November 2018

Investigating the Roles of Fucosylation and Calcium Signaling in Melanoma Invasion

Tyler S. Keeley
University of South Florida, tkeeley11@gmail.com

Investigating the Roles of Fucosylation and Calcium Signaling in Melanoma Invasion

by

Tyler S. Keeley

A dissertation submitted in partial fulfillment
of the requirements for the degree of
Doctor of Philosophy
with a concentration in Cancer Biology
Department of Cell Biology, Microbiology, and Molecular Biology
College of Arts and Sciences
University of South Florida

Major Professor: Shengyu Yang, Ph.D.
Co-Major Professor: Eric Lau, Ph.D.
Srikumar Chellappan, Ph.D.
Conor C. Lynch, Ph.D.
Alvaro Monteiro, Ph.D.

Date of Approval:
November 8, 2018

Keywords: invadopodia, fucose, FUK, FUT1, STIM1

Dedication

I dedicate this dissertation to my family and close friends, those who inspired me, and helped me to remember why I started this endeavor in the first place. Their belief in me helped make this work possible.

Acknowledgements

First and foremost, I must extend my most heartfelt appreciation to Dr. Yang for his willingness to take as his first graduate student. His guidance and training truly expanded my knowledge and understanding of cancer and laboratory practices. I must also thank Dr. Shengchen Lin for being a tremendous help in the lab and always being willing to answer the small questions I had.

I would also like to extend my thanks to my committee members, Dr. Eric Lau, Dr. Srikumar Chellappan, Dr. Conor Lynch, and Dr. Alvaro Monteiro. Their guidance throughout the years has helped with experimental design, and has been critical in my presentation development.

Research now is never an individual effort, and I would like to extend my appreciation to Dr. Lau and his lab members for the collaborative efforts that have helped me get to this point. His advice, reagents, and willingness to troubleshoot experiments with me as we started the fucose project was crucial to the success of the project. Additionally, I have to thank the core facilities at Moffitt for their contributions to the experiments conducted that we could not have completed on our own.

I couldn't have made it this far without the help of several key individuals outside of the lab setting. First, I would like to thank Maria Hernandez for helping me with scheduling committee meetings, especially after our lab moved to Penn State. Along those lines, I would like to thank Melissa Quintana for her role in scheduling these meetings for Dr. Monteiro. My sincere thanks also goes to Charity Sauder, Michele Herr, Jaci Wildner, and Lisa Harmon at Penn State for helping to make the transition to Penn State smooth. They helped to make me feel particularly welcome as they helped find ways for me to become engaged with the graduate students and make connections quickly. Those mentioned in this paragraph truly made my life easier after the move.

Of course, I would like to acknowledge the Cancer Biology Ph.D. program for the opportunities presented to me over the last five years. Dr. Ken Wright, Cathy Gaffney, and Janet Opel have been instrumental in ensuring that I made it here by making certain deadlines were reached. Particularly, I would like to thank Dr. Wright for taking the time to sit down with me once the move had been announced and to guide me to the right decision for me.

Finally, my family and friends deserve my thanks for always being supportive on this venture. My wife, Kristen, for taking a leap of faith on me and following me to Tampa from Massachusetts. My parents, Howard and Cidalia, for constantly reminding me that this step will set me up for great things moving forward. My brother, Zak, and my closest friends, Ryan and Jason, for always being close, even when separated by the miles. My grandparents Howard and Hazel, and my aunt and uncle, Bev and Bill, for always being interested in what my work entailed. I have been incredibly fortunate to have had your support over these years, and I am forever grateful for your backing.

Table of Contents

List of Tables

List of Figures

Abstract

Melanoma is the deadliest form of skin cancer. Prognosis for early stage melanoma patients is excellent, and surgery is often curative for these patients. However, once patients have presented with invasive disease, the average 5-year survival rate drops significantly from over 90% to between 10 and 15%. Several therapies have been developed to target a commonly mutated oncogene BRAF, or its downstream effectors. Unfortunately, while these treatments show robust initial response, most patients relapse within a year. Moreover, therapy-resistant tumors are often more invasive and metastatic. Therefore, it is important to investigate the molecular mechanisms underlying melanoma invasion and metastasis, and to prevent melanoma cell dissemination and metastatic progression. Invadopodia are proteolytic membrane protrusions used by metastatic cancer cells to degrade the extracellular matrix and to facilitate cancer cell invasion and metastasis. In my thesis research I have focused on protein fucosylation and store-operated calcium entry, two separate mechanisms involved in invadopodial regulation.

Post translational modifications of proteins are essential for their structure and function. Many cell surface proteins require modifications such as glycosylation for protein-protein interactions, cell adhesion, and signal transduction. Fucosylation is a form of glycosylation that adds L-fucose on glycan structures of proteins. There is evidence indicating that fucosylation plays an important but cancer-type and branching dependent role in cancer progression. Emerging evidence indicates that the fucose salvage pathway and protein fucosylation are altered during melanoma progression and metastasis. Here, we report that the fucose salvage pathway inhibits invadopodia formation and extracellular matrix degradation by promoting α(1,2) fucosylation of cell surface proteins. The activation of the fucose salvage

pathway decreases invadopodia numbers and inhibits the proteolytic activity of invadopodia in WM793 melanoma cells. Inhibiting fucokinase, one of the critical enzymes in the fucose salvage pathway, in melanoma cells abrogates L-fucose-mediated inhibition of invadopodia, suggesting dependence on the fucose salvage pathway. The inhibition of invadopodia formation by L-Fucose treatment or fucokinase overexpression could be rescued by treatment with α(1,2), but not α(1,3/4) fucosidase, implicating an α(1,2) fucose linkage-dependent inhibitory effect. The ectopic expression of FUT1, an α(1,2) fucosyltransferase, is sufficient to inhibit invadopodia formation and ECM degradation. Our findings indicate that the fucose salvage pathway can inhibit invadopodia formation, and consequently, invasiveness in melanoma via α(1,2) fucosylation. Re-activation of this pathway in melanoma could be useful for preventing melanoma invasion and metastasis.

Calcium is a critical second messenger involved in a multitude of biological processes from cell proliferation to muscle contraction. In melanoma, previous studies have found that activation of the store operated calcium entry (SOCE) channel promotes tumor invasion and metastasis, *in vitro* and in xenograft models. The expression levels of STIM1, an essential component of the store operated calcium channels, has been found to increase with later stages of melanoma. In melanoma cell lines, the over expression of STIM1 enhances invadopodia number whereas STIM1 knockdown inhibits invadopodia formation. Similarly, gelatin degradation activity is enhanced with STIM1 overexpression and abrogated with STIM1 knockdown, implicating STIM1 as an important factor in the regulation of invadopodia formation and melanoma invasion. Though the studies published have shown a significant role of STIM1 in tumor progression, a robust transgenic animal model has not yet been established. Here, we developed a novel transgenic mouse model which, upon 4-hydroxytamoxifen (4OHT) treatment, induces the $BRAF^{V600E}$ mutation and PTEN, STIM1, and STIM2 deletions in melanocytes via an inducible Cre-lox system. Our investigation found that the loss of STIM1 exacerbates tumor growth and results in tumor formation significantly more quickly than STIM1 wild type mice. Whereas PCR analysis of 4OHT-treated skin showed

deletion of STIM1 and PTEN, immunohistochemical staining of these genes in tumors did not convincingly demonstrate complete deletion. Therefore, it remains to be determined whether the effects we observed are due to STIM1 and STIM2 loss. These findings need to be corroborated in the future.

Our studies focus on two important mechanisms required for melanoma progression and metastasis. We found that α(1,2) fucosylation is able to inhibit invadopodia formation, and melanoma cell invasion. The reestablishment of α(1,2) fucosylation in melanoma could potentially be exploited to inhibit melanoma metastasis. Additionally, early evidence points to STIM1 having a tumor suppressive role in melanoma oncogenesis and tumor growth based on the transgenic mouse model. Although the phenotype is unexpected, further investigation of this model will likely provide important insight for the complicate roles of SOCE in melanoma initiation and progression.

Introduction to Melanoma

Melanoma is the 5th and 6th most common cancer in men and women respectively in 2018[1] and is the deadliest form of skin cancer.[2,3] Despite significant progress in cancer diagnosis and therapeutic modalities, the incidence and mortality rates have continued to rise.[1,4–6] Between 2009 and 2016, the risk of developing invasive melanoma increased from 1 in 58 to 1 in 54, and the life time risk of developing *in situ* melanoma increased from 1 in 78 to 1 in 58.[4] When melanoma is detected early, the prognosis is favorable, with average 5 year survival rates >90%.[4,7] Once melanoma has begun to invade the local tissue and metastasize, the average 5-year survival rates drop to 10-15%.[3,7] Patients with 3 or more metastases have a 1 year mortality rate of over 95%.[5]

Melanoma staging is determined through the TNM system, which takes into account the tumor size and ulceration status (T), the number and location of lymph nodes that have been detected as involved (N), and the presence of local and distant metastases (M). Several prognostic factors that have been linked to poor clinical outcome, and are taken into account when determining staging, include ulceration[7,8], mitotic rate[7,8], satellites[8], and primary tumor thickness[7,9,10]. It has been determined that the thickness of the primary tumor – "Breslow Depth" – is the most important factor in predicting survival.[7,9] Surgery is often curative when melanomas are detected early and the tumor thickness is ≤1mm, however, survival rates drop steeply with increasing thickness.[3] Early stage melanomas are localized to the epidermis and have not yet started disseminating.[11] Late stage melanoma cells are invasive, and are able to invade the local tissue.[12] These cells can either intravasate into blood or lymphatic vessels, or take on pericyte-like characteristics, to disseminate through or migrate along the vessel.[13–15] Disseminated cells seeded in different organs develop secondary tumors, or stay in a quiescent state until conditions are

favorable for growth.[16] Fortunately, our understanding of the causes of melanoma is growing, and hopefully, we will begin to see a plateau and decline of mortality rates with continuing education and improved detection.

1.1 Metastatic Sites

In order for metastasis to occur, the tumor must invade through the local tissue, intravasate into the vessels, evade the immune system and survive the circulatory system, adhere to the endothelial lining of a capillary, extravasate from the vessel, and finally colonize the new tissue.[12,17–19] Metastatic colonization is inefficient, with a minute population of disseminated cells developing secondary tumors.[5,18,20] Melanoma has a propensity to metastasize to certain tissues such as the lungs, brain, and skin, however, it has been observed that melanoma tumor cells can disseminate to any viscera and tissue.[5,12,21,22] Several of the more common metastatic sites are highlighted in Table 1.

Table 1: Common Sites of Melanoma Metastasis[21]

Organ	Prevalence at autopsy
Lymph Nodes	74%
Lungs	71%
Liver	58%
Brain	55%
Bone	49%
Adrenal Glands	47%
GI Tract	44%
Skin	11%

Lymph nodes have been reported to be the most frequent site of metastasis in melanoma patients.[12] As the thickness of the primary melanoma increases, so does sentinel lymph node involvement.[8,19] Melanoma has the propensity to rapidly metastasize, with lymph node metastases observed within an average of 16 months after initial disease presentation[17], and close to 50% of patients with invasive melanoma displaying lymphatic invasion.[13] Lymph node metastases are prognostic of the metastatic potential of primary tumors.[19,23]

Distant organs that are susceptible to melanoma metastases include the lungs[5,24], bone[5,24], liver[19,20,24], small intestine[20], and brain[5,19–21,24]. Cutaneous melanomas commonly metastasize to the

lungs.[17] Melanoma cells within tumors that express $\alpha_v\beta_3$ integrins tend to develop lung metastases.[17] A postmortem study found that in melanoma patients, lung metastases were present in over 70% of individuals.[21] Melanoma has been found to metastasize to the bone in ~49% of patients and to the liver in up to 58% of postmortem patients.[21] Unfortunately, due to poor detection, clinical liver metastases are only diagnosed in 10-20% of melanoma patients.[5] Melanoma is the most common cancer to metastasize to the small intestine, possibly due to CCL25 production by intestinal cells which acts as a chemoattractant for CCR9-bearing melanoma cells, and facilitates homing to the small intestine.[17] Similar to liver metastases, only a small population, between 1-7%[5], of patients have metastases clinically detected, however, upon autopsy investigation, metastases in the small intestine are found in between 44-58% of melanoma patients.[5,21] Melanoma is a particularly aggressive cancer type which is able to metastasize rapidly to almost any organ. This robust metastatic phenotype significantly contributes to lethality among melanoma patients.

1.2 Commonly Mutated Drivers

Several oncogenes and tumor suppressors have been found to be commonly mutated in melanoma including BRAF, Neuroblastoma RAS (NRAS), phosphatase and tensin homolog (PTEN), p53, and cyclin-dependent kinase inhibitor 2A (CDKN2A). BRAF is the most commonly mutated oncogene in melanoma with a mutation rate of ~40%, and 80-90% of those mutation being $BRAF^{V600E}$.[2,3,25–36] This glutamic acid substitution of valine at position 600 causes constitutive activation of BRAF, which in turn continuously activates the mitogen activated protein kinase (MAPK) pathway to promote tumor cell growth, survival, migration, and invasion.[2,25,27,30] However, the mutation of BRAF alone is not sufficient to induce melanoma formation.[37] Oncogenic BRAF mutations are found in 80-90% of benign nevi, indicating that while it might be a necessary event to induce melanocyte proliferation, the mutation of a single oncogene is insufficient to cause a malignant transformation.[3,10,27,28,32,36,37] Further studies have found that

Table 2: Combination Treatments

Combined with	MEK inhibitor	Immunotherapy	Radiation	Chemotherapy
BRAF inhibitor	2,25,28,38,40,43,46,73,74	65,76		299,300
Immunotherapy		301–305	63	306

$BRAF^{V600E}$ is often coupled with inactivation of tumor suppressor genes such as PTEN, p53, and CDKN2A.[28,36,37] There are numerous FDA approved $BRAF^{V600E}$ inhibitors, with impressive clinical efficacies in melanoma patients.[28,38–46] However despite robust initial response, most patients become resistant to these targeted therapies after 6-7 months with a small percentage remaining disease-free past 1 year.[25,39,47] Resistance has been reported to develop through BRAF splice variant expression, gene amplification, or NRAS activating mutations.[3,28,39,41,48] Additionally, resistance can develop through the activation of signaling pathways that bypass targets of inhibition. Activating mutations in MEK[3,47,49,50], MITF amplification[51], and upregulation of COT expression[52] are examples of MAPK agonists resulting in the activation of ERK despite BRAF inhibition. Other mechanisms such as enhanced NF-κB signaling[53] and upregulation of signaling receptors such as PDGFR[54], IGF-R1[55], and FGFR3[56] have also been implicated in conferring therapeutic resistance in melanoma. Multiple studies have been conducted to investigate combination treatments to discover novel treatment regimens to combat resistance and extend patient survival summarized in Table 2.

Another frequently mutated oncogene in melanoma in the MAPK pathway is NRAS. It is the second most commonly mutated protein in melanoma with a mutation rate of ~20%.[2,3,26–31,33–35,41] Mutant NRAS leads to the activation of the MAPK pathway, as well as the PI3K pathway.[25,30,57] NRAS mutations in melanoma can disrupt antitumor immunity by inhibiting the expression of major histocompatibility complexes and recruiting myeloid-derived suppressor cells and regulatory T-cells leading to decreased lymphocyte infiltration and a less immunogenic tumor type.[25,29] Mutations of NRAS and BRAF are mutually exclusive with only ~0.6% analyzed melanoma tumors expressing both mutated oncogenes.[25–27,34] Incidentally, there is evidence that mutations of both proteins in the same cell leads to senescence.[35]

BRAF and NRAS mutations alone are insufficient to promote tumorigenesis and additional mutations are required for malignant transformation. PTEN is a frequently mutated tumor suppressor in melanoma. PTEN is a lipid phosphatase that dephosphorylates the 3'-position of the inositol ring of phosphatidylinositols and inhibits Akt activation.[2,30] Loss of PTEN activity can be due to inactivating mutations, chromosomal deletion, methylation induced transcriptional silencing, or miRNA dependent mechanisms.[25] Mutations of PTEN occur in about 10-35% of melanomas and have been observed in both NRAS and BRAF mutant tumors.[28,30,35,38] A retrospective study found that PTEN protein expression is completely lost or reduced in ~80% of analyzed melanoma samples.[30] The combination of a mutated oncogene with the loss of PTEN activity is sufficient to drive melanoma progression.

One of the best known tumor suppressor genes is p53, which is frequently mutated in many cancer types.[58] p53 is mutated in ~20% of melanomas.[28] Mutated p53 is found in thicker invasive melanomas and contributes to advanced progression in chronically sun damaged skin.[10] Ultra-violet (UV) radiation causes DNA damage, which must be repaired in order for a cell to progress through the cell cycle to division.[59] When DNA damage is detected, p53 is one of the proteins responsible for halting cell division until the DNA has been repaired.[60] p53 mutations in melanoma occur later in tumor progression as p53 expression is high in primary tumors compared to nevi, but lost in matched metastatic tumors.[36] Inactivating mutations of p53 are found at a much higher frequency in metastases than primary tumors, further supporting p53 mutations are a late event in melanoma.[10]

Another tumor suppressor gene that is frequently mutated in melanoma is CDKN2A. This gene inhibits cell cycle progression as it encodes two proteins, p16 and p14arf, that inhibit cyclin dependent kinases and activate p53, respectively.[35] CDKN2A is mutated in 25-40% of families with hereditary cases of melanoma.[28,37] Inactivation of CDKN2A has been reported in as high as 88% of sporadic melanoma.[36,37,61] Similar to p53 or PTEN, loss of CDKN2A is thought to occur later in melanoma progression as inactivation is not typically observed in precursor lesions, but occurs once the melanomas have become

invasive.[10,36] UV radiation is thought to be responsible for CDKN2A loss by causing DNA damage in the region of the CDKN2A gene.[2] In addition to promoting general tumor growth, the continuous passage through the cell cycle without regulation allows for tumor cells to accumulate further mutations that might confer a survival advantage[62], further promoting heterogeneity and evolution of the tumor.

There are many genes and proteins that have been implicated in tumor formation. It is generally understood that one mutation is not sufficient to generate melanoma, but rather accumulated mutations of oncogenes and tumor suppressors work in tandem to prompt tumor formation and tumor progression.

1.3 Treatments for Melanoma

The most effective treatment for early stage melanoma is surgery, which can be curative.[3,10,17] However, with later stages of disease, surgery alone is not sufficient to successfully treat melanoma. Treatment options that are considered for patients with later stages of disease include adjuvant treatment with small molecule inhibitors[28,32,34,38,39,41,46,48], radiation[17,63,64], and immunotherapy[8,25,38,63–72] following surgery (Table 3). Limitations of current therapy are due to resistance mechanisms that melanoma cells develop to survive targeted therapy treatment. Combination treatments are being investigated to combat relapse mechanisms and enhance patient responses. Some treatments aim to block signaling cascades by

Table 3: Current Therapy Modalities for Melanoma

Treatment	Reasons Used	References
Surgery	• Curative intent in early stages • Removal of lymph nodes with curative intent	10,17
Radiation	• Alternative to surgery for *in situ* disease • Adjuvant therapy following surgery • Palliative relief after metastasis	17,63,64
Molecular Targeted Therapies	• Blocking of protein active sites to inhibit signaling driving tumorigenesis	28,32,34,38,39,41,46, 48
Immunotherapies	• Block signaling events that lead to immune cell exhaustion through CTLA-4 or PD1 • Adjuvant therapy to boost immune cell function	8,25,38,63–72
Combination Treatments	• Target multiple proteins of the same signaling cascade • Target multiple proteins in different signaling pathways	2,38,43,63,65,68,75

administration of small molecule inhibitors to target multiple proteins in the same or parallel signaling pathways.[2,25,28,38,40,43,46,73,74] Other treatment regimens combine small molecule inhibitors, antibodies, chemotherapies, and/or immunotherapies in order to inhibit melanoma development while simultaneously augmenting the immune response to the tumor cells.[2,25,28,38,40,43,46,63,65,68,73–75] The most promising combination treatments have delayed disease progression by ~15 months in patients treated with a BRAF and a MEK inhibitor[38] and overall survival by ~20 months in patients treated with a BRAF inhibitor and immunotherapy.[76] Although responses and median survival rates are improving compared to the standard of care, there is still much to be desired.

Melanoma has the ability to metastasize rapidly and indiscriminately, causing treatment difficulties. Metastases can develop quickly once melanoma cells have begun to invade, or occur years to decades after apparent successful removal of the primary tumor.[18] Up to 12% of patients that develop metastatic melanoma have no identifiable primary tumor[5] and upwards of 50% of melanomas develop from benign tumors, further contributing to treatment challenges.[32,57]

1.4 Major Proteins Involved in Cytoskeletal Rearrangement

Cancer cells use the same migratory mechanisms involved in embryonic morphogenesis, wound healing, and lymphocyte trafficking to migrate through tissue to local vessels.[77] The actin cytoskeleton plays a significant role in cell movement. Actin polymerization promotes cell migration through the elongation of polarized cells and generation of traction forces.[77] There are two main actin structures in the leading edge of migrating cells termed lamellipodia and filopodia. Filopodia are actin rich protrusions that are transient in nature, protrude the cell membrane, promote cell-cell adhesion, act as sensors for the cell to probe the microenvironment, and sometimes generate focal adhesionions.[78] Lamellipodia are thin, sheet-like protrusions of the cell membrane formed by rapid actin branching.[79] Filopodia are thought to act as sensors of the extracellular matrix (ECM) and seek out small gaps in the fibers, whereas

lamellipodia provide the protrusive force resulting in membrane protrusion and cell crawling.[80] As the cell crawls forward, the actin filaments at the rear of the cells are degraded, and the globular actin segments are recycled to the leading edge of the migrating cell, where they are incorporated into actin filaments, to continue the migration.[81]

Actin branches are repeatedly being formed and disassembled to facilitate the continual push of the cell membrane at the leading edge of migrating cells.[82] Extracellular stimuli through integrins or receptor tyrosine kinases (RTKs) activates Neuronal Wiskott-Aldrich Syndrome Protein (N-WASP), leading to actin nucleation by activation of the Arp2/3 complex[79], which can be promoted by WASP interacting protein (WIP).[79,83] Ena/VASP regulate actin branching by bundling actin filaments and preventing capping of actin barbed ends.[79] Existing branches are transient in nature and are rapidly disassembled by cofilin to maintain the constant pool of actin monomers available to the cell and create barbed ends at which further polymerization can occur.[84] Cortactin interacts with cofilin to inhibit its actin severing abilities.[84,85] The Rho family of GTPases have been implicated in actin dynamics, particularly RhoC, which has been shown to regulate cofilin activity.[86] Rho-associated kinases (ROCK) regulate cell migration and invasion through organization of the actin cytoskeleton.[87] Many studies have been conducted investigating the molecular mechanisms of the aforementioned proteins, including the role they play in cancer progression.

1.5 Invadopodia

Invadopodia are proteolytic actin-rich protrusions of the cell membrane on the ventral side of the cell.[80] Invadopodia formation can be divided into the following stages: initiation, assembly, and maturation.[88] Initiation begins when the cell develops focal adhesions, and signaling events through growth factors or integrins result in the recruitment of actin nucleating proteins.[88] Assembly occurs when actin polymerization extends actin filaments and results in protrusion of the cell membrane.[88] Maturation results in the degradation of the ECM through recruitment and secretion of matrix metalloproteinases,

such as MT1-MMP, MMP2, and MMP9.[88–90] These invasive structures are important to tumor cell invasion as they lead to the restructuring and degradation of the ECM through the recruitment, secretion, and activation of MMPs.[17,91,92]

Since invadopodia are actin-based protrusions, they require similar molecular machinery as filopodia and lamellipodia.[89] Invadopodia have been shown to be as long as 12μM, and have a lifetime of anywhere from 20 minutes to 2 hours.[79,80,89,93] Invadopodia form on the ventral side of the cell, under the nucleus, and form perpendicular to the cell surface.[79,80,94,95] Once invadopodia have developed, degradation of the ECM follows, typically through the combination of physical force as well as the recruitment, secretion, and activation of proteinases.[86,96–98] Invadopodia have been shown to act as docking and secretion sites for endosomes[99], which might contribute to the development of metastasis.[100] Cancer cells have been demonstrated both *in vitro* and *in vivo* to form invadopodia to penetrate the basement membrane, surrounding stroma, and vasculature.[83,95,101] Understanding the mechanisms by which invadopodia are formed and dysregulated in cancers provides insight and possible targets to study to abrogate, or at least delay, tumor cell invasion.

1.6 Signaling Cascades and Key Proteins in Invadopodia

Invadopodia initiation begins with signaling through plasma membrane proteins such as integrins and RTKs. The signal transduction cascades from these membrane receptors facilitates the recruitment of scaffolding proteins, kinases, and actin related machinery to promote invadopodia assembly and maturation.[89,102–104] There is evidence that invadopodia are generated at lipid rafts, and several important proteins in invadopodia assembly, such as Arp2/3, Tks5, and MT1-MMP, localize to these rafts.[105–107] Various growth factors that have been shown to initiate invadopodia formation include PDGF, EGF, VEGF, HGF and TGFβ.[89,98,108] β1 and β3 integrins have been shown to be the primary adhesion molecules found at invadopodial puncta. β1 integrin is thought to be more involved than β3 integrin and forms signaling

complexes with Src, epidermal growth factor receptor (EGFR), and focal adhesion kinase (FAK) at invadopodia.[104] One of the essential kinases in invadopodia formation is Src. Src phosphorylates scaffolding proteins and facilitates the interaction between multiple proteins important in cytoskeletal rearrangement.[79] One such scaffolding protein is known as Tks5. Following activation by Src, Tks5 binds to N-WASP and cortactin, facilitating their interaction and function in invadopodia formation.[79,89,105,109] Tks5 also enables the degradation of the ECM through the recruitment of degradative enzymes.[101,105,110] Cortactin plays an important role in the activation of key players in actin polymerization and assembly of invadopodia.[94] Cortactin acts as a scaffolding protein to facilitate the interaction between N-WASP and Arp2/3 and has been shown to be an important regulator of protease secretion, localization of MMPs to actin puncta, and ECM degradation.[79,96] The phosphorylation of cortactin by Src leads to dissociation with cofilin, and promotes the recruitment of Arp2/3 and N-WASP.[95,101,105,110,111] Cofillin dissociation from cortactin severs actin filaments to generate new barbed ends for actin polymerization and membrane protrusion.[84,85] As invadopodia mature, degradative enzymes are recruited to degrade the ECM. MT1-MMP, MMP2, MMP9, sepharase, cathepsin B, gelatinase A, ADAM proteinases, and uPAR are recruited or secreted at invadopodia to facilitate the cleavage of various components of the ECM and lead to degradation.[104,112]

Part One: An Investigation into the Modulatory Role of Fucose in Melanoma Invasion

Note to Reader

Portions of this part have previously been published in *PLOS ONE*, 2018, 13(6): e0199128 and have been reproduced under the terms of the Creative Commons Attribution License CC-BY 2018.

2.1 Introduction

2.1.1 Fucose

Fucose is a natural deoxyhexose with similar structure to glucose, except for its lack of a hydroxyl group on carbon 6.[113] Mammalian cells utilize fucose in the L-enantiomer, whereas they generally make use of other deoxyhexoses in the D-enantiomer.[114] L-fucose is incorporated onto glycoproteins and glycolipids and is important in the synthesis of N- and O-linked glycans in mammalian cells.[115,116] Fucosylated glycans are important in a range of cellular functions from modulating the inflammatory response, to cell adhesion and communication, to fertilization.[117] Specificity of cell-cell interactions can be partially determined by the presence of fucosylated lectin-like adhesion molecules on the cell surface.[118] Several cell membrane receptors and proteins that have been shown to be fucosylated include EGFR, TGFβ, E-cadherin, and various integrins.[119] Additionally, selectin ligands have been shown to be fucosylated which enhances their binding to selectins, and loss of fucosylation on selectin ligands abrogates selectin binding.[120] Since cancer can dysregulate many cellular functions to promote growth and metastasis, aberrantly fucosylated glycans can play an important role in tumorigenesis and progression.

Post-transitional modifications are stringently regulated to perform specific cellular functions. Aberrant fucosylation has been reported in many cancer types, including melanoma.[121] In some cases fucosylation is upregulated, whereas in other cases fucosylation is downregulated. Different phenotypes stemming from differential fucosylation can be linked to specific fucosylation residues as there are four major types of branching.[115] Changes in fucosylation have been previously observed to affect metastatic properties of cancer such as cell adhesion and recognition by immune cells.[122] Lewis antigens (Le) refer to specific orientations of monosaccharides with differing orientations of terminal fucosylation, and in some cases, sialylation (Fig. 1-1). Augmented exhibition of Le antigens in tumors has been shown to drive tumorigenic properties in multiple cancer types, including melanoma.[123] Increased levels of fucosylated sLe^x and sLe^a antigens correlate with poor prognosis, as these antigens promote metastasis by strengthening tumor cell interactions with epithelial cells.[115,118] In gastric cancer, it was found that fucosylation is enhanced in early stages, but also diminished in late stages and metastasis as glycans are defucosylated.[124] However, there are also reports indicating that some metastatic cancer cells have

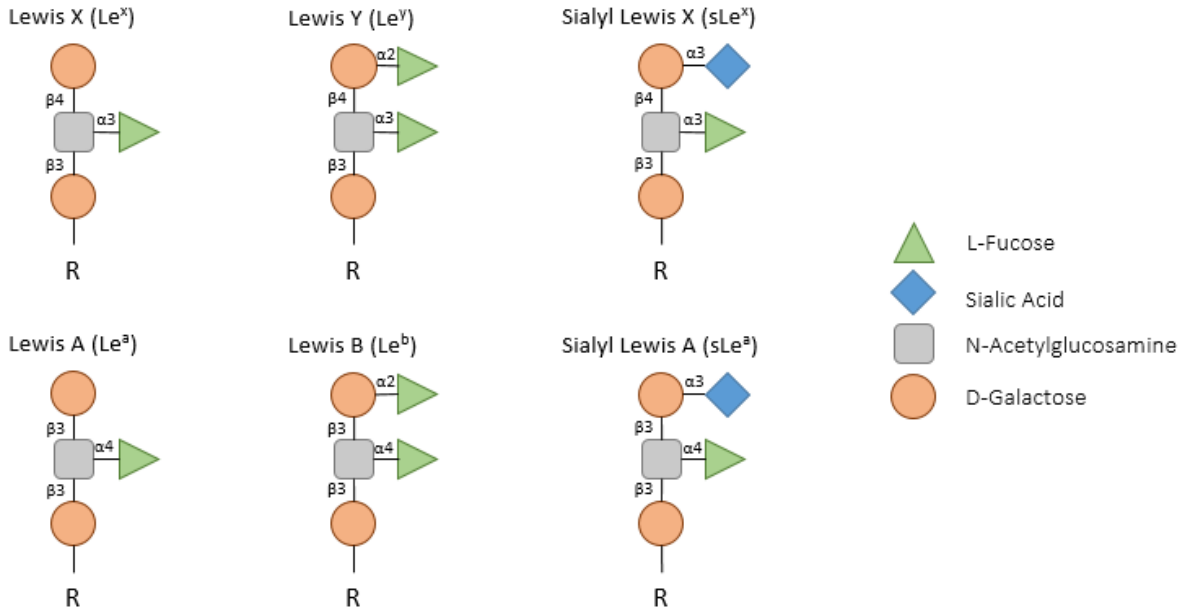

Figure 1-1: Visual Representation of Lewis antigens and associated fucose branches commonly found on the surface of cells

increased fucosylation when compared to non-metastatic cells.[125] Overall levels of fucosylation have been shown to increase in cancer types such as breast and colorectal[126], but the variation in branching types of fucosylation plays important roles in cancer progression.

2.1.2 L-fucose metabolism

There are two known pathways by which mammalian cells synthesize GDP-Fucose (Fig. 1-2). In the *de novo* pathway, GDP-mannose in the cytosol is utilized as a substrate for GDP-mannose 4,6-dehydratase (GMD), and converted to GDP-4-keto-deoxymannose. The keto intermediate is quickly converted by the FX protein to GDP-fucose. The epimerase portion of FX converts the keto intermediate to GDP-4-keto-6-deoxygalactose, and the reductase portion of FX then catalyzes the final reaction to

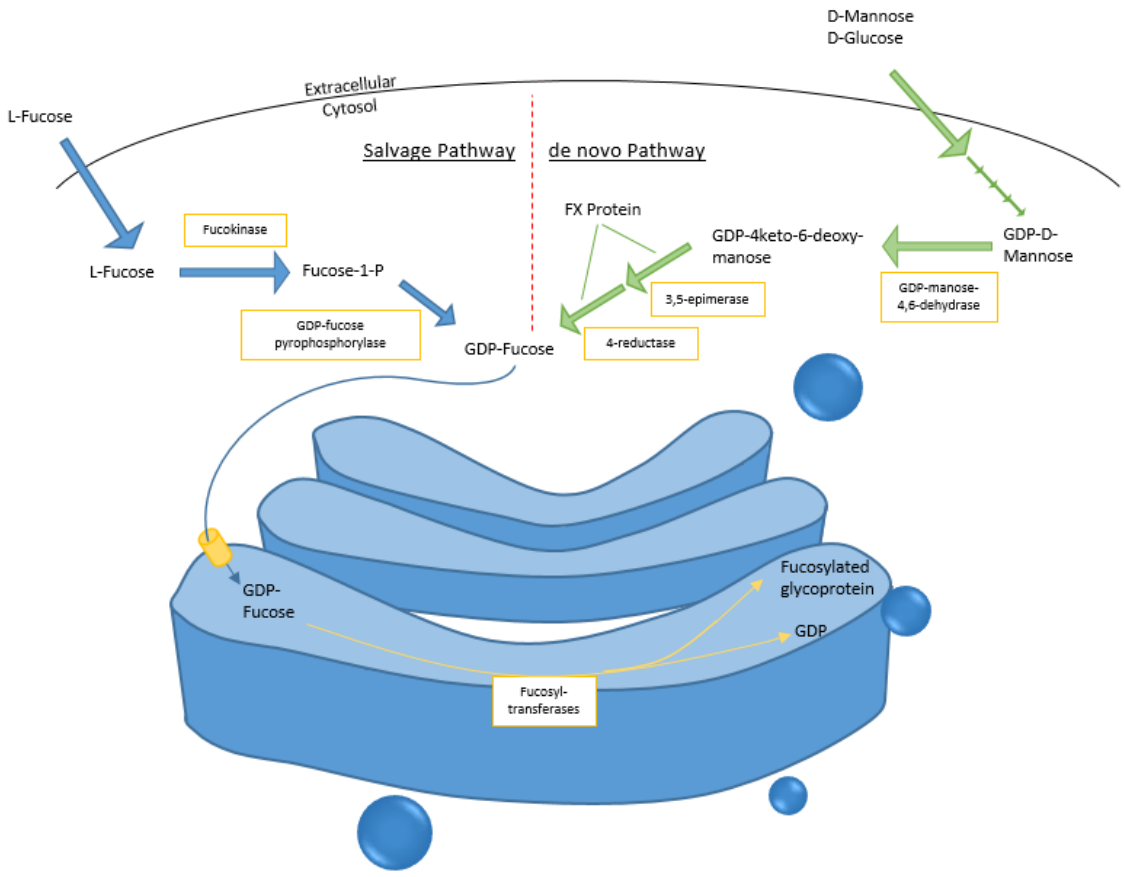

Figure 1-2: Schematic of the fucose salvage and *de novo* pathways

result in GDP-fucose.[115] The second pathway is known as the salvage pathway. L-fucose is transported into the cytosol from the extracellular space, or from lysosomal compartments. L-fucose from the extracellular space is believed to enter the cell through L-fucose specific transporters, although which remain unclear. Free L-fucose in the cytosol is converted to fucose-1-phosphate by fucokinase (FUK), which is then converted to GDP-fucose by GDP-pyrophosphorylase.[115] In general, it is believed that the main source of L-fucose for the salvage pathway comes from diet.[115] However, when dietary sources are insufficient, L-fucose can be catabolized from preexisting fucosylated glycans. The glycans are endocytosed and catabolized in lysosomes, where L-fucosidases cleave L-fucose from the glycans to be used by the salvage pathway.[115,116,127] In melanoma cells, it has been reported that the salvage pathway contributes ~40-50% of GDP-fucose.[128] Once synthesized, GDP-fucose is shuttled into the Golgi apparatus, where it is used as a substrate for fucosyltransferases.

2.1.3 Fucosyltransferases: Regulators of Fucosylation Branching

Fucosyltransferases (FUTs) are membrane-bound proteins that utilize GDP-fucose as a substrate to transfer L-fucose onto oligosaccharides, glycans, lipids, and proteins to form fucosylated glycoconjugates.[129,130] Eleven FUTs and 2 protein-O-FUTs (POFUTs) have been discovered to this point. FUTs conjugate L-fucose onto oligosaccharides in various conformations, such as α(1,2), α(1,3), α(1,4), and α(1,6) orientations (Fig. 1-3).[115] As fucose is conjugated to oligosaccharides, the first carbon of fucose is bound to the second (1,2), third (1,3), fourth (1,4), or sixth (1,6) carbon of galactose or N-Acetylglucosamine (GalNAc).[131] The linkage is considered α when the oxygen atoms in the carbon rings are in a *cis* conformation, whereas β linkages occur when the oxygen atoms in the carbon rings are in a *trans* conformation.[132] POFUTs directly conjugate L-fucose onto serine or threonine amino acids within EGF or THBS repeats.[133] Core fucosylation (α(1,6)) is only conjugated by FUT8, which conjugates L-fucose to the primary GalNAc branch on N-glycans.[133] Core fucosylation has been shown to play an important

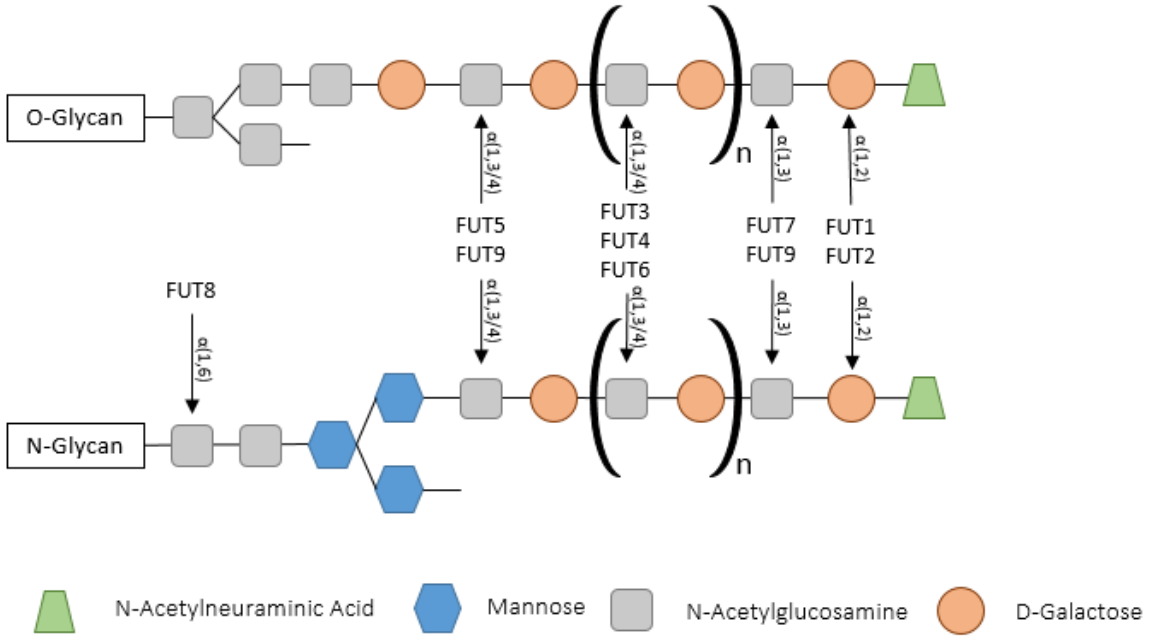

Figure 1-3: Visual representation of the various sites of fucosylation and the respective FUTs that conjugate L-fucose to the monosaccharides

role in the signaling of various membrane bound proteins, such as EGFR[119,121] and TGFβ[117,121]. T-cell receptors are heavily core fucosylated, which ensures proper activation of downstream signaling.[134] Terminal fucosylation refers to L-fucose conjugated to GalNAc or galactose monosaccharides in an α(1,2), α(1,3) or α(1,4) conformations.[116,133] Terminal fucosylation is highly diverse, contributing to the generation of Lewis antigens on a multitude of proteins.[135] The specificity of branched fucosylation, and therefore the precise signaling mechanism initiated, is dictated by FUTs.

FUT 1 and 2 are the two transferases that conjugate L-fucose in the α(1,2) branching to terminal galactose on both O- and N-glycans.[115] FUT1 is implicated in the synthesis of H antigens, and has been shown to contribute to endothelial cell tube formation and leukocyte-synovial fibroblast proliferation and adhesion.[136] Its role in immunity was demonstrated as the overexpression of FUT1 in transgenic mice promotes thymocyte maturation and arrest through increased T-cell receptor signaling and apoptosis.[134] FUT1 has been demonstrated to contribute to Lewis^{y} (Le^{y}) antigen production.[137] FUT2 contributes to

α(1,2) fucosylation of H antigens in salivary glands and epithelial tissues[124], and ABO blood type antigens in body fluids, the gut, and secretory glands.[138,139]

FUT3-7, and 9-11 are responsible for the addition of L-fucose to GalNAc monosaccharides in α(1,3) and α(1,4) orientations on O- and N-glycans.[115] Carbohydrate lectins are fucosylated in patterns similar to Lewis antigens in order to facilitate binding with selectins expressed on the surface of platelets, endothelial cells, and leukocytes.[115] FUT3 conjugates L-fucose in both α(1,3) and α(1,4) branching and contributes to the synthesis of Lewis^a(Le^a) Lewis^b(Le^b), Lewis^x(Le^x), and sialyl-Lewis^x(sLe^x) antigens.[124,130,135] FUT4 and 5 also conjugate both branching of L-fucose to glycans, and are thought to contribute to the formation of the same Lewis antigens as FUT3, as well as the sialylated precursor selectin ligands in leukocytes.[124,130,133,135] The formation of the precursor selectin ligands generated by FUT4 are likely responsible for leukocyte function and trafficking.[129] FUT6 additionally contributes to both forms of branching, however, its activity is limited to synthesis of Le^x and sLe^x antigens.[124,130,133,135] In addition to the conjugation of L-fucose in the α(1,3) and α(1,4) orientations, FUT7 is involved in the recruitment of neutrophils and T-cells to areas of inflammation and lymphoid trafficking to distal lymphoid organs – likely due to its contribution to sialylated precursor selectin ligands in leukocytes.[115,130,135] FUT9 has only been reported to be involved in the synthesis of Le^x antigens.[130,135] Most of the α(1,3) and α(1,4) FUTs have redundant function, particularly in the generation of Lewis antigens. However, in cancer, there tends to be differential expression or activity of some, but not all FUTs, indicating that they might play a more specific role in disease regulation or progression.

FUT8 is the only transferase to conjugate L-fucose to the initial GalNAc residue on N-glycans in an α(1,6) conformation (core fucosylation).[135,140] FUT8 has been shown to be integral in TGFβ signaling as knockout of FUT8 results in a lack of core fucosylation of receptor type II, which inhibits the binding of TGFβ1 to type I and II receptors.[117] Additionally, core fucosylation has been previously shown to be

important in EGF, TGFβ, and HGF signaling.[121] Core fucosylation of E-cadherin increases cell adhesion by facilitating tighter E-cadherin-dependent adhesions.[126]

2.1.4 α(1,2) Branching

It is thought that enriched fucosylation might lead to increased adhesion and metastatic potential through the expression of Lewis antigens.[141] There have been studies in melanoma[128,142,143], oral/head and neck[144], gastric[145], pancreatic[146], and hepatocellular[147,148] carcinomas indicating that α(1,2) fucosylation inhibits tumor formation and is decreased during tumorigenesis and disease progression (Table 4). A recent investigation into the role L-fucose and fucokinase (FUK) of the salvage pathway played in melanoma progression with regard to α(1,2) fucosylation was conducted. The investigators found that L-fucose treatment and/or FUK overexpression inhibited cell migration and invasive potential as demonstrated by scratch assays and Matrigel-embedded spheroid assays. In mouse models, FUK overexpression and L-fucose treatment resulted in slower tumor growth and fewer lung metastases. Assessment of human melanoma patient specimens in a tissue microarray revealed that primary tumors with low UEA-1 staining correlated with significantly lower probability of survival compared to primary tumors with high UEA-1 staining. Similarly, metastases exhibited significantly lower UEA-1 staining compared to primary tumors, suggesting that loss of α(1,2) fucosylation might promote melanoma metastasis.[128] It has been previously reported that approximately 25% of melanoma cell lines lack FUT1 expression.[126,149] Transfection of FUT1 to BL6 cells has been reported to inhibit the metastatic ability of these cells[142] suggesting that metastatic ability is suppressed by α(1,2) fucosylation and melanoma cells might reduce or eliminate FUT1 expression as a mechanism to promote tumorigenic properties. A siRNA screen for glycosyltransferases in melanoma cell lines found that the knockdown of FUT1 and 2 increased cell invasion. Further screening of primary and metastatic melanomas through fluorescent staining indicated that α(1,2) fucosylation is higher in primary tumors than in metastatic tumors.[121] This data

indicates that the loss of α(1,2) correlates with the progression of primary tumors to metastasis. A study in melanoma cell lines determined that the knockdown of FUT1 or 2 increases the invasive potential of the cells. Histological analysis of tumor samples found that α(1,2) fucosylation is reduced in metastatic tissues compared to primary tumors.[122] The current literature suggests that loss of α(1,2) fucosylation is important for melanoma tumor progression.

2.1.5 α(1,3/4) Branching

Compared to α(1,2) fucosylation, α(1,3/4) fucosylation has been shown to have a much more consistent effect on various cancer types. Studies comparing α(1,3/4) fucosylation in cancer and normal tissues have found that it is up regulated in breast[150,151], liver[148,152], ovarian[153,154], colorectal[141], pancreatic[155–157], gastric[158,159], lung[160], and prostate[161–163] cancers (Table 4). α(1,3/4) fucosylation conjugated by FUTs 3-7 & 9-11 has been shown to be enhanced in tumors and metastases in these cancer types.

A similar phenotype is found in melanoma. One study investigated the role of sLe^x in melanoma through the overexpression of FUT3 in melanoma cell lines. Moderate expression of sLe^x significantly increased the development of tumor nodules in the lungs compared to control transfected cells. Interestingly, cells that exhibited high expression of sLe^x died in the lung vasculature through Natural Killer cell rejection.[164] Several studies found that lung colonization and tumor growth of melanoma cells could be diminished by inhibiting selectin interaction with sLe^x through the use of peptide mimics.[165,166] E-selectin on epithelial cells has been implicated in several studies as the target of sLe^x. The overexpression of sLe^x antigen in multiple cancer types allows for stronger interactions with the endothelial lining of blood vessels demonstrated by slower rolling speed under shear forces, and promotes the ability of circulating tumor cells to extravasate from the blood vessel into the surrounding tissue[156,159,161,163,167]. In addition to enhancing sLe^x expression, several α(1,3/4) FUTs have been shown to alter cell surface signaling. α(1,3/4)

Table 4: Changes of Fucosylation in Cancer

Cancer Type	Changes in α(1,2) fucosylation	Reference
Melanoma	• α(1,2) fucosylation inhibits tumor formation • 25% of melanoma cell lines lack FUT1 expression • FUT1 expression is decreased in tumors • α(1,2) fucosylation inhibits invadopodia & invasion	128,142,143 126,149 121,128 143
Oral/Head & Neck	• α(1,2) fucosylation inhibits tumor formation • FUT1 expression is decreased in tumors • α(1,2) fucosylation high in tumors, lost at invading front	144
Gastric	• α(1,2) fucosylation inhibits tumor formation	145
Hepatocellular	• α(1,2) fucosylation inhibits tumor formation • FUT1 expression is decreased in tumors	147,148 148
Ovarian	• α(1,2) fucosylation is elevated through FUT1 overexpression	307
Prostate	• α(1,2) fucosylation is elevated through FUT1 overexpression • FUT1 expression is increased in tumors	308 308,309
Colorectal	• α(1,2) fucosylation increased in tumor tissues	141,310,311
Pancreatic	• α(1,2) fucosylation is elevated through FUT1 overexpression in primary tumors & lost in metastases	136,146

	Changes in α(1,3/4) fucosylation	Reference
Breast	• α(1,3/4) fucosylation upregulated in tumor tissue	150,151
Melanoma		164
Oral/Head & Neck		312
Liver		148,152
Ovarian		153,154
Prostate		161–163
Colorectal		141
Pancreatic		155–157
Gastric		158,159
Lung		160

	Changes in α(1,6) fucosylation	Reference
Breast	• Core fucosylation increased in tumor tissue	172,313
Melanoma		121
Liver		121,126,148,173
Ovarian		121,126,174,175
Colorectal		126,141,176,177
Pancreatic		157
Lung		181–183
Gastric	• Core fucosylation increased in tumor tissue • Core fucosylation decreased in tumor tissue	145,179 178,180
Prostate	• Core fucosylation increased in castrate resistant tissue	314
Thyroid Papillary Carcinoma	• Core fucosylation increased in tumor tissue	315–317

fucosylation of growth factor receptor signaling pathway such as TGFβ, VEGFA, EGF, and FGF2 have been implicated in promoting tumor development.[151,168,169] Inhibition of α(1,3/4) fucosylation impedes migration, proliferation, and MAPK activity. One of the consequences of TGFβ exposure is the induction of epithelial to mesenchymal transition (EMT), during which E-cadherin expression is diminished, and N-cadherin is elevated.[170] Loss of α(1,3/4) fucosylation by knockdown of FUT3/6 abrogates the loss of E-cadherin expression after TGFβ stimulation, thereby inhibiting EMT and preventing migration.[168] Additionally, enhanced α(1,3/4) fucosylation has been shown to decrease the expression of apoptotic proteins, such as procaspase-3, and increase the expression of anti-apoptotic proteins, such as pPKB and pBad, leading to an increased resistance to cell death.[171] Since multiple FUTs catalyze α(1,3/4) fucosylation, it is difficult to determine which are most important in tumor progression. Different FUTs have been implicated in various cancer types, indicating each cancer type might rely more on one FUT to catalyze sLe^x that is different from other cancer types. To this point, there have been few studies examining the role of α(1,3/4) fucosylation in melanoma, but studies that have been conducted agree with the literature published in other cancer types indicating that augmentation of α(1,3/4) fucosylation enhances tumorigenic and metastatic properties.

2.1.6 α(1,6) Branching

FUT8 is the only known transferase that conjugates L-fucose residues to core GalNAc monosaccharides on N-glycans. Studies investigating core fucosylation have been conducted in melanoma[121], breast[172], liver[121,126,148,173], ovarian[121,126,174,175], colorectal[126,141,176,177], pancreatic[157], gastrointestinal[145,178–180], and lung[181–183] cancers (Table 4). Many of the studies found that FUT8 expression is elevated in cultured cell lines and therefore found that loss of FUT8 inhibits invasion[121,173], migration[173,184], proliferation[173,183], colony formation[183], tumor growth[121,185,186], and metastasis[121,185]. Core

fucosylation is important in mediating EMT induced by TGFβ as knockdown of FUT8 attenuated TGFβ induced EMT and inhibited de-differentiation.[185,187] It has been demonstrated that core fucosylation of plasma membrane proteins such as β1-integrin[188], β-catenin[187,189], EGFR[186,188,190], c-Met[186], and E-cadherin[183,189] regulates activity and signaling. In melanoma, a siRNA screen found that the knockdown of FUT8 inhibits melanoma cell migration and invasion. By examining α(1,6) fucosylation in primary and metastatic tumors through fluorescent staining, it was determined that tumor metastases exhibit higher α(1,6) fucosylation than primary tumors. Knockdown of FUT8 in melanoma cells in murine xenograft models significantly inhibits lung metastases and metastatic tumor burden in the lung following flank and intracardiac injection. Glycomic analysis identified L1-CAM as a critically core fucosylated protein in melanoma metastasis, as once core fucosylation of L1-CAM is lost, L1-CAM is cleaved and inhibits melanoma cell invasion.[121] Another study in melanoma cell lines determined that the knockdown of FUT8 decreases invasion ability. Examination of α(1,6) fucosylation in histological samples determined that FUT8 is highly expressed in metastatic tissues.[122] As FUT8 is the only known transferase capable of conjugating core fucosylation to glycans, it might prove to be a valuable target for cancer therapy.

2.2 Methods

2.2.1 Cell culture

WM793 and WM245 melanoma cells were cultured in HyClone RPMI-1640 Media supplemented with 10% FBS and 1% Penicillin/Streptomycin. Cells were treated for 48 hours with 25μM or 50μM [L-fucose (Biosynth, F8060)] as indicated prior to experimentation.

2.2.2 Gelatin coated coverslips

Glass cover slips (Fisherbrand 18Cir.-1, 12-545-100) were acid washed overnight in 1M HCl at 60°C. After thorough rinsing with diH2O, coverslips were washed with 1xPBS and stored in 20% EtOH. To coat, coverslips were removed from 20% EtOH and washed with 1xPBS. After last wash was removed, 100μL of

0.2% bovine gelatin (Sigma, G9391) in 0.2M NaHCO3 was applied to each coverslip, and allowed to stand for 20 minutes. After three washes of 1xPBS, 100µL of 0.5% Glutaraldehyde (Sigma, S7776) was applied to each coverslip and allowed to stand for 15 minutes. Coverslips were then washed extensively (10x) in 1xPBS to remove any residual glutaraldehyde. After final wash, coverslips were set gelatin side up into 12-well plates and either used immediately, or stored at 4°C for future use.

2.2.3 Texas Red gelatin labeling and coating

The labeling and coating of Texas Red gelatin were performed was previously described[191,192] with modifications. A 2% gelatin solution was made in 0.2M NaHCO3 pH 8.3. Texas Red-X Succinimidyl Ester (Invitrogen, T6134) was dissolved DMSO (Fisherbrand, BP231) at a concentration of 10mg/mL. 50µL of the reactive dye solution was mixed into 1.5mL of the filtered gelatin and allowed to incubate for 1 hour at room temperature with continuous stirring, protected from light. Unbound dye was then removed using a HiTrap desalting column. Recovered gelatin was diluted 1:8 and protected from bacterial growth with 2mM sodium azide (Sigma, S2002), and stored at 4°C. Acid washed coverslips (see above) were removed from 20% EtOH and washed three times with 1xPBS. After final wash, 100µL of poly-D-lysine (Sigma, P6403) was applied to each coverslip and allowed to stand for 20 minutes. Following another three washes in 1xPBS, 100µL of glutaraldehyde was applied to each coverslip and allowed to stand for 15 minutes. After three more washes of 1xPBS, 80µL of Texas Red labeled gelatin was applied to each coverslip and allowed to stand, protected from light, for 10 minutes. Excess gelatin was reclaimed and recycled. Coverslips were washed three times with 1xPBS, then quenched with 100µL of 5mg/mL sodium borohydride (Sigma, 452882) and allowed to sit for 15 minutes. Coverslips were then set into 12-well plates with gelatin side up, and washed three times with 1xPBS, then stored at 4°C protected from light, or used immediately.

2.2.4 Proliferation assay

WM793 cells were plated into 12-well plates at equal densities in triplicate for each condition. After 4 hours, the media was changed on all plates, and one plate was washed once with 1xPBS and fixed with 10% buffered formalin as Day 0. At each 24-hour interval, another plate was washed and fixed. After plates were fixed for 5 days, cells were stained with crystal violet for 15 minutes. Plates were then washed in DI water until washes remained clear. The plates were then dried, inverted on paper towels overnight. Any residual water was aspirated. The cell bound stain was solubilized with 300µL 10% Glacial Acetic Acid per well, and placed on a shaker for 10 minutes. 50µL of each well was then transferred to a 96-well plate, and the absorbance read at 562nm.

2.2.5 cDNA constructs

The pLenti-GFP, pLenti-GFP-hFUK, pLKO, and pLKO-hFUK-shB3 constructs were generously provided by Dr. Eric Lau. The CTRL shRNA (SHC016-1EA) and hFUKsh37856 (TRCN0000037856) were obtained from Sigma. Human FUT1 was subcloned from the Harvard Plasmid Repository (HsCD00345675) to pLenti-CMV-blast empty as follows: hFUT1 was amplified with BamHI and XhoI cutting sites, as well as a C-terminal flag tag using sense primer 5'-ATCAG GATCCCATGTGGCTCCGGAGCCATCGTC-3' and antisense primer 5'-ACTCCTCGAGTCACTTGTCGTCATCGTCTTTGTAGTCAGGCTTAGCCAAT GTCC-3'. The amplified product and the pLenti-CMV-blast vectors were digested using BamHI and XhoI and run on a 1% agarose gel. Digested vector and hFUT1 were purified using Wizard® Plus SV Gel and PCR Clean-Up System (A9282). The purified products were ligated for 2 hours at room temperature, and transformed to DH5α bacteria, and plated to ampicillin^{+} LB agarose plates. Multiple colonies were picked the following day, and amplified for Midi Prep DNA generation.

2.2.6 Stable cell lines

HEK293T cells were used to package lentiviral particles as previously described.[193] Lentiviral vector cDNA (5µg) was combined with pSPAX (5µg), pMD2G (5µg) and polyethylenimine (Fisher, NC9197339) and

added dropwise to 10cm plates of 60% confluent 293T cells. After 48 hours, virus was collected after each 14 hour interval for 4 days. Virus containing media was first centrifuged at 3000g for 15 minutes at 4°C to spin down cellular debris, then ultracentrifuged at 20,000rpm for 2 hours at 4°C to pellet virus. Pellets were suspended in growth medium and snap frozen in LN2, then stored at -80°C for future use. Virus was then used to infect WM793 cells, and after 48 hours, cells were subjected to antibiotic selection. Surviving cells were verified of complete selection by fluorescent microscopy for the hFUK constructs, or western blotting for the hFUT1 constructs.

qPCR: The qPCR primers for hFUK are as follows:

hFUK Fwd: 5'-CTGTATCCAGGCCAGTCACC-3' Rev: 5'-CAGATTGTGCACTCCCAGGT-3'

GAPDH Fwd: 5'-TGAAGGTCGGAGTCAACGG-3' Rev: 5'-AGAGTTAAAAGCAGCCCTGGTG-3'

WM793 cells were seeded at $5x10^5$ cells in 6cm plates and allowed to incubate overnight. The following day, plates were washed once with 1xPBS and total RNA was isolated using Qiagen RNeasy kit (Cat#74106). Two micrograms of total RNA was used for reverse transcription. cDNA was diluted 1:10 and used for qPCR with Power SYBR1Green PCR Master Mix (Applied Biosystems, 4367659).

2.2.7 Invadopodia assay

WM793 cells were plated to 6cm dishes and allowed to grow for 48 hours. Parental WM793 cells were treated with 25µM L-fucose or control water. Plates were washed once with 1xPBS and cells dissociated using enzyme free cell dissociation solution (Millipore, S-004-C). Cells were seeded to gelatin coated coverslips at $1x10^5$ cells per coverslip and allowed to incubate for 4 hours. Coverslips were then washed once with 1xPBS and fixed using fresh 4% paraformaldehyde (Sigma, 158127) for 20 minutes at room temperature. Cells were then stained with fluorescent phalloidin stains (Alexa Fluor phalloidin-488, -594, and -647) based on the experimental conditions, and imaged for quantitation using wide-field microscopy. Samples were imaged using an Axiovert S100 upright microscope through a 63x/1.3 FLUAR Plan Apochromatic oil immersion objective. An attached Axiocam 503 mono charge-coupled camera and ZEN

2.3 blue edition (Zeiss) software were used to capture images. For representative images, samples were imaged using a Leica SMI8 inverted microscope, TCS SP8 confocal scanner, and a HC PL APO 63x/1.4 CS2 oil immersion objective. The 488, 552, and/or 638 STED lasers were used to excite the samples, and a tunable acousto-optical beam splitter was used to minimize crosstalk between fluorochromes. Sample emission was captured with Leica HyD hybrid detectors and images were prepared with the Leica Application Suite X. To calculate percent degraded gelatin, ImageJ software (NIH) was used to determine total cell area in pixels. The suspected area of degradation was then duplicated, converted to 32-bit, and the threshold was set. Using the measure function, the percent area of selection that was degraded was calculated. The percent of the degradation of the gelatin under the entire cell was then calculated by multiplying the percent of degradation in the selected area by the total area of selection, then dividing by the entire cell area.

2.2.8 Invadopodia precursor assay

WM793 cells were plated at $1x10^5$ cells per coverslip and allowed to settle for 1 hour in complete RPMI. After 1 hour, cells were washed once with 1xPBS, and 1mL of 1% FBS RPMI (starvation media) was added to each well. The cells incubated for 18 hours, then FBS was added to the media to make up to 10% FBS for each well. Coverslips were fixed in 4% PFA every 15 minutes and images for quantitation and representation were acquired as mentioned.

2.2.9 Fucosidase treatment

After cell dissociation using enzyme free solution, cells were washed three times in 1xPBS, then incubated in PBS with 0.08U/mL fucosidase (New England Biolabs, α(1,2):P0724S, α(1,3/4):P0769S) for 30 minutes at 37°C. Next, cells were washed three times in 1xPBS, then used in further experiments.

2.2.10 Flow cytometry

Cells were harvested using enzyme free dissociation media, washed once with 1xPBS, and incubated with 1x PKH26 (Sigma, MINI26) for 1 minute at room temperature. Next, cells were washed three times in

1xPBS, then fixed in 2% paraformaldehyde in PBS for 45 minutes at room temperature and protected from light. Cells were then washed once with 1xPBS and blocked with 0.2% IgG- and protease-free BSA (Jackson ImmunoResearch, 001-000) for 30 minutes at room temperature. Cells were washed twice in 1xPBS and stained with 0.2µg/mL FITC-UEA-1 (Vector Labs, FL1061) for 1 hour at room temperature and protected from light. After two more washes with 1xPBS, cells were analyzed by flow cytometry. For levels of FITC-UEA-1 staining. FITC-UEA-1 staining levels were calculated as a ratio of the median UEA-1 values divided by median PKH26 values (where each condition was relative to the control). For flow cytometric experiments using GFP-EV- or GFP-FUK-expressing cells, the cells were harvested as above, divided in half for staining with PKH26 or with TRITC-UEA1 (EY Labs, R-2201-2) and analyzed by flow cytometry as described above.

2.2.11 Western blotting

Cells were seeded to 6cm plates at $5x10^5$ cells per plate and allowed to incubate overnight. The following day, plates were washed once with ice cold 1xPBS, then lysed with a rubber policeman and ice cold RIPA buffer (150mM NaCl, 5mM EDTA, 50mM Tris pH 8.0, 1% NP-40) with 1mM phosphatase (ThermoScientific, 88667) and 1mM protease (Roche, 04693159001) inhibitor cocktails added. The following antibodies were used: FLAG (Sigma, F3165) at 1:5000 dilution in 5% BSA (Fisher, BP1600) in TBST; GAPDH (Sigma, G8795) at 1:5000 dilution in 5% BSA in TBST.

2.2.12 Bioinformatics

FUT1 and FUT2 mRNA expression data was retrieved from 5 previously published microarray datasets (GSE84 01, GSE46517, GSE 7553, GSE15605 and GSE3189).[194–197] The expression level data of FUT1 (probeset 206109_at) and FUT2 (probeset 208505_s_at) were plotted as scatted dot plot using Graphpad Prism 7.0 and the statistical analysis was performed using two samples, two-tailed t-test.

2.2.13 Matrigel invasion assay

Matrigel invasion by WM793 cells was performed using invasion Boyden chamber (8µm) as described previously.[191,192,198,199]

2.3 Results

2.3.1 L-fucose treatment inhibits invadopodia formation and extracellular matrix degradation

There have been a number of studies that have investigated the effect of L-fucose and L-fucose-containing extracts, termed fucoidan, in breast[200–205], lung, colorectal[203,206–208], and melanoma[128,209] cancers. In each of these studies, L-fucose or fucoidan significantly attenuated tumor growth and metastasis *in vivo*, and inhibited cell proliferation, migration, invasion, and colony formation *in vitro*. Our laboratory was particularly interested in melanoma. Although the study conducted by Lau et. al.[128] determined that melanoma progression was promoted by the inhibition of FUK, whether the manipulation of FUK or L-fucose treatment affects invasive structures that tumor cells utilize to metastasize, particularly invadopodia, is not known. Since FUK expression is suppressed in invasive and metastatic melanoma cells, and L-fucose supplementation inhibited melanoma metastasis, we examined the effects of L-fucose treatment on invadopodia formation. We have previously demonstrated that the

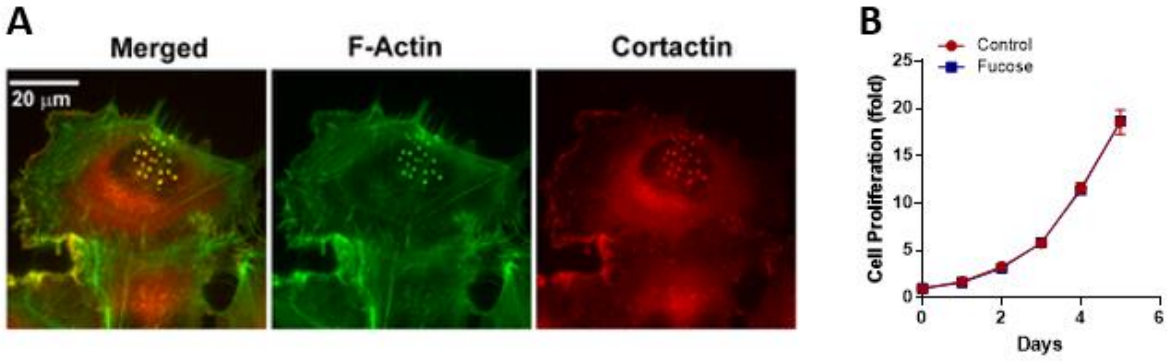

Figure 2-1: L-fucose treatment does not affect WM793 cell proliferation. A, Representative images showing invadopodia in WM793 cells revealed by F-actin and cortactin double staining. **B**, the effect of L-fucose treatment on WM793 cell proliferation.

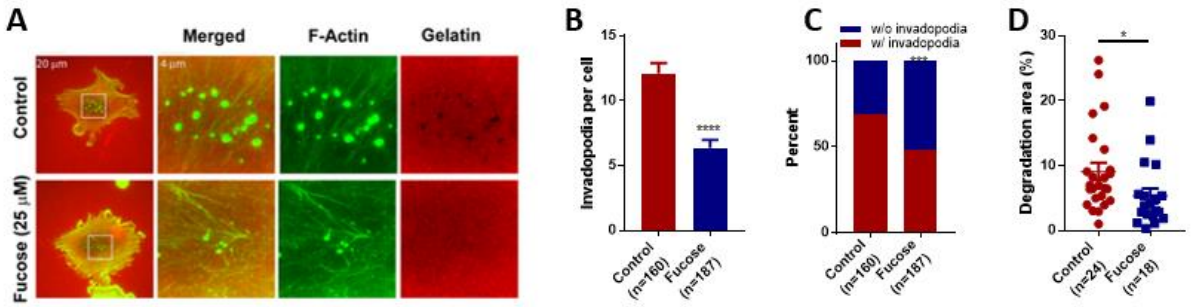

Figure 2-2: Fucose treatment inhibits invadopodia formation and ECM degradation. A, representative invadopodia assay images showing the effects of 25μMLfucose treatment on the formation of invadopodia and degradation of TexasRed labeled gelatin by WM793 cells. **B-D**, quantitation of the effect of fucose treatment on the average invadopodia number per cell (**B**), proportion of invadopodia-positive WM793 cells (**C**) and gelatin degradation area by WM793 cells (**D**). *, *** and **** indicate p<0.05, 0.001 and 0.0001, respectively. The p values were determined by two tailed, two sample t-test (in **B, D**) or two-tailed Fisher exact test (**C**). Numbers in parenthesis indicates the number of cells used in quantitation. Representative results from at least three independent replicates were presented.

WM793 melanoma cell line is an excellent model to study invadopodial regulation.[191] When plated on gelatin coated glass coverslips under normal growth condition, approximately 70% of WM793 cells were able to assemble arrays of robust invadopodia generally in areas underneath the nuclei.[191] These invadopodial puncta are cortactin and F-actin positive protrusions on the ventral site of the cell (Fig. 2-1A), and are able to degrade fluorescently labeled gelatin[191]. L-fucose treatment had no effect on the proliferation of WM793 cells (Fig. 2-1B). However, when pre-treated with 25 μM L-fucose for 48 hours, the average numbers of invadopodia per cell was decreased by approximately 50% compared to vehicle control (dH_2O)-treated WM793 cells (Fig. 2-2A and 2-2B). The percentage of invadopodia-positive cells was also decreased from ~70% in control cells to ~40% in L-fucose treated cells (Fig. 2-2C). To determine how the degradative capacity of invadopodia was affected by L-fucose, we further evaluated the effects of L-fucose-treatment on the degradation of fluorescence-labeled gelatin. The degradation of gelatin by invadopodia would leave black dots on a bright fluorescence background. Indeed there was a significant decrease in gelatin degradation in the L-fucose treated cells (Fig. 2-2A and 2-2D.). The inhibition of gelatin degradation by L-fucose treatment was also observed in WM245, a melanoma cell line derived from radial growth phase melanoma (Fig. 2-3A). Taken together, our data indicate that the number and degradative capability of invadopodia are inhibited by L-fucose treatment.

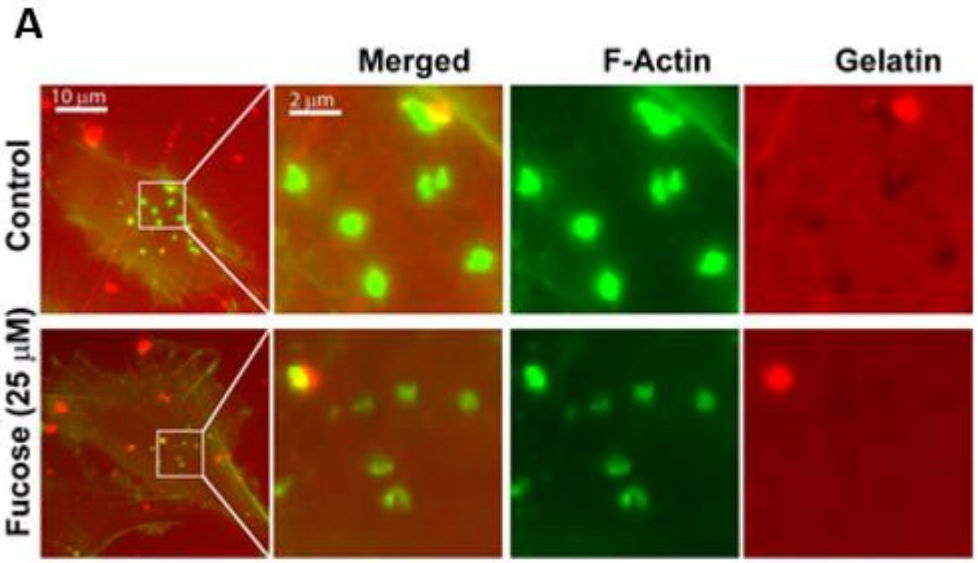

Figure 2-3: L-fucose treatment inhibits invadopodia formation and ECM degradation in WM245 cells. A, representative images showing the effects of L-fucose treatment on invadopodia formation and gelatin degradation in WM245 melanoma cells.

2.3.2 Overexpression of FUK abrogates invadopodia formation and delays invadopodia initiation

To determine whether activation of the fucose salvage pathway is sufficient to inhibit invadopodia formation, we ectopically expressed hFUK in WM793 cells. The expression of FUK was verified by qPCR (2-4A). The expression of FUK increased the fucosylation of cell surface proteoglycans without affecting cell proliferation (Fig 2-4B to 2-4D). The control and FUK OE cells were seeded to gelatin coated coverslips and the formation of invadopodia was determined by phalloidin staining. Similar to L-fucose treatment, we found that the ectopic expression of FUK resulted in about 50% drop in average invadopodia per cell (Fig 2-5A and 2-5B). Additionally, the proportion of invadopodia positive cells was reduced by about 40% in FUK OE group (Fig 2-5C). We also found that the overexpression of FUK attenuated the degradative ability of invadopodia in WM793 cells (Fig 2-5D). Taken together, our data indicate that augmenting the fucose salvage pathway by ectopic expression of FUK is sufficient to inhibit invadopodia formation and ECM degradation.

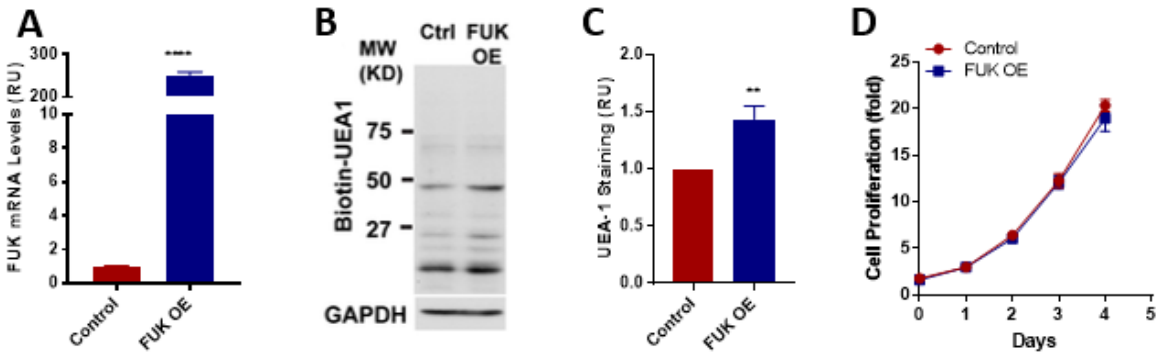

Figure 2-4: The ectopic expression of FUK in melanoma cells promotes cell surface fucosylation. A, qPCR analysis of WM793 cells following infection with an hFUK overexpression vector. **B**, the effect of FUK overexpression on the fucosylation of WM793 cell surface proteoglycans. The plasma membrane proteins from control and FUK OE WM793 cells were separated using SDS-PAGE and detected by biotin-UEA1. **C**, the effect of FUK overexpression on cell surface fucosylation as detected by UEA1 staining and flow cytometry. **D**, the effect of FUK overexpression on WM793 cell proliferation. ** and **** indicates $p<0.01$ and $p<0.0001$, as determined by two-tailed, two sample t-test.

To understand the mechanism by which the fucose salvage pathway regulates invadopodia, we determined the effects of ectopic FUK expression on invadopodial initiation. WM793 cells were starved in 1% FBS overnight to reduce the basal invadopodial assembly. The cells were then stimulated with 10% FBS and the extents of FBS-induced invadopodial formation were quantified at indicated time points over one hour (Fig 2-6A). We found that FBS stimulation remarkably induced invadopodial formation in control cells, as we previously reported.[191] In contrast, FBS-induced invadopodia initiation was significantly inhibited in WM793 cells expressing ectopic FUK (Fig 2-6A), suggesting that the fucose salvage pathway in melanoma regulates invadopodial initiation.

2.3.3 FUK is required for L-fucose-mediated inhibition of invadopodia formation

As the phosphorylation of L-fucose by FUK is a crucial first step in the generation of GDP-L-fucose for fucosylation, we next investigated whether FUK is required for L-fucose-mediated inhibition of invadopodia formation. By combining 2 shRNA targeting hFUK, we were able to reduce the mRNA transcript levels of FUK in WM793 by about 70% (Fig 2-6B). To determine whether FUK is required for L-fucose-mediated inhibition of invadopodia formation, control or FUK knockdown WM793 cells were

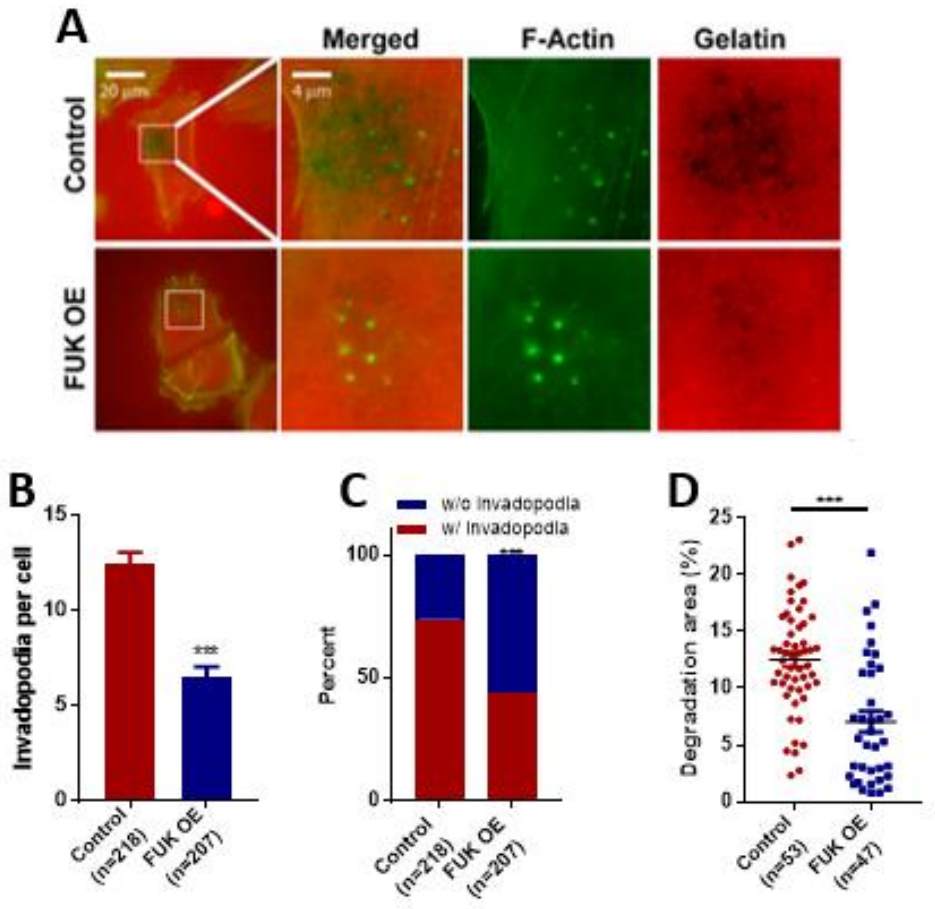

Figure 2-5: The ectopic expression of FUK in melanoma cells inhibits invadopodia formation and gelatin degradation. A, representative images showing the effects of ectopically expressed FUK on invadopodia formation and TexasRed gelatin degradation in WM793. **B** and **C**, quantitation of the effect of ectopically expressed FUK on the invadopodia number per cell (**B**) and the proportion of invadopodia positive cells (**C**) in WM793. **D**, quantitation of the effects of FUK overexpression on gelatin degradation. *** indicates $p<0.001$, as determined by two-tailed, two sample t-test (**B** & **D**) or two-tailed Fisher's exact test (**C**). Numbers in parentheses indicates the number of cells used in quantitation. Representative results from at least three independent replicates were presented.

incubated for 48 hours with 20μM L-fucose, and then the effect of L-fucose treatment on invadopodia formation were evaluated by phalloidin staining. As shown in Figs 2-6C and 2-6D, FUK knockdown itself has no significant effect on invadopodia formation. However, the depletion of FUK significantly reduced the L-fucose-mediated inhibition (Fig 2-6C and 2-6D). Taken together, our data suggests that FUK is essential for L-fucose-mediated inhibition of invadopodia assembly.

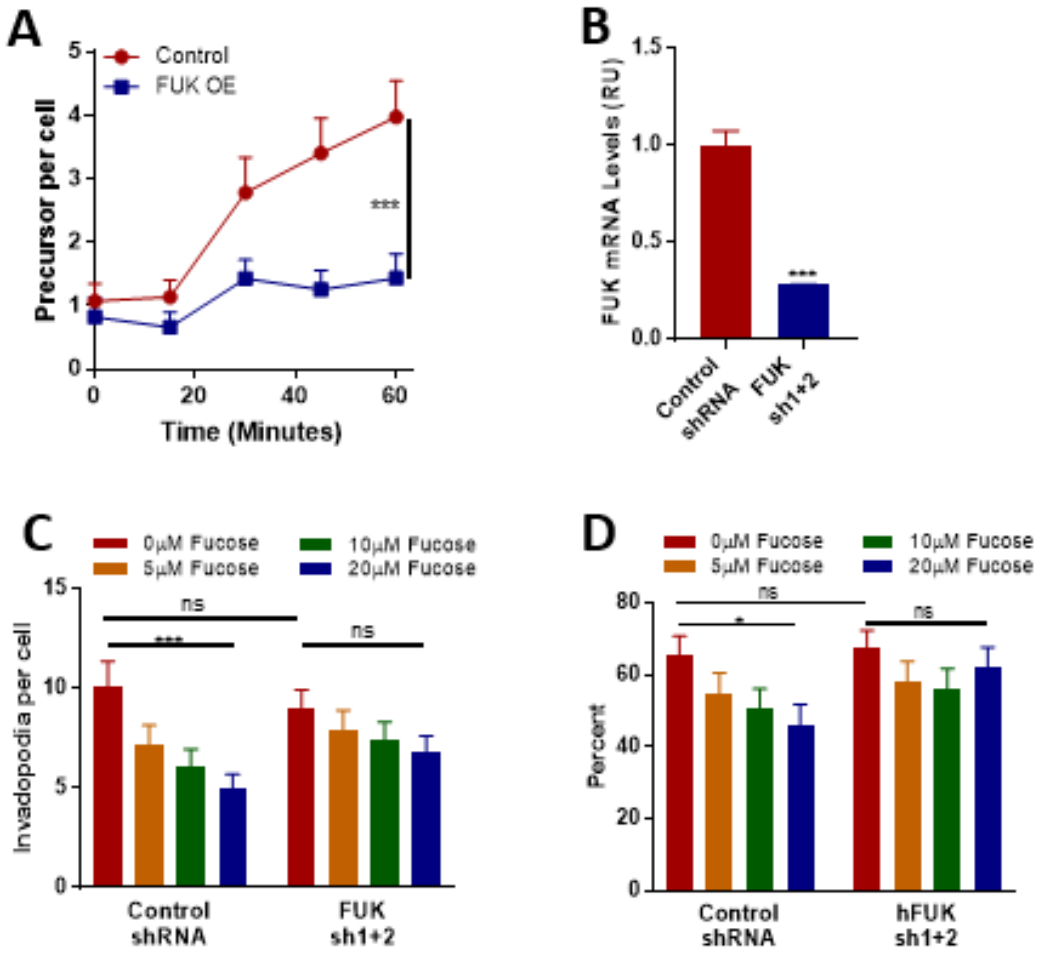

Figure 2-6: The ectopic expression of FUK in melanoma cells delays invadopodial initiation. A, the effects of ectopic FUK on the initiation of the assembly of invadopodia induced by 10% FBS. **B**, qPCR assay showing the effects of FUK sh1+sh2 on the mRNA transcript levels of FUK in WM793 cells. **C**, quantitation of the effects of FUK knockdown on L-fucose-mediated inhibition of invadopodia formation at increasing concentrations of L-fucose in WM793 cells. **D**, percentages of cells exhibiting invadopodia following FUK knockdown in titrated concentrations of L-fucose. * and *** indicates $p<0.05$ and $p<0.001$, as determined by two-tailed, two sample t-test (**B-D**). Representative results from at least three independent replicates were presented.

2.3.4 α(1,2) fucosylation is responsible for the inhibition of invadopodia formation by L-fucose

We noted that the L-fucose- and FUK-mediated inhibition of invadopodia was abrogated when cells were lifted with trypsin instead of by protease-free dissociation methods. We reasoned that the neutralization of fucosylation effects by trypsin digestion might be due to proteolysis of fucosylated transmembrane proteins. To determine whether plasma membrane protein fucosylation is mediating the inhibition of invadopodia formation, we used fucosidase to remove the fucosylation of cell surface proteoglycans. Proteoglycans can be modified by α(1,2), α(1,3) or α(1,4) branched fucosylations (Fig 2-

Figure 2-7: α(1,2) fucosidase, but not α(1,3/4) fucosidase cleaves cell surface α(1,2) fucosylation. A, schematic illustration showing the modification of glycans by α(1,2), α(1,3) and α(1,4) branched fucosylations. **B,** the effects of L-fucose and fucosidase treatment on cell surface α(1,2) fucosylation, as determined by UEA-1 staining and flow cytometry.

7A). Control or L-fucose-treated WM793 cells were lifted from the plates using protease-free dissociation buffer and incubated with fucosidase to remove branched fucosylation, and the effects of fucosidase treatments on cell-surface α(1,2) fucosylation were evaluated by UEA-1 lectin staining. As shown in Fig 2-7B, L-fucose treatment increased cell surface UEA-1 staining, suggesting an increase in α(1,2) L-fucose linkages. The increase in UEA-1 staining was abrogated by treatment with α(1,2) fucosidase (but not with α(1,3/4) fucosidase), confirming the specificity of fucosidase treatment and UEA-1 staining (Fig 2-7B). Interestingly, treatment with α(1,2) fucosidase sufficed to completely abrogate the inhibition of invadopodia by L-fucose (Fig 2-9A-2-9D). To determine whether FUK-mediated inhibition of invadopodia was dependent on α(1,2) fucosylation, we treated control of FUK OE WM793 cells with α(1,2) fucosidase. The treatment with α(1,2) fucosidase partially rescued the inhibition of invadopodia formation by FUK (Fig 2-8A-2-8E). The removal of α(1,2) fucosylation by fucosidase also restored the proportion of invadopodia-positive cells in FUK OE group. In contrast, the treatment with α(1,3/4) fucosidase did not rescue invadopodia formation in L-fucose-treated or FUK-overexpressing WM793 cells (Fig 2-10A-2-11D), suggesting that the inhibition of invadopodia by the fucose salvage pathway is mediated by cell surface α(1,2) fucosylation but not by the α(1,3/4) fucosylation.

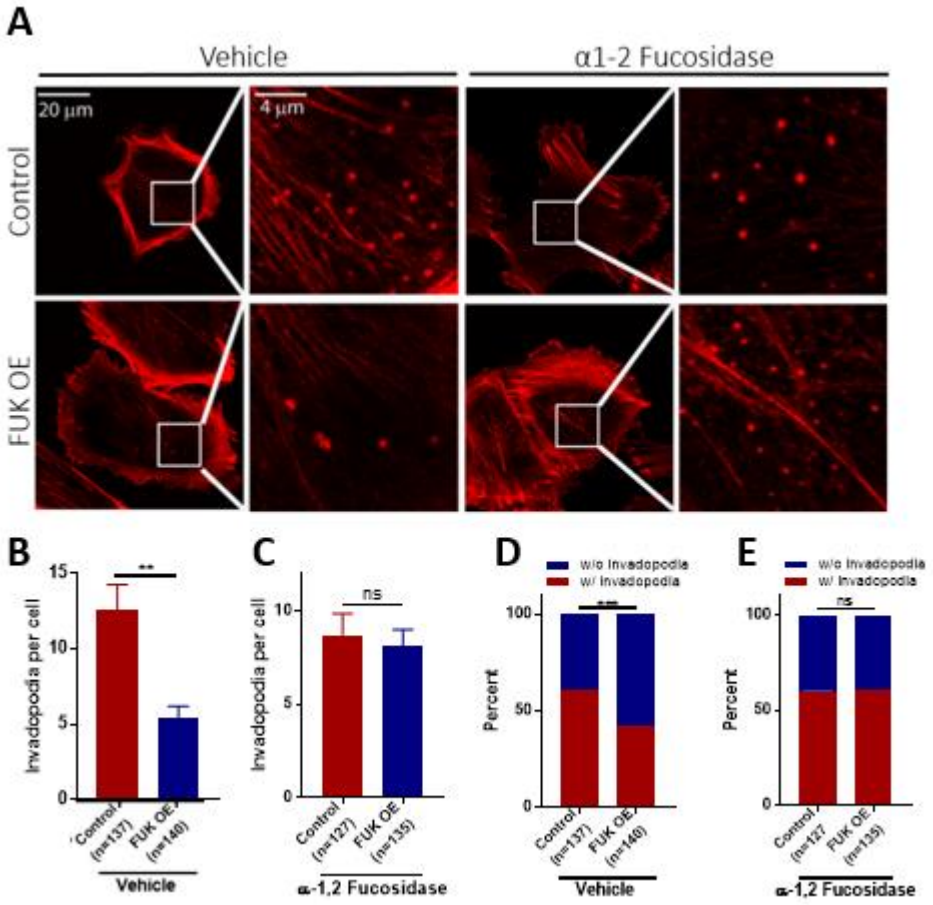

Figure 2-8: The fucose salvage pathway inhibits invadopodia through α(1,2) fucosylation. A, representative invadopodia assay images showing the effect of α(1,2) fucosidase treatment on FUK-mediated inhibition of invadopodia formation in WM793 cells. **B-E**, quantitation of the effect of α(1,2) fucosidase treatment on the invadopodia number per cell (**B & C**) and the proportion of invadopodia positive cells (**D & E**) in control or FUK OE WM793 cells. ** and *** indicates $p<0.01$ and 0.001, respectively, as determined by two-tailed, two sample t-test (**B, C**) or two-tailed Fisher's exact test (**D, E**). ns, not statistically significant. Numbers in parentheses indicates the number of cells used in quantitation. Representative results from at least three independent replicates were presented.

Fucosyltransferase 1 and 2 (FUT1 and FUT2) are the fucosyltransferases responsible for the transfer of L-fucose to glycans via α(1,2) linkages and has been shown to be involved in inhibition of melanoma cell migration and adhesion.[195] We examined the changes of FUT1 and FUT2 expression levels during melanoma progression in five previously published datasets (GSE8401, GSE46517, GSE 7553, GSE15605 and GSE3189).[194–197] As shown in Fig 2-12A, FUT1 mRNA levels were downregulated in malignant melanoma when compared to benign nevi or normal skin from human patients (Fig 2-12A). The levels of FUT1 were further suppressed in metastatic melanoma when compared to primary melanoma

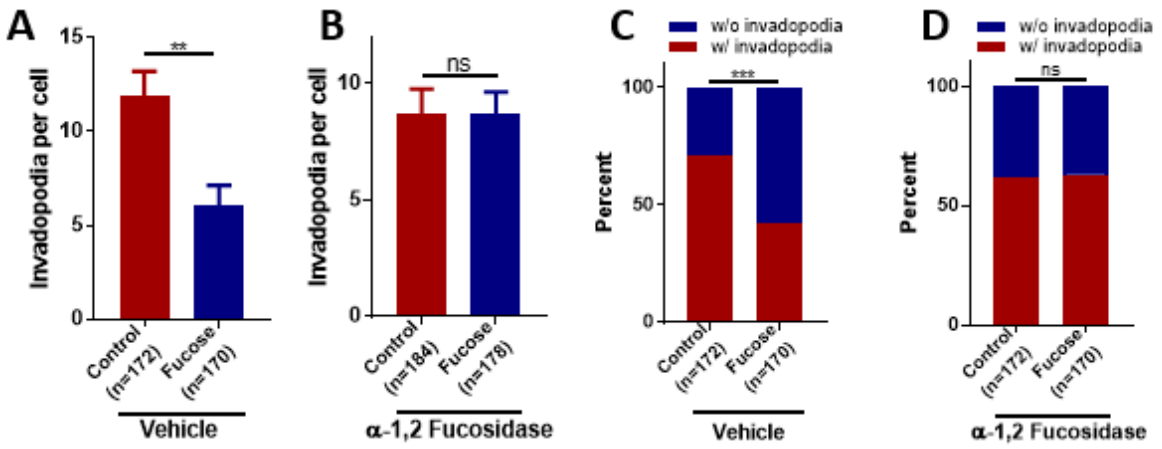

Figure 2-9: L-fucose treatment inhibits invadopodia through α(1,2) fucosylation. A-D, quantitation of the effect of α(1,2) fucosidase treatment on the invadopodia number per cell (**A & B**) and the proportion of invadopodia positive cells (**C & D**) in control or L-fucose treated WM793. ** and *** indicates p<0.01 and 0.001, respectively, as determined by two-tailed, two sample t-test (**A, B**) or two-tailed Fisher's exact test (**C, D**). ns, not statistically significant. Numbers in parentheses indicates the number of cells used in quantitation. Representative results from at least three independent replicates were presented.

(Fig 2-12A). In contrast, there was no clear correlation between FUT2 mRNA levels and melanoma progression in these datasets. Although in some datasets there appeared to be down-regulation of FUT2 mRNA in metastatic melanoma when compared to primary melanoma (GSE46517, GSE15605), in other datasets there was either no changes or increases in FUT2 expression with melanoma progression (GSE8401, GSE7553, GSE3189). Therefore, to further evaluate whether α(1,2) fucosylation is sufficient to inhibit invadopodia, we ectopically expressed Flag-tagged FUT1 in WM793 cells (Fig 2-13A). As shown in Fig 2-13B and 2-13C, ectopic expression of FUT1 resulted in approximately 50% reduction in the average number of invadopodia when compared to the vector control cells (Fig 2-13C). Additionally, analysis of the percentage of cells that presented invadopodia showed an approximate 40% reduction in the cells overexpressing FUT1 as compared to the empty vector control cells (Fig 2-13D). In line with the previous experiments, FUT1 overexpression also inhibited the Matrigel invasion activity of WM793 (Fig 2-13E and 2-13F), suggesting that α(1,2) fucosylation mediated by FUT1 is sufficient to inhibit invadopodia formation and melanoma invasion.

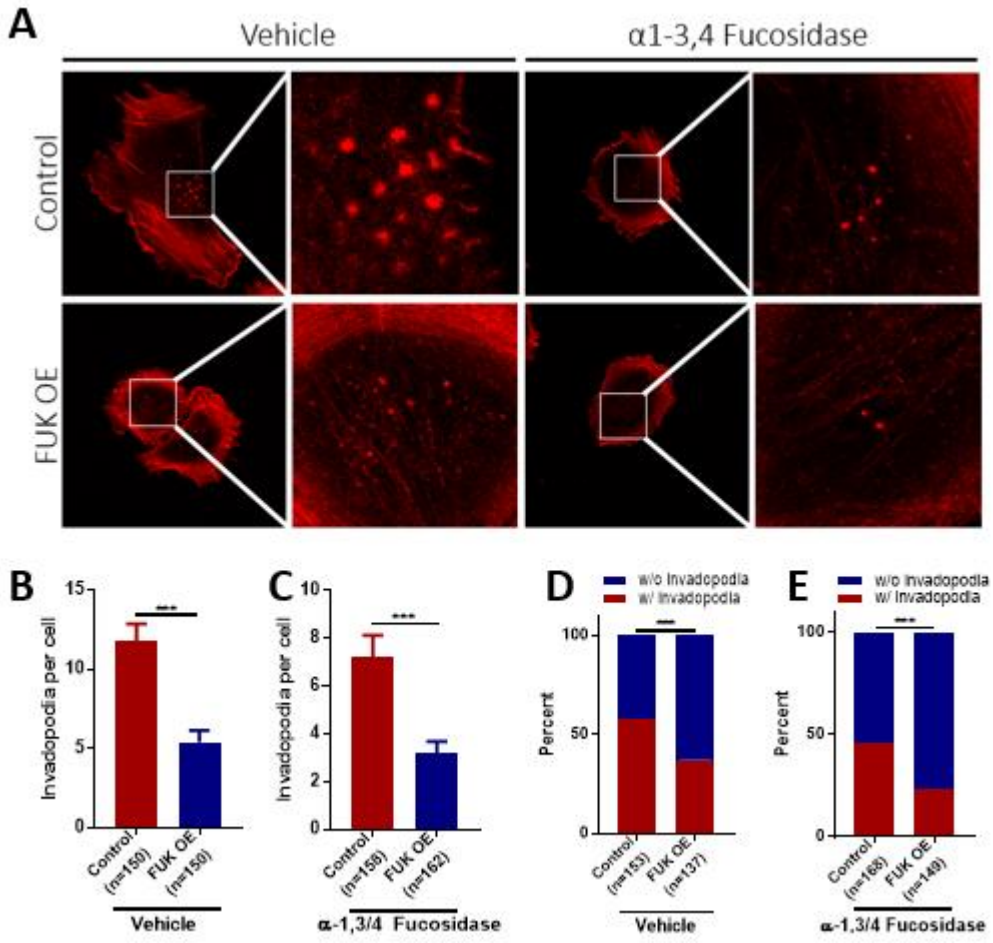

Figure 2-10: α(1,3/4) fucosidase cannot rescue invadopodia formation in FUK overexpression cells. A, representative invadopodia assay images showing the effect of α(1,3/4) fucosidase treatment on FUK-mediated inhibition of invadopodia formation in WM793 cells. **B-E**, quantitation of the effect of α(1,3/4) fucosidase treatment on the invadopodia number per cell (**B & C**) and the proportion of invadopodia positive cells (**D & E**) in control or FUK OE WM793. *** indicates 0.001, respectively, as determined by two-tailed, two sample t-test (**B, C**) or two-tailed Fisher's exact test (**D, E**). ns, not statistically significant. Numbers in parentheses indicates the number of cells used in quantitation. Representative results from at least three independent replicates were presented.

2.4 Discussion

The differential deregulation of fucosylation has been correlated with tumorigenesis and tumor progression in various cancers.[126,128,142,210,211] More recently, a systemic glycomics study suggested that the role of glycosylation in melanoma progression could be linkage dependent.[121]

The activity of FUK in catalyzing the crucial phosphorylation of L-fucose in the salvage pathway is reportedly attributable for up to 40% of total cellular fucosylation[128,212]. In metastatic melanoma, although the expression of FUK is suppressed by the PKCε-ATF2 pathway, the ectopic expression of FUK or

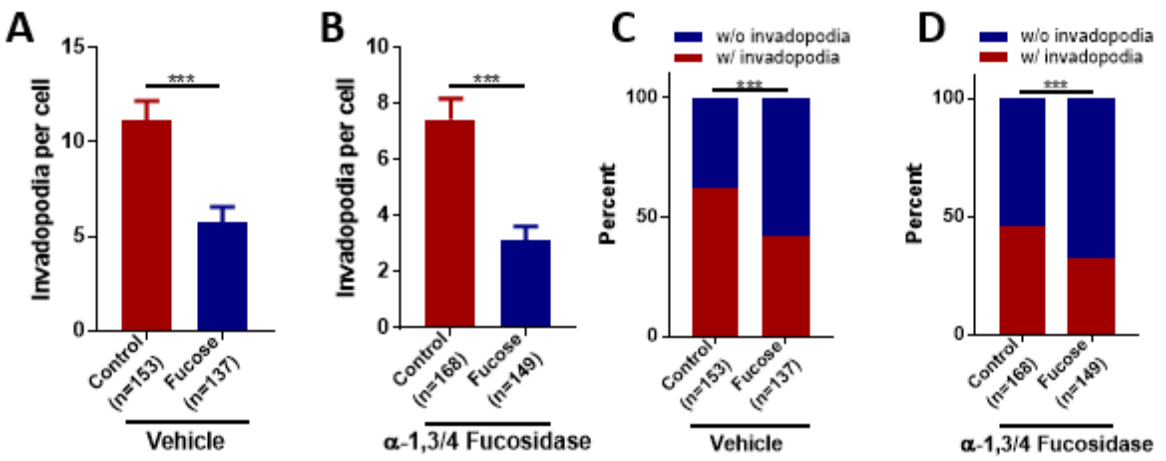

Figure 2-11: L-fucose mediated invadopodia inhibition cannot be rescued by α1(3,4) fucosidase. A-D, quantitation of the effect of α(1,3/4) fucosidase treatment on the invadopodia number per cell (**A & B**) and the proportion of invadopodia positive cells (**C & D**) in control or L-fucose treated WM793. *** indicates p<0.001, as determined by two-tailed, two sample t-test (**A, B**) or two-tailed Fisher's exact test (**C, D**). ns, not statistically significant. Numbers in parentheses indicates the number of cells used in quantitation. Representative results from at least three independent replicates were presented.

treatment with L-fucose significantly inhibits melanoma cell migration/invasion in vitro and lung metastasis in mouse models. These data indicate that the FUK-mediated salvage pathway represents an important determinant of invasive/metastatic capacity and therapeutically actionable target for suppressing melanoma.

However, the mechanisms by which FUK and the fucose salvage pathway regulates melanoma progression are not completely understood. Here, we present evidence that the ectopic expression of FUK and L-fucose treatment inhibit the formation and the proteolytic activities of invadopodia, suggesting that the fucose salvage pathway might control melanoma invasion through invadopodia-mediated ECM remodeling. It is interesting to note that the depletion of FUK in WM793 melanoma cells at least partially abrogated the L-fucose-mediated inhibition of invadopodia formation, suggesting that the downregulation of FUK in metastatic melanoma might desensitize melanoma cells to the anti-metastatic effects of L-fucose. FUK overexpression and L-fucose treatment similarly inhibit invadopodia in melanoma cells. However, in some experiments it appeared that L-fucose treatment might decrease invadopodial

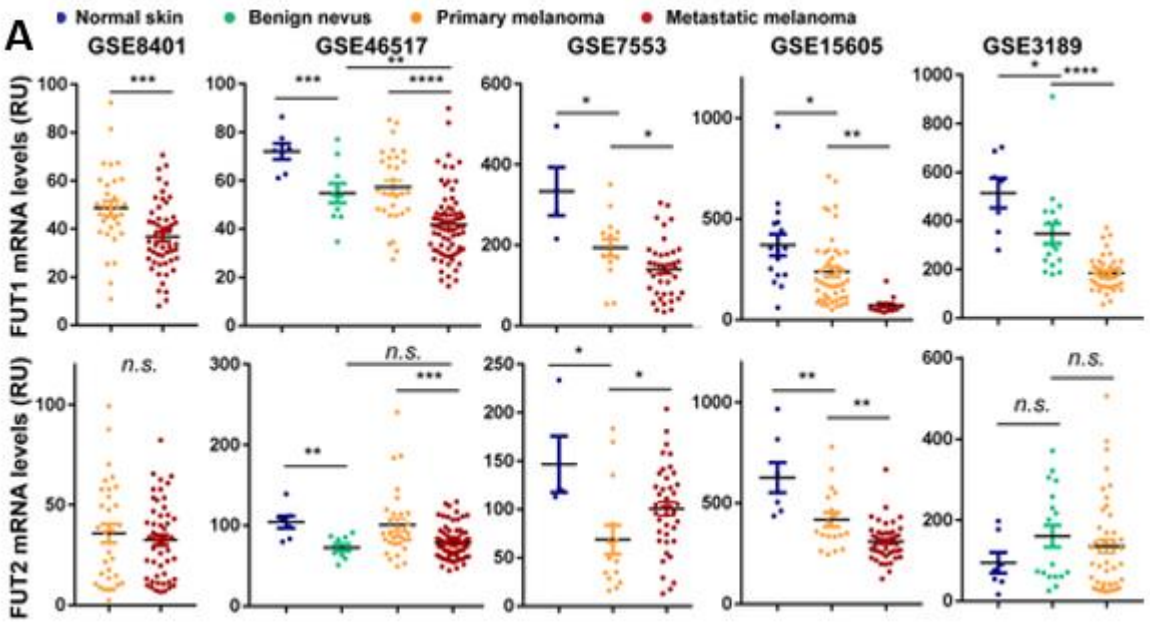

Figure 2-12: FUT1 mRNA expression, but not FUT2 mRNA expression is downregulated in advancing stages of melanoma. **A**, comparing the expression levels of FUT1 and FUT2 mRNA in normal skin, benign nevi, primary melanoma and metastatic melanoma in five microarray datasets. *, *** and **** indicates p< 0.05, 0.001 and 0.0001, as determined by two-tailed, two sample t-test.

size (Fig 2-2A and 2-3A), while FUK overexpression might result in larger invadopodia. The underlying mechanism and potential significance for such difference remained to be determined.

Core-fucosylation (α(1,6) fucosylation) catalyzed by FUT8 is highly elevated in metastatic melanoma, and promotes melanoma progression and metastasis by regulating L1CAM cleavage and L1CAM-mediated invasion.[121] In contrast, α(1,2) branched fucosylation of glycans attenuates melanoma growth and metastasis[121,128], suggesting that the modification of glycans by different fucosyltransferases might have drastically different functional consequences. Treatment of melanoma cells with α(1,2) fucosidase but not α(1,3/4) fucosidase sufficed to abrogate the inhibition of invadopodia by L-fucose and FUK, suggesting the inhibitory effects of the fucose salvage pathway are mediated through the α(1,2) fucosylation of plasma membrane glycans. The ectopic expression of FUT1, an α(1,2) fucosyltransferase, sufficed to recapitulate the inhibition of invadopodia assembly and ECM degradation, further supporting this notion. It is interesting to note that the expression of FUT1 and FUT2, the two α(1,2)

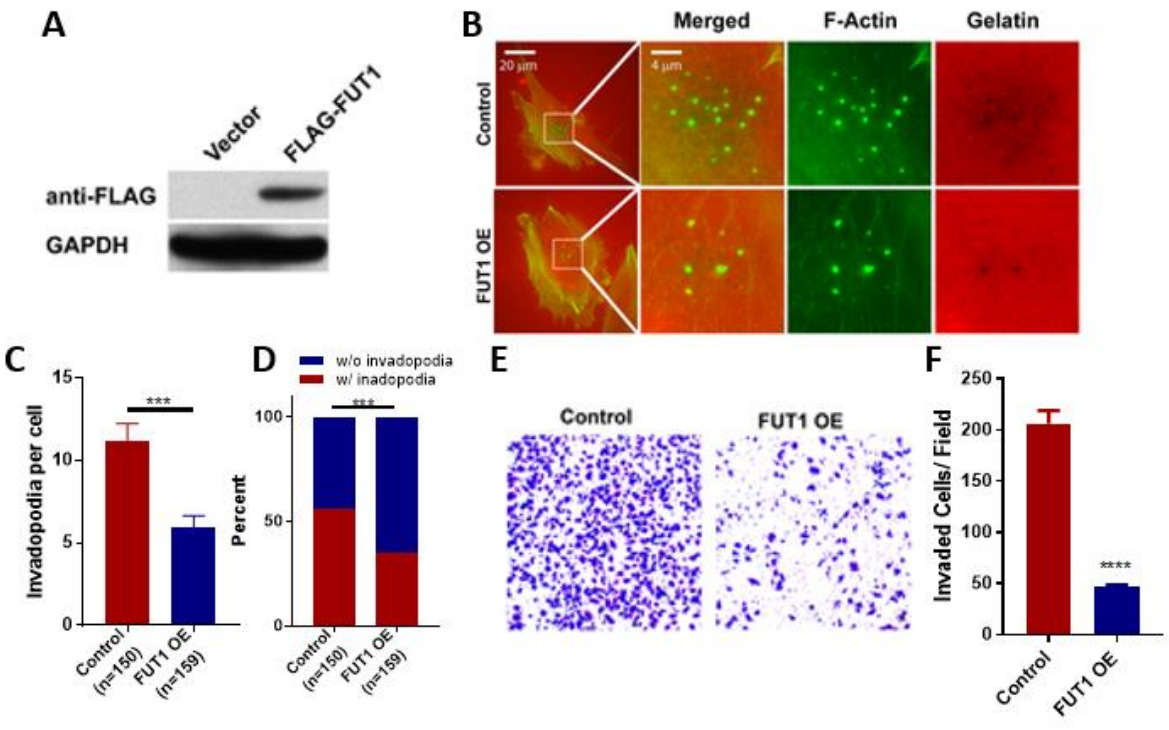

Figure 2-13: The ectopic expression of α(1,2) fucosyltransferase FUT1 inhibits invadopodia in WM793 cells. A, the ectopic expression of Flag-FUT1, as determined using anti-FLAG Western blotting. **B,** representative invadopodia assay images showing the effect of ectopically expressed FUT1 on invadopodia formation and gelatin degradation in WM793 cells **C and D,** quantitation of the effect of ectopically expressed FUT1 on the invadopodia number per cell (**C**) and the proportion of invadopodia positive cells (**D**) WM793. **E** and **F,** representative images (**E**) and quantitation data (**F**) showing the effects of FUT1 overexpression in WM793 cells on Matrigel invasion. ******* and ******** indicates 0.001 and 0.0001, as determined by two-tailed, two sample t-test (**C, F**) or two-tailed Fisher's exact test (**D**). Numbers in parentheses indicates the number of cells used in quantitation. Representative results from at least three independent replicates were presented.

fucosyltransferases, are suppressed during melanoma progression[121], and the levels of α(1,2) fucosylation are inversely correlated with the survival of melanoma patients.[128] Although all fucosyltransferases use GDP-L-fucose as fucosylation donors, it is possible that the fucose salvage pathway might preferentially provide GDP-L-fucose for certain fucose transferases through compartmentalization or spatial-temporal regulation.

There are several plasma membrane proteins that might lead to the inhibition of invadopodia when modified by α(1,2) fucosylation. One such protein is CD44. CD44 is a multifunctional cell surface adhesion receptor that interacts with various components of the ECM including hyaluronan, ostepontin, collagens and MMP-9.[110,213] High expression of CD44 has been shown to negatively affect patient outcome

in those with malignant melanoma.[214,215] Studies investigating the role of CD44 in tumorigenesis have determined that CD44 promotes cell adhesion and blocking CD44 with an antibody inhibits cell adhesion.[150,216] Additionally, after processing with MT1-MMP, the enzymatic products of CD44 have been demonstrated to promote tumor cell migration.[217] In regards to invadopodia, CD44 has been implicated as important in invadopodia formation and maturation.[104] CD44 promotes the phosphorylation of cortactin at invadopodia, as well as the recruitment of MMP9 to invadopodia in breast cancer cells.[88] The knockdown of CD44 inhibits invadopodia formation.[218] CD44 is also referred to as P-glycoprotein, and has been shown to be fucosylated.[120,146,161,213,219] sLe^x antigen expression increases on CD44 after FUT3, 6, or 7 overexpression in prostate cancer cells, contributing to cell adhesion through E-selectin.[161] A similar phenomenon has been observed in breast cancer cells, where high expression of CD44 on invasive cancer cells, and low CD44 expression on non-metastatic cancer cells demonstrates that sLe^x antigens interact with CD44.[219] A study in rat colon carcinoma cells found that CD44 is α(1,2) fucosylated after FUT1 overexpression, and contributes to tumorigenicity.[220] Thus far, there have not been any studies investigating fucosylated CD44 in melanoma progression. It might be possible that L-fucose treatment of melanoma cells, FUK overexpression, or FUT1 overexpression enhances α(1,2) fucosylation of CD44, thus diminishing sLe^x antigen expression and inhibiting invadopodia formation.

Another cell surface protein that might inhibit invadopodia formation after α(1,2) fucosylation is β1 integrin. β1 integrin is an important signaling factor which promotes the protrusion of the cell membrane and invadopodia formation.[89,221] It has been demonstrated that invadopodia formation through β1 integrin signaling is mediated by the presence of collagen in the ECM.[97] The inhibition or knockdown of β1 integrin interrupts invadopodia formation, implicating it as an important factor in invadopodia.[89,95] There are multiple reports indicating that β1 integrin fucosylation is crucial for its function.[121,124,150,222–224] β1 integrin can be α(1,2) fucosylated through FUT1 as demonstrated in bladder cancer cells, where α(1,2) fucosylation contributes to activation of β1 integrin.[225] Several studies in various

cell types have demonstrated that core fucosylation mediates integrin activity and promotes ligand binding, migration, and metastasis in cancer cells[121,124,182,224], whereas defucosylation of integrins inhibits adhesion and migration.[150,223] Additionally, it has been demonstrated that β1 integrin is core fucosylated in metastatic melanoma cells.[226] Since β1 integrin can be fucosylated, and has been shown to be α(1,2) fucosylated, it might be possible that enhanced α(1,2) fucosylation of β1 integrin on melanoma cells inhibits invadopodia formation.

A third potential candidate is EGFR. EGFR has been previously determined to be fucosylated.[119,186,188,190,227,228] One study suggests that loss of fucosylation of EGFR mediated by α-L-1-fucosidase results in activation of EGFR and its signaling pathways in breast cancer and CRC cell lines.[119] In lung cancer cells, the role of fucosylation and EGFR signaling is more complicated. α(1,3) fucosylation mediated by FUT4 and FUT6 overexpression has been shown to prevent EGFR dimerization and inhibit signaling. At the same time the overexpression of FUT8 promotes the dimerization and activation of EGFR.[190] Similarly, the overexpression of FUT7 in lung cancer cells leads to enhanced activation of EGFR and AKT/mTOR signaling pathway to promote cell proliferation.[227] α(1,3) fucosylation mediated by FUT4 was found to be increased on EGFR in breast cancer cells, leading to activation of EGFR signaling.[228] Through the use of an L-fucose analog in HCC cells, one study demonstrated that decreased core fucosylation of EGFR suppressed downstream signaling events, and correlates with inhibited colony formation in soft agar and tumor growth *in vivo* therefore indicating that during HCC progression, core fucosylation of EGFR contributes to it signaling.[188] Similarly, it was demonstrated in HCC cells that the loss of FUT8 inhibited EGFR signaling, perhaps leading to ablated tumor formation in xenograft models.[186] The current literature has indicated that EGFR has the potential to be fucosylated, but to this point there have not been studies investigating fucosylation of EGFR in melanoma. EGFR is a known factor in invadopodia formation as it has been shown that EGF stimulation induces invadopodia formation and EGFR inhibition prevents invadopodia formation.[98,104] It is thought that EGFR forms signaling complexes with other

membrane-bound proteins, such as β1 integrin, at invadopodia.[104] Being that EGFR has been demonstrated to be involved in invadopodia formation and has the potential to accept multiple forms of fucosylation, it might be possible that α(1,2) fucosylation of EGFR in melanoma cells inhibits its association with other RTKs or integrins and prevents invadopodia signaling.

The assembly and maturation of invadopodia are controlled by many glycosylated plasma membrane proteins such as integrins, growth factor receptors, ion channels/exchangers, matrix metalloproteases, etc. Our findings that the modulation of FUK and the fucose salvage pathway inhibits both the initiation of invadopodial assembly and the proteolytic activity of invadopodia establishes a foundation for future exploration of how the fucose salvage pathway regulates the functions of such crucial invadopodial proteins, and importantly, metastatic capacity in melanoma.

Part Two: An investigation into the role of STIM1 in melanoma formation, progression, and metastasis through a novel transgenic mouse model

3.1 Introduction

3.1.1 Calcium and Homeostasis

The calcium ion (Ca^{2+}) is a crucial second messenger in cellular signaling and is involved in many physiological functions ranging from regulating enzymatic activity, cellular motility, muscle contraction, cell cycle control to angiogenesis.[229–232] Extracellular concentrations are typically greater than 1mM, whereas normal cytosolic concentrations are between 10-100nM.[233] In order to protect the cell from Ca^{2+} overload, several organelles, such as the endoplasmic reticulum (ER) act as Ca^{2+} sinks to take up excess Ca^{2+}. ER Ca^{2+} concentrations generally range between 21µM to 2mM.[233] Ca^{2+} leakage into the cytosol is constantly occurring, therefore homeostasis is maintained by the constant uptake of Ca^{2+} from the cytosol to Ca^{2+} sinks through Ca^{2+} pumps.[230,233] In general, cells maintain low cytosolic Ca^{2+} until physiological processes necessitate the release of Ca^{2+} from internal stores. Once internal stores are depleted, and Ca^{2+} is effluxed to the extracellular space, the internal stores must be replenished by Ca^{2+} influx from the extracellular space.[234]

There are Ca^{2+} pumps, exchangers, channels, transporters, and buffering proteins to ensure that cytosolic Ca^{2+} homeostasis is maintained.[230,234–236] Channel proteins are found on the plasma membrane, as well as intracellular store membranes to allow the passage of Ca^{2+}.[234] There is a very narrow range of tolerable Ca^{2+} concentrations within a cell. The dysregulation of Ca^{2+} homeostasis can lead to extended periods of high Ca^{2+} concentration and cell death.[235] it has been observed that dysregulation of Ca^{2+}

homeostasis in cancer cells can lead to promotion of cell proliferation, apoptosis avoidance, gene transcription, migration, and metastasis.[230,237]

Table 5: Studies of STIM1 in Cancers

Cancer Type	Effect of STIM1	Reference
Breast	• Knockdown inhibits migration, SOCE, and cell seeding to lungs	[244]
Cervical	• Overexpression promotes proliferation, migration, angiogenesis tumor growth, • Knockdown inhibits tumor growth and angiogenesis • Inhibition of STIM1 localization to plasma membrane interface blocks SOCE	[245] [246]
Gastric	• Knockdown inhibits proliferation, migration, invasion, tumor growth, and lung metastasis	[247,248]
Colorectal	• Overexpression promotes migration and motility properties • Knockdown inhibits migration and SOCE • Overexpression promotes migration, invasion, lung & liver metastases, and correlates with poor survival. • Knockdown inhibits migration, invasion, lung & liver metastases, and correlates with improved survival.	[250] [251]
Lung	• Knockdown inhibits proliferation, colony formation, and tumor growth • Knockdown inhibits migration, invasion, and tumor metastasis	[253] [254]
Hepatocellular	• Knockdown inhibits migration, invasion, and promotes focal adhesions	[255]
Prostate	• Knockdown inhibits migration and invasion	[256]
Melanoma	• Overexpression promotes invadopodia formation and gelatin degradation • Knockdown inhibits invadopodia formation, gelatin degradation, Ca^{2+} oscillations, and cell seeding in lungs • Knockdown inhibits proliferation, migration, SOCE, and lung seeding	[191] [257]
Glioblastoma	• Knockdown inhibits colony formation, proliferation, tumor growth, and arrests cells in G0/G1 phases	[290]

3.1.2 Store Operated Calcium Entry

Cells utilize store operated calcium entry (SOCE) to replenish depleted ER Ca^{2+} stores.[233] There are two families of proteins that are involved in the formation of store operated channels (SOCs), stromal interaction molecule (STIM) and ORAI proteins.[235] There are two STIM proteins on the ER membrane and

three ORAI proteins on the cell membrane that can be involved in SOC formation, with STIM1 and ORAI1 as the main contributors.[238]

There are three variants of ORAI, all of which can interact with STIM proteins to form Ca^{2+} entry channels.[234] ORAI1 is a 301 amino acid long protein that exists as a transmembrane protein on the plasma membrane.[233] The channel is formed by the hexameric aggregation of ORAI1 proteins around a central pore, of which the C-termini interact with STIM.[234,235] Although the ORAI1 proteins form the pore on the plasma membrane, this pore is not formed or activated unless Ca^{2+} stores have been depleted, and STIM1 is involved.[233]

STIM1 is a 685 amino acid long protein located primarily on the ER membrane and acts as the Ca^{2+} sensor for the ER store.[233] The STIM1 protein consists of a pair of EF-domains, of which one binds Ca^{2+}, a sterile alpha motif (SAM) which interacts with the open EF domain, a transmembrane portion, coiled-coil domains, STIM1-ORAI activating region (SOAR)/CRAC activation domain (CAD), and a polybasic tail which

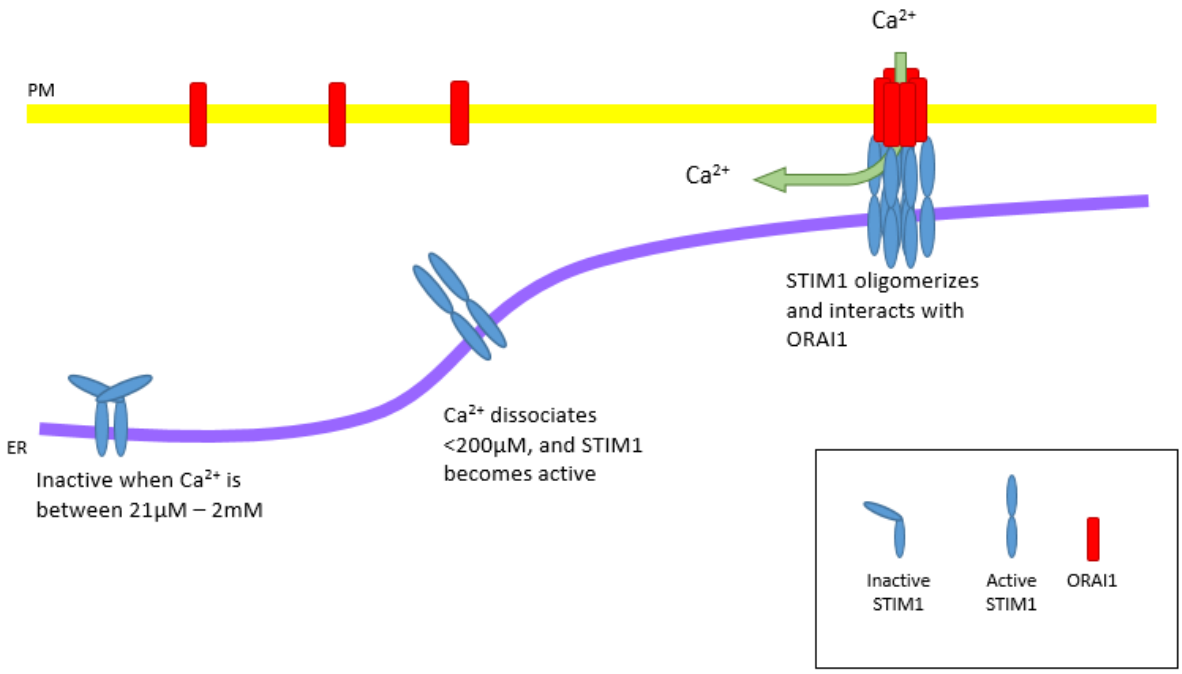

Figure 3-1: Simplified schematic of SOCE channel formation. STIM1 dimers are inactive when bound to Ca^{2+}. Drops in ER Ca^{2+} concentration cause Ca^{2+} to dissociate with STIM1 and induce a conformational change. STIM1 oligomerizes and translocates along the ER membrane. ORAI1 on the PM forms a hexameric unit and interacts with STIM1 to open a pore and allow Ca^{2+} influx to the cytoplasm.

interacts with the plasma membrane and ORAI.[234] The EF domains in the ER remain bound to Ca^{2+} until Ca^{2+} is effluxed from the ER and the $Ca^{2=}$ concentration drops to a point at which the bound ions dissociate and induce a conformational change.[234,239] The dissociation of Ca^{2+} from the EF domain of STIM1 occurs at ~200μM, whereas for STIM2 it is ~400μM, indicating that STIM2 responds to changes near resting state and STIM1 reacts to significant decreases in Ca^{2+} concentration.[234,239] When activated, STIM1 dimers oligomerize and shuttle along the ER membrane to the ER-PM junction, where ORAI1 then accumulates and generates hexamers, allowing influx of Ca^{2+} to the cytosol.[233]

SOCE begins with ER depletion, which occurs after inositol triphosphate (IP_3) binding to inositol triphosphate receptor (IP_3R) on the ER membrane and induces Ca^{2+} release into the cytoplasm.[240,241] Ca^{2+} depletion in the ER allows for Ca^{2+} to shuttle along the concentration gradient from the extracellular space into the cytosol through SOC channels (Fig. 3-1). Ca^{2+} dissociates with STIM1 dimers, causing a conformational change and translocation to ER/PM junctions where ORAI proteins aggregate to form an entry for Ca^{2+}.[234,235,239,242] The multimerization of STIM1 is mediated by lipid rafts.[233] When the ER Ca^{2+} store is refilled, STIM1 binds to Ca^{2+}, undergoes an inactivating conformational change, and dissociates from ORAI1.

3.1.3 STIM1 in melanoma

The role of STIM1 and SOCE have been extensively studied in breast[230,241,243,244], cervical[243,245,246], esophageal[243], gastric[247–249], colorectal[249–252], lung[241,253,254], hepatocellular[241,255], prostate[256], and melanoma[191,241,257] cancers, as summarized in Table 5. Many of these studies demonstrate that STIM1 overexpression promotes cancer cell migration, invasion, tumor growth, and metastasis.

In melanoma, overexpression of STIM1 increases the average number of invadopodia per cell and enhances gelatin degradation whereas the knockdown of STIM1 inhibits invadopodia formation and ECM degradation as demonstrated by invadopodia assays utilizing gelatin coated coverslips.[191] IHC staining of

melanoma tumors indicates that metastases have higher STIM1 expression than primary tumors, and the expression of STIM1 increases as the stage of disease becomes more advanced.[191,257] SOCE is thought to promote invadopodia formation as treatment of melanoma cells with Ca^{2+} chelators or SOCE inhibitors decreases invadopodia number and gelatin degradation.[191] Knockdown of STIM1 in melanoma cells inhibits cell proliferation, migration and lung metastases in tail vein injection mouse models.[191,257] The majority of the published literature has concluded that STIM1 expression is enhanced in many clinical tumor types, including melanoma, and is important in promoting migration and invasion of cancer cell lines.

3.1.4 Murine models of melanoma

Mouse models have significantly advanced our understanding of melanoma development and response to treatments, but also come with limitations.[258,259] Currently, mouse models are unable to completely recapitulate conditions that are observed in patient progression, particularly the clonal nature of melanoma cells within a tumor.[258] Therefore, different mouse models are used to examine different aspects of cancer development and metastasis. Several models have been developed in which melanoma cells are implanted subcutaneously or directly into metastatic sites.[260] Subcutaneous implantation involves the injection of tumor cancer cells below the surface of the skin to develop tumors over the course of days to weeks.[259] Syngeneic cells that are known to be metastatic can be utilized in order to model intravasation, survival in circulation, extravasation, distal site survival, and growth at distal sites.[5,259,261] Cells can also be injected directly into a metastatic site, such as the brain or lungs, and a tumor allowed to grow to examine how metastases function.[5] This approach is limited in that the tumors that develop lack a complete microenvironment and are often clonal based on culture conditions.[20,258] Additionally, these models sometimes lack immune interaction as only syngeneic cell lines can be used in immune competent mice.

Patient derived xenograft (PDX) models involve implanting a piece of surgically resected tumor from the patient, including stromal cells in the tumor microenvironment, to severely immunocompromised mice.[259] These models are utilized in an effort to understand and predict patient response. Treatments to the models occur in parallel with treatment of the patient to monitor for genomic changes and resistance mechanisms.[259,262] However, these models are inefficient and tumors do not always develop after inoculation. Additionally, these models are limited in that being in immunocompromised mice, the impact of the immune system cannot be assessed.[259,262] While these models are able to model the local tumor microenvironment and treatment response, the immune response cannot be examined.

Metastasis is the main cause of death in melanoma patients.[17] Metastatic colonization is an inefficient process, with a low percentage of circulating cells able to develop into secondary tumors.[5,18] In order to examine metastatic colonization, intravenous models are utilized.[5] Tumor cell injection into the tail vein, heart, or portal vein are commonly used to study metastatic colonization at various distant organs.[263,264] Studies of melanoma seeding typically utilize the tail vein injection model as the injected cells will often seed in the capillaries of the lungs, and thus model lung "metastases".[259] In cases where bone metastases are being examined, melanoma cells are injected into the heart.[265] Even though intravenous injections are a commonly used model of "metastasis", the model is not able to study the metastatic dissemination from a primary tumor.[259]

In an effort to accurately model cancer in animals, genetically engineered animals have been designed and studied to investigate tumor initiation through metastasis. In melanoma, there have been many studies conducted in mice, but the relevance to human melanoma formation is not complete. Genetically engineered mouse (GEM) model melanomas are dermal in nature, and have few shared characteristics with human melanomas.[266] Even so, they are the most similar and efficient model to study genetic aberrations leading to melanoma. These models are able to develop complete tumor

microenvironments, which does not occur with tumor cell implantation, and are thought to more accurately recapitulate tumor progression including initiation, dissemination, and metastasis.[5] GEM models have been used to model various oncogenes, tumor suppressors, and combinations of both to obtain insight into the mechanisms of how respective proteins affect melanoma.[266] In 2002, a GEM model of Cre-mediated PTEN knockout was generated.[267] Five years later, a Cre-inducible model was created to examine the role of $BRAF^{V600E}$ in lung tumor formation.[268] With mutant BRAF and PTEN loss playing such a critical role in melanoma formation, the two models were crossed to develop a model that resembled human melanoma. In 2009, it was published that a novel melanoma GEM model was created, which incorporates melanocyte specific Cre-induced BRAF mutation and PTEN knockout. After topical 4-hydroxytamoxifen (4OHT) treatment, mutant BRAF alone only results in hyperplasia, whereas when coupled with PTEN loss, all mice rapidly develop primary and metastatic tumors.[269] In 2008, STIM1 knockout mice were generated to examine the role of STIM1 in T-cell function.[270] To this point, a GEM model has not been developed to examine the role of STIM1 in melanoma progression. Based on previous data from the laboratory, our aim was to combine these preexisting GEM models to develop an inducible melanoma model that incorporates the loss of STIM1 in melanoma initiation, development, and metastasis.

3.2 Methods

3.2.1 Cell culture

WM793, WM115, and B16/F10 melanoma cells were cultured in HyClone RPMI-1640 Media supplemented with 10% FBS and 1% Penicillin/Streptomycin.

3.2.2 cDNA Constructs

STIM1 was knocked out using pLentiCRISPRv2-sgSTIM1. The STIM1 sequences used are:

Human Fwd: 5’-TGTGCGCCCGTCTTGCCCTG-3’

Human Rev: 5’-CAGGGCAAGACGGGCGCACA-3’

Mouse Fwd: 5’-ACAGTGGCTCATTACGTATG-3’

Mouse Rev: 5’- CATACGTAATGAGCCACTGT-3’

STIM1 was knocked down using pSuper-shSTIM1 with the target sequence of 5’-AGAAGGAGCTAGAATCTCAC-3’

3.2.3 Migration Assays

Matrigel invasion by WM793 and WM115 cells was performed using invasion Boyden chamber (8μm) as we previously described previously.[191,192,198,199] Wound healing assays were performed with B16/F10 cells. Briefly, cells were allowed to grow to confluence before a scratch was made with a pipette tip. The wells were washed to remove floating cells and 1% FBS media was added to each well. Images were taken on the same field at 0 and 12 hours.

3.2.4 Soft Agar Assay

In preparation for the experiment, 1.5% agarose solution and 2x RPMI culture media were made. Agarose (Fisher, BP165-25) was added to ddH_2O, then autoclaved to complete solvation and sterilize the solution. 2x RPMI powder (HyClone, Cat #SH30011.02) was dissolved in ddH_2O and pH was balanced to 7.4. The media was sterilized by passage through a 0.22μm bottle top filter (Corning, 431097), after which 2x Penicillin/Streptomycin solution and stored at 4°C. Before using 2x RPMI, FBS was added to an aliquot up to 20%. Solutions were kept at 42°C to prevent solidification. 0.75% agarose solution was made by combining 1.5% agarose solution with 2x RPMI, and was used to coat the bottom of wells in 12-well plates and allowed to cool. Cells were layered in a 0.375% agarose solution over the bottom layer, and allowed to cool. Over the top, 1mL of complete media was added, then changed every 2 days. Colonies were resolved using p-iodonitrotetrazolium violet (PINTV) staining.

3.2.5 Mouse Models

C57BL/6 Subcutaneous Xenograft: All mice experiments were performed in compliance with protocols approved by the Institutional Animal Care and Use Committee (IACUC) of the Moffitt Cancer Center. B16/F10 cells expressing the empty vector, or STIM1 knockout were trypsinized and washed using 1x PBS. Next, $1x10^5$ cells were injected in 100µL of PBS under the flank skin. Tumor measurements were taken three times per week, until tumors reached endpoints.

Transgenic Mouse Model: Mouse husbandry and tumor studies were done in compliance with protocols approved by the IACUC of the Moffitt Cancer Center, and Penn State College of Medicine. Tumors were induced by topical application of 4OHT dissolved in DMSO for 10 minutes, with residual liquid removed to combat non-specific tumor formation.

3.2.6 Cytokine Array

When treated mice were 50 days old, they were sacrificed and tumor tissue was harvested and flash frozen in liquid nitrogen. Tumor samples of similar mass from three mice with similar tumor sizes from $STIM1^{WT/WT}$ or $STIM1^{lox/lox}$ groups were combined, homogenized with a Dounce Homogenizer in an ice bath, then lysed with ice cold RIPA buffer (150mM NaCl, 5mM EDTA, 50mM Tris pH 8.0, 1% NP-40) supplemented with phosphatase and protease inhibitor tablets. Homogenate was then sonicated and spun down to remove debris. The lysate was then utilized in the cytokine array (RayBiotech, AAM-CYT-3-2). 150µg of protein was diluted in cytokine array blocking buffer up to 1mL, then added to array membranes and incubated overnight at 4°C. Membranes were then incubated with biotinylated antibody cocktail for 2.5 hours at room temperature. Detection was performed by exposing the membranes to detection buffer mix and exposure to autoradiography film.

3.2.7 Peripheral Blood Determination

Peripheral blood from mice of indicated genotypes was taken by retro-orbital bleeding and analyzed on a Heska HemaTrue Hematology Analyzer for the presence of white blood cells, lymphocytes, granulocytes, and monocytes.

3.2.8 Western blotting

Cells were seeded to 6cm plates at $5x10^5$ cells per plate and allowed to incubate overnight. The following day, plates were washed once with ice cold 1xPBS, then lysed with a rubber policeman and ice cold RIPA buffer (150mM NaCl, 5mM EDTA, 50mM Tris pH 8.0, 1% NP-40) supplemented with 1mM phosphatase (ThermoScientific, 88667) and 1mM protease (Roche, 04693159001) inhibitor cocktails. The following antibodies were used: STIM1 (Cell Signaling Technology, 5668) at 1:1000 dilution in 5% BSA (Fisher, BP1600) in TBST; GAPDH (Sigma, G8795) at 1:5000 dilution in 5% BSA in TBST.

3.2.9 PCR Genotyping

Mouse tail specimens ranging from 3-5mm in length were digested overnight in 600µL TNES buffer (50mM Tris, 0.4M NaCl, 100mM EDTA, 0.5% SDS) supplemented with 350µg of proteinase K at 55°C. After tissue was completely digested, 167µL of 5M NaCl was added and samples were vortexed vigorously for 15 seconds. Samples were centrifuged at 18,000rcf for 20 minutes at 4°C. The supernatant was removed to fresh tubes, 800µL of cold 100% ethanol was added, and gently inverted several times to precipitate DNA. Centrifugation was repeated as described. Ethanol supernatant was discarded, and DNA pellets were gently washed with 1mL cold 70% ethanol. Centrifugation was repeated, supernatant discarded, and residual ethanol was allowed to evaporate. DNA pellets were resuspended in 200µL ddH_2O, and incubated at 55° for 30 minutes.

BRAF, PTEN, Cre PCR - 2µL of DNA, 1.2µL of 10x DreamTaq Buffer, 0.96µL of 2.5mM dNTP, 0.6µL of Fwd primer, 0.6µL of Rev primer, 0.06µL of DreamTaq, and 6.58µL ddH_2O were mixed for each sample and run

on a thermocycler on the following program: 94°C for 3 minutes, 94°C for 30 seconds, 60°C for 1 minute, 72°C for 1 minute (repeat steps 2-4 for 35 cycles), 72°C for 2 minutes, then 10°C hold. Primers:

BRAF Fwd: 5'-TGAGTATTTTTGTGGCAACTGC-3' Rev: 5'-CTCTGCTGGGAAAGCGGC-3'

PTEN Fwd: 5'- CAAGCACTCTGCGAACTGAG-3' Rev: 5'-AAGTTTTTGAAGGCAAGATGC-3'

Cre Fwd: 5'-ACGTTGATGCCGGTGAACG-3' Rev: 5'-CCACCAGCTTGCATGATCTC-3'

STIM1 & STIM2 PCR: 0.5µL of DNA, 1.2µL of 10x DreamTaq Buffer, 1.2µL of 2.5mM dNTP, 0.24µL of Fwd primer, 0.24µL of Rev primer, 0.05µL of DreamTaq, and 8.59µL of ddH_2O were mixed for each sample and run on a thermocycler on the following program: 94°C for 1 minute, 94°C for 1 minute, 60°C for 1 minute, 74°C for 1 minute (repeat steps 2-4 for 40 cycles), 74°C for 1 minute, then 10°C hold. Primers:

STIM1 Fwd: 5'-CAGAACCGTTACTCTAAGGAGCAC-3' Rev: 5'-CATATGTTAGGCATGTACTCTGTCAAC-3'

STIM1Δ Fwd: 5'-CTGCTGAGCTACACACATTCC-3' Rev: 5'-CATATGTTAGGCATGTACTCTGTCAAC-3'

STIM2 Fwd: 5'-TACAGAGTGCAGTGTGCCTC-3' Rev: 5'-CCAGGTCATTGTCACTAGGCACAAGC-3'

STIM2Δ Fwd: 5'- TACAGAGTGCAGTGTGCCTC-3' Rev: 5'-TCTGAACAAGTTTCCCAATCCTA-3'

PCR products were run on 2% agarose gel to resolve bands.

3.2.10 Immunohistochemistry

Mouse tissues were fixed in 10% buffered formalin for 48 hours before being embedded in paraffin and sectioned. Slides were deparaffinized at 55°C for 45 minutes, then cleared in two washes of CitriSolv (VWR, 89426-270). Tissues were then rehydrated through graded alcohol solutions. Antigen retrieval was conducted using 10mM sodium citrate solution pH 6.0 that was heated to ~90°C for 20 minutes. Endogenous enzyme activity was blocked by incubation in 3% H_2O_2. For STIM1 staining, the Vector® M.O.M.™ Immunodetection Kit (Vector Laboratories, PK-2200) was utilized. PTEN staining was completed using ABC-AP Staining Kit (Vector Laboratories, AK-5000). Both stains were visualized with Vulcan Fast Red (Biocare, FR805) development. The following antibodies were used: STIM1 (ThermoFisher, MA1-19451)

at 1:200 and PTEN (Cell Signaling Technologies, 9559S) at 1:50. Slides were counterstained with hematoxylin before being washed and dehydrated in several quick washes of 100% ethanol and mounting.

3.3 Results

3.3.1 STIM1 promotes migration and anchorage independent growth

STIM1 has been demonstrated in several studies to be elevated in melanoma tumors compared to benign nevi, and also increases expression in progressing stages and metastasis.[191,241] The same studies determine that STIM1 expression facilitated enhanced SOCE and invasive activity through SOCE and invadopodia formation.[191,241] Our first objective was to generate stable cell lines of several human and murine cell lines with STIM1 knockdown or STIM1 knockout and to confirm changes of STIM1 expression by western blot (Fig. 3-2A, C, & E). We found that the loss of STIM1 by knockdown or knockout inhibits cell migration, consistent with previously published results (Fig. 3-2B & D). We next examined the effect

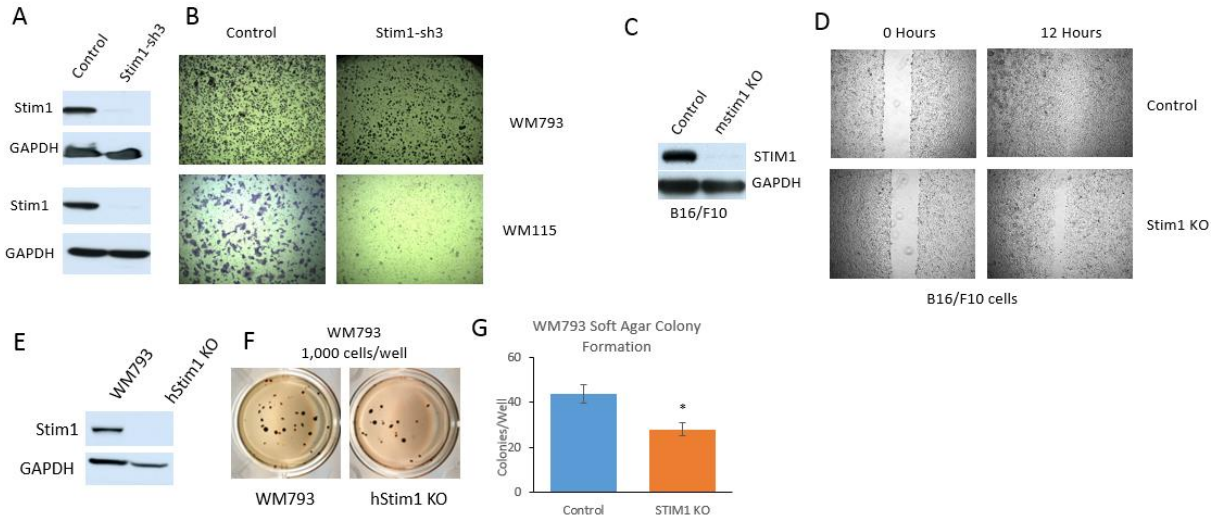

Figure 3-2: Loss of STIM1 inhibits migration and colony formation. A Western blot analysis of STIM1 shRNA infected stable cell lines in WM793 (top) and WM115 (bottom) melanoma cell lines. **B** Melanoma cell transwell migration was inhibited by the knockdown of STIM1. **C** Western blot analysis of STIM1 sgRNA infected stable cell lines in murine B16/F10 melanoma cells. **D** Scratch assay after 12 hours demonstrated that STIM1 KO cells migrated slower than empty vector control cells. **E** Western blot analysis of STIM1 sgRNA infected WM793 cells. **F** Representative wells of control cells and STIM1 KO cells. **G** Quantitation of colony formation assay * indicates $p<0.05$. Representative results from at least three independent replicates were presented. Statistical analysis determined by two-tailed, two sample t-test.

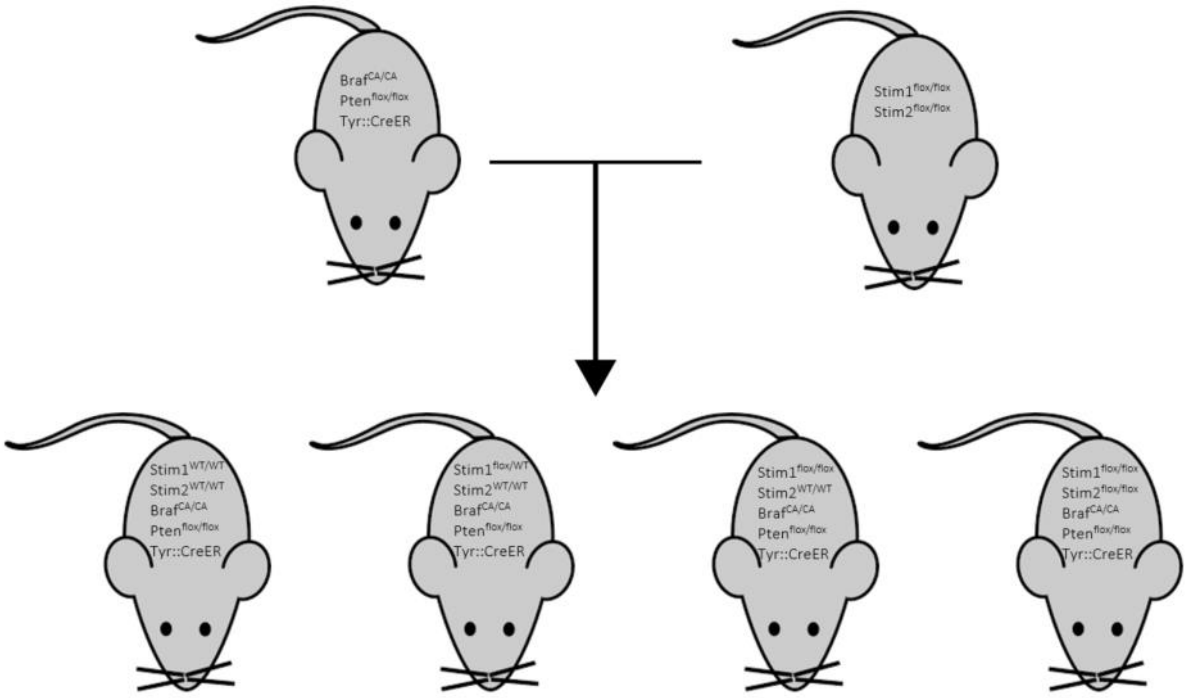

Figure 3-3: Illustrated representation of our breeding strategy and desired genotypes.

of STIM1 on colony formation. Loss of STIM1 inhibited colony formation (Fig. 3-2F & G), indicating that STIM1 contributes to anchorage independent growth.

3.3.2 Development of a STIM1 inducible knockout model of melanoma progression and metastasis

Since STIM1 has been demonstrated to promote melanoma progression and metastasis[191,241], we began considering a novel method to model STIM1 in melanoma initiation, progression, and metastasis. We were able to purchase BRAF$^{CA/CA}$/PTEN$^{lox/lox}$/Cre mice from the Jackson Lab, and were generously given STIM1$^{lox/lox}$/STIM2$^{lox/lox}$ mice from Dr. Yoshihiro Baba of Osaka University. Our experimental approach was to cross the two strains of mice together to generate melanocyte-specific mutant BRAF with PTEN deletion and variations of STIM1 expression (Fig. 3-3). PCR genotyping confirmed whether the mice were homozygous for the floxed BRAF and PTEN, as well as whether the mice were STIM1$^{WT/WT}$, STIM1$^{WT/lox}$, or STIM1$^{lox/lox}$ (Fig. 3-4A). Based on the treatment regimen detailed by Dankort et. al.[269], we treated the

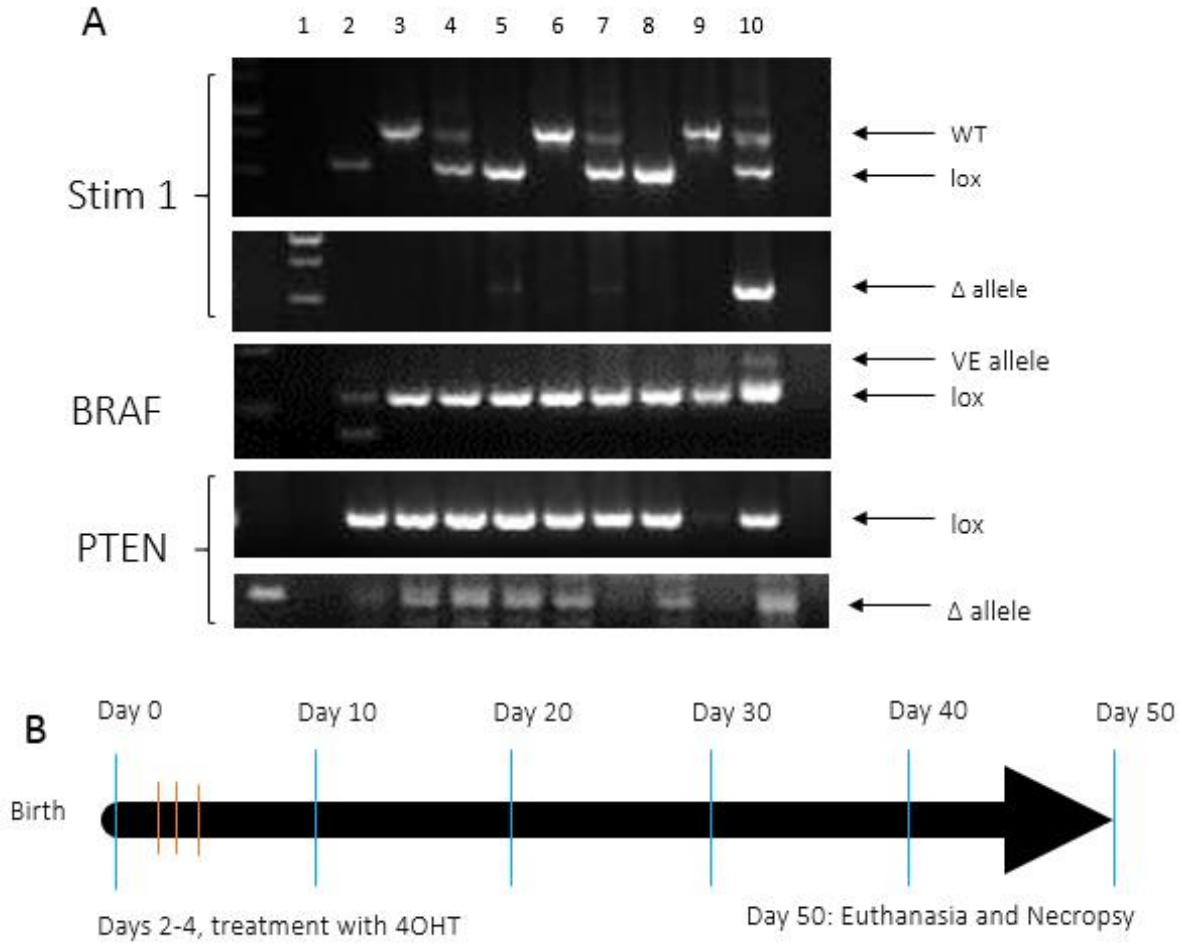

Figure 3-4: 4OHT treatment induces genomic alterations. A PCR analysis of genomic DNA isolated from tail snips treated with 4OHT. All mice were homozygous for $BRAF^{V600E}$, $PTEN^{lox}$, and $STIM2^{WT}$. Lanes 1, 5, & 8 were from homozygous $STIM1^{lox}$ mice, lanes 4, 7, & 10 were from heterozygous mice, and lanes 3, 6, & 9 were from homozygous $STIM1^{lox}$ mice. Δ refers to the modified allele after Cre activity. **B** Timeline of mice used in the study.

indicated pups on post-natal days 2-4, then allowed the pups to grow until day 50, at which point the mice were euthanized, and necropsy was performed (Fig. 3-4B).

Tumor measurements were conducted three times per week. We found that the $STIM1^{lox/lox}$ tumors grew faster and were approximately 50% larger on Day 50 than the $STIM1^{WT/WT}$ tumors (Fig. 3-5A). Interestingly STIM1 and STIM2 null tumors were approximately two-fold larger than the $STIM1^{WT/WT}$/$STIM2^{WT/WT}$ tumors, indicating that the loss of both STIM molecules exacerbated tumor growth. We were curious to know whether the loss of STIM1 and STIM2 significantly affected tumor formation and examined tumor free survival. The generated Kaplan-Meier analysis shows that $STIM1^{WT/WT}$

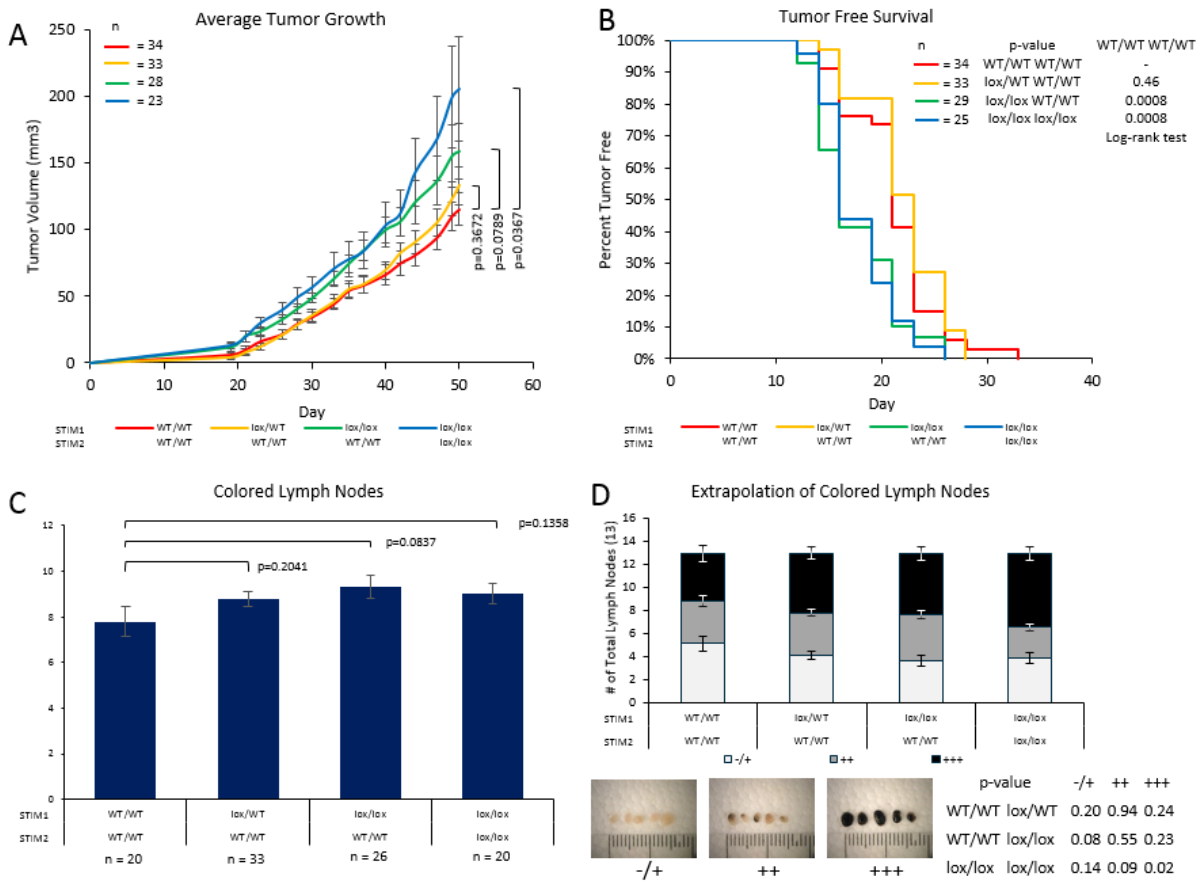

Figure 3-5: STIM1 knockout enhances tumorigenic properties. A Tumor growth curves for mice treated with 4OHT on post-natal days 2-4. **B** Kaplan Meier analysis of tumor free survival in mice after 4OHT treatment. **C** Necropsy analysis of lymph node involvement defined by the presence of pigment in the lymph nodes. **D** Quantitation of percentage of involved lymph nodes based on degree of pigmentation. Statistical analysis determined by two tailed, two sample t-test (**A**, **C**, **D**) or log-rank t-test (**B**).

and STIM1 heterozygous mice generated tumors later than the STIM1$^{lox/lox}$, or the STIM1$^{lox/lox}$/STIM2$^{lox/lox}$ mice (Fig. 3-5B). Upon necropsy, we found that there was significant lymph node involvement in all the mice. Additional analysis of the lymph node involvement found that there were three distinct phenotypes of metastatic lymph nodes; no metastasis, partial metastasis, and complete metastasis. Metastasis was defined by the presence of black pigmentation in the lymph nodes. Nodes were considered having no metastasis based on a lack of visible pigmentation. Partial and complete metastases were characterized as lymph nodes that displayed some black pigmentation, or were completely black. We found that as mice lost STIM1 alleles, the percentage of lymph nodes without pigmentation dropped, and the percentage of lymph nodes that demonstrated dramatic color change coincidentally rose (Fig. 3-5D). The percentage of

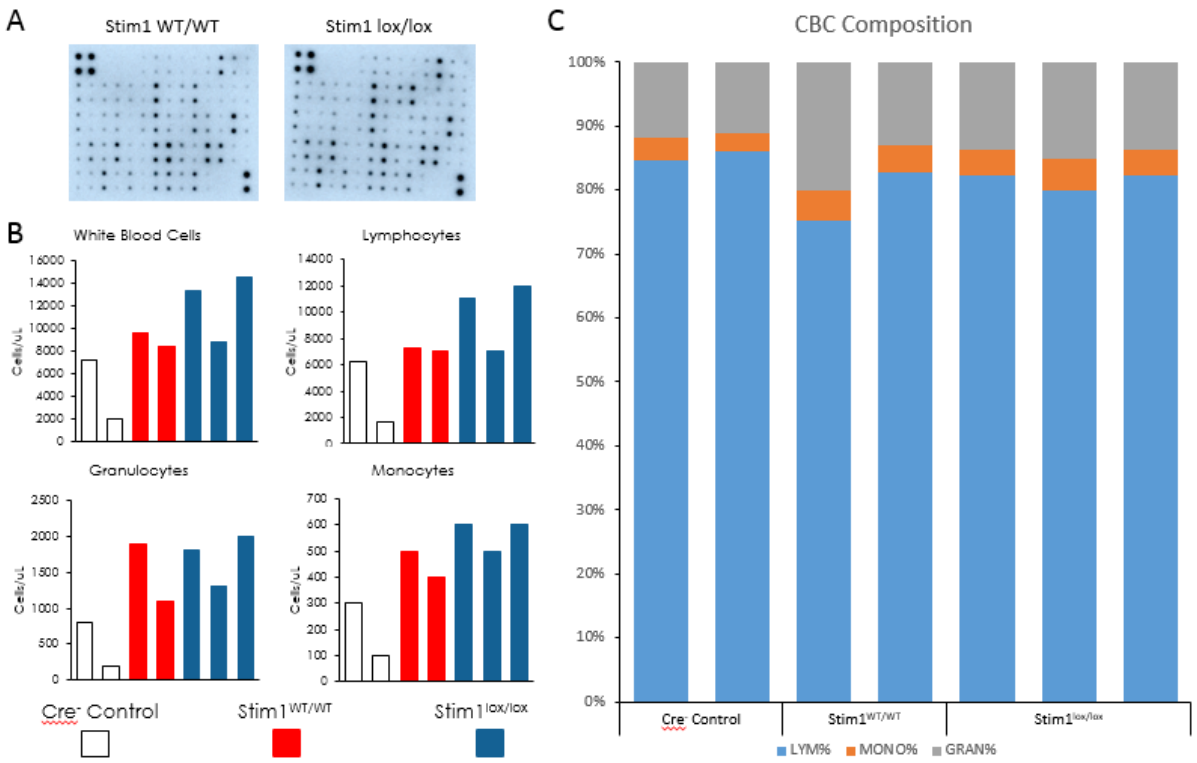

Figure 3-6: STIM1 knockout does not significantly affect peripheral immune system. A Murine cytokine array performed on tumor samples from mice that were homozygous for $STIM1^{WT}$, or $STIM1^{lox}$. **B** Breakdown of analyzed circulating blood cells taken by retro-orbital bleed from each of the mice analyzed. (C) Circulating blood cell composition for the mice analyzed. Grey indicates percentage of granulocytes, orange indicates percentage of monocytes, and blue indicates percentage of lymphocytes.

lymph nodes considered partially metastatic did not change between cohorts. Quantitation of affected lymph nodes did not demonstrate a significant difference between cohorts (Fig. 3-6C). One should caution that the presence of black pigmentation in the lymph nodes is not an accurate criteria of melanoma metastasis. It is possible that the black pigment in the lymph nodes is a result of immune cells taking up melanin prior to circulating to the lymph nodes. Further pathological analysis is required to determine the effect of STIM1 loss on melanoma metastasis in this model.

Since SOCE is crucial for immune response in both T-cells[271] and B-cells[272], we are curious whether the increased melanoma growth in STIM1/STIM2 knockout models is due to changes in the tumor immune microenvironment. First, an analysis of cytokines secreted in the tumor was conducted. Similar sized samples were taken from three tumors of similar size from $STIM1^{WT/WT}$ or $STIM1^{lox/lox}$ mice, and

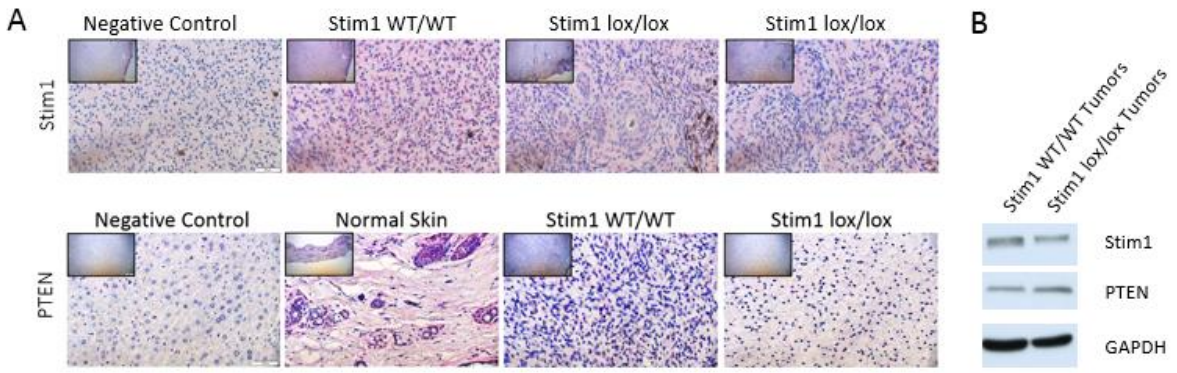

Figure 3-7: Immunohistochemical analysis indicates incomplete protein deletion. **A** IHC staining of STIM1 (top) and PTEN (bottom) indicating incomplete deletion. Scale bar indicates 50µm **B** Western blot analysis of tumor lysate indicating approximately 50% reduction of STIM1 expression.

homogenized to extract protein. After lysate was generated for each condition, 150µg of total protein was incubated on cytokine array membranes to investigate whether noticeable shifts in cytokine expression could be observed. It was determined that there was not a significant shift of any examined cytokines between the tumor conditions (Fig. 3-6A). Additionally, we conducted flow cytometric analysis of circulating blood cells to examine whether there were changes in the immune periphery. Overall, there was not a significant difference in populations of white blood cells, lymphocytes, granulocytes, or monocytes (Fig. 3-6B & C).

Next we conducted immunohistochemical staining of tumor tissues for STIM1 and PTEN. Interestingly, we found that although there was a decrease of STIM1 in tumor tissue, there was not a complete ablation (Fig. 3-7A). This could be explained by other cell types present in the tumor, such as infiltrating lymphocytes, fibroblasts, keratinocytes, etc., and will need to be more closely examined in the future. Protein lysate generated from the tumors indicate that STIM1 protein expression is reduced by approximately 50% in the knockout tumors. Taken together, the data suggest that loss of STIM1 promotes tumor growth and tumor initiation. However, as there is not a complete loss of STIM1, further experimentation will have to be conducted to confirm and validate our results.

3.4 Discussion

Calcium is a critical component of cellular physiology and disruption of Ca^{2+} balance is sufficient to cause cellular and organismal problems detrimental to overall health.[230,235,237,243,273] SOCE is the main mechanism by which Ca^{2+} enters cells, and STIM1 expression is often upregulated in carcinomas. Due to a lack of *in vivo* work modeling the effect that STIM1/STIM2 plays in melanoma initiation, progression, and metastasis, we generated a novel transgenic mouse model to investigate the effect of STIM1/STIM2 loss in melanoma. Unfortunately, we ran into several difficulties that made our model problematic to work with or derive conclusions from. We found in pilot studies that the treatment regimen had to be optimized as residual 4OHT on the mice would result in severe oral and genital tumors. The residual 4OHT was likely being consumed by the pups by licking, or by the mother during grooming. When the pups lick one another, 4OHT enters the digestive system and would stimulate PTEN loss and BRAF mutation activation in melanocytes around the mouth and genitals during intake and excretion. If indeed the mother was ingesting the residual 4OHT, it is possible that it made it into the milk, and subsequently to the pups.

Although the role of SOCE has been studied in cancer cell migration, invasion and metastasis, little is known about its function in tumor initiation and growth. In the BRAF/PTEN melanoma model, we found that the loss of STIM1 accelerated tumor initiation and growth, which was further exacerbated when STIM1 loss was combined with STIM2 loss. Although these results are unexpected, it should be noted both STIM1 and STIM2 were previously predicted to be tumor suppressors based on the loss of their chromosomal loci in some tumors.[274–283] It might be possible that STIM1 in the murine melanocytes does has a tumor suppressive function. Therefore, the loss of STIM1 combined with mutated BRAF and PTEN would lead to the enhanced initiation and tumor growth observed in our experiments. If STIM1 is tumor

suppressive, the suppressive nature might be masked in cultured cells due to accumulated mutations, and therefore appear to have a oncogenic effect when overexpressed *in vitro* and in xenograft models.

Another mechanism that might explain our results is that different STIM1 variants are responsible for the difference between our study and previous studies. STIM1 was initially thought of to be a tumor suppressor gene that arrested rhabdomyosarcoma cell growth.[283] Since then it has been determined that there are at least two different variants of STIM1, with the second variant known as STIM1L.[284] While there have not been any studies investigating if STIM1L is expressed in melanoma, it is thought that knockdown of STIM1 will also affect STIM1L, and therefore might result in data that appears contrary to previous results.[285] If indeed there are different variants of STIM1, and one of them acts as a tumor suppressor, then it is within the realm of reason that our knockdown may preferentially target the tumor suppressive variant, therefore leading to enhanced tumor growth, as we have observed.

Our results are also reminiscent of a study conducted in prostate cancer, where STIM1 expression was decreased in advancing stages of cancer.[286] Further studies in prostate cancer reported that reduced SOCE inhibits apoptosis, and the overexpression of STIM1 promotes apoptosis in prostate cancer cells.[287–289] Similarly, while STIM1 overexpression was shown to promote cell migration, it also inhibits cell proliferation by promoting senescence and arresting cells in the G_0/G_1 phase.[286] However, being that some STIM1 expression appears to persist in our IHC staining, it is not clear whether this phenotype is being recapitulated.

In our IHC stains, the specificity of the antibody was considered for nonspecific staining that might show incomplete knockout. The antibody we chose to use has been demonstrated to work in IHC studies before.[191] However, the staining's completed in that study was conducted in human tissues, whereas our studies were conducted in mouse tissues, and the STIM1 antibody was created in mouse. It is possible that a different STIM1 antibody created in a different species would behave differently and give a better staining. This antibody has been tested for use in IHC in STIM1 knockdown cells previously in our

laboratory where the knockout cells were negative, indicating positive specificity of the antibody to STIM1. The simplest way to ensure that STIM1 is knocked out in the tumor melanoma cells would be to complete a double staining of STIM1 with a melanocyte specific marker, such as S100. It has been shown that three days of treatment are sufficient to induce PTEN deletion and BRAF mutation, but it might be possible that this treatment regimen is not inducing complete STIM1 knockout in all melanocytes of the treated area. This incomplete deletion might lead to various cellular clones with STIM1 expression, adding further heterogeneity to an already complex microenvironment. As mentioned, STIM1 expression in prostate cancer cells arrest cells in G_0/G_1 phase, while the knockout cells could theoretically continue to proliferate and give rise to tumors. However, the opposite has also been reported in that the knockdown of STIM1 in glioblastoma cells also leads to G_0/G_1 arrest.[290] In our knockdown model, we may not see complete loss of STIM1 staining because those cells that have lost STIM1 may not be proliferating, and remain arrested within the tumors. In a similar manner, the loss of SOCE has been previously reported to induce quiescence in glioblastoma cells.[291] Considering this observation, if the same principle applies to melanoma, then the cells which have lost STIM1 expression might have transitioned to a quiescent state, whereas other melanoma cells which have not completely lost STIM1 expression continued to proliferate. Again, the simplest way to test these hypotheses is to conduct double staining with a melanocyte or neural crest specific marker. Another possibility is that the cells lacking STIM1 might be providing a survival advantage to other cells either through paracrine signaling, or another mechanism that we have not investigated. The current model was limited by the treatment regimen and spontaneous tumor formation due to Cre leakage.

The possibility also exists that STIM1 may play a complex role in tumor development, and the extent of that complexity has not been determined. It is interesting to note that the TGFβ signaling pathway has both tumor-suppressing and metastasis-promoting functions.[292,293] In normal cells, TGFβ promotes cell homeostasis by regulating differentiation, apoptosis, and inflammation. However, once

cells have become tumorigenic or malignant, TGFβ promotes immune avoidance, EMT, migration, and metastasis.[292,293] It might be possible that STIM1 is tumor suppressive during early stages of melanoma, then promotes migration and metastasis in later stages. Therefore, the loss of STIM1 would mitigate the tumor suppressive function and result in tumors forming earlier and growing more quickly than $STIM1^{WT/WT}$ tumors.

4.1 Summary, Future Work, and Discussions

The thesis research investigated melanoma invasion and metastasis using two very different, but complimentary, approaches. Our investigation into how fucosylation inhibits melanoma invasion through modulation of invadopodia was conducted entirely *in vitro*. The study investigating the role of the SOCE protein STIM1 in melanoma progression mostly focused on developing a novel transgenic mouse model to address how the loss of STIM1 would affect melanoma initiation, growth, and metastasis. Our purpose for both studies was to investigate molecular mechanisms to further our understanding of melanoma invasion in an effort to combat metastasis.

4.1.1 α(1,2) Fucosylation Inhibits Melanoma Invasion

The first project took into account previous studies of fucosylation in melanoma and posed the question: how does fucosylation affect invadopodia formation? Tumor cells utilize invadopodia to invade the local matrix as the cells migrate towards vasculature. Reports in the literature indicated that L-fucose treatment could interfere with melanoma growth and metastasis, and a branch of fucosylation known as α(1,2) fucosylation appeared to be lost in melanoma metastasis compared to the primary tumors.[121,128] Our study was the first to demonstrate that the fucose salvage pathways inhibits invadopodia initiation and formation. We found that α(1,2) fucosylation of cell surface proteins is responsible for the inhibition of invadopodia formation. Later stages of melanoma have been shown to downregulate FUT1 expression, which we found inhibits invadopodia formation through α(1,2) fucosylation.

This study provides new insight into how α(1,2) fucosylation plays a role in inhibiting melanoma progression and invasion. Melanoma metastasis is the main cause of death in patients.[17] Invadopodia play

an important role in melanoma cell invasion in the metastatic cascade and our results suggest that the invasive nature of melanoma cells might be attenuated by α(1,2) fucosylation. Although we were able to determine that α(1,2) fucosylation on the cell surface inhibits invadopodia formation, it has not been determined which plasma membrane bound proteins are significantly α(1,2) fucosylated to inhibit invadopodia formation. The primary goal for a continuation of this study would be to determine which cell surface proteins that are involved in invadopodia signaling are significantly fucosylated after L-fucose treatment or FUK overexpression. To accomplish this, glycomics and mass spectrometry can be utilized, specifically on cell membrane containing fractions of cell lysate to focus the investigation. Additionally, experiments can be conducted with radiolabeled L-fucose to confirm possible targets. Those target proteins should then undergo manipulation to confirm the mechanistic involvement in invadopodia formation and the necessity of α(1,2) fucosylation sites. As α(1,6) fucosylation has been determined to be advantageous to melanoma metastasis, it might be worth investigating how it impacts invadopodia formation. Relevant proteins might prove interesting targets for treatment through the use of fucosidase.

Mouse models investigating the effect of L-fucose treatment and FUK overexpression in tumor growth and metastasis have already been investigated.[128] In line with these studies, experiments should be conducted with FUT1 overexpression melanoma cell lines to determine the effect of FUT1 on tumor growth, and to determine if FUT1 overexpression does indeed inhibit metastases. Being that EGFR expression is enhanced following the development of resistance to BRAF inhibition[28,48], and α(1,2) fucosylation of EGFR might inhibit invadopodia formation, it might be of interest to combine current treatment regimens with L-fucose analogs or supplement patient diet with L-fucose to further combat melanoma progression. Therefore, an experimental mouse model combining L-fucose treatment with other melanoma treatment options should be considered to determine if L-fucose treatment improves overall and progression free survival.

L-fucose, fucose containing extracts, and fucose-containing liposomes are being investigated as potential treatments in various cancer types. L-fucose treatment has been shown to inhibit tumor growth *in vivo* in melanoma.[128] Since it has been shown that tumor cells will exploit certain FUTs to ensure fucosylation that promotes tumorigenic properties, one might wonder how L-fucose treatment inhibits melanoma growth and progression. It is possible that excess free L-fucose is taken up and conjugated by other FUTs onto structures that are able to mask or override tumorigenic structures. L-fucose treatment has been shown to increase fucosylated protein concentration within tumors, contributing evidence to this hypothesis.[128,200] In metastases, sLe^x has been demonstrated as critical to facilitate adhesion to endothelial cells. L-fucose treatment might affect this interaction as free L-fucose could be conjugated by other FUTs that limit or prevent the synthesis of sLe^x. Another possibility is that the excess free L-fucose encourages an immune response against the tumor through the activation of cytolytic immune cells such as T-cells and NK cells.[128,294] If this phenomenon is consistently noted through further studies, it might lead to advances in dietary treatments of melanoma. With L-fucose naturally occurring in various seaweed species, it might be worth considering if supplementation of brown seaweed into current diets might help slow tumor progression or have preventative effects. One hypothesis, is that average consumption of approximately 15g of seaweed per day may inhibit melanoma formation.[295]

Though trends in fucosylation branching have been identified through several cancer types, further study must be conducted to identify fucosylation changes in cancer progression. Many questions still remain regarding the role of fucosylation in cancer progression. For example, it will be interesting to determine how fucosylation patterns change after treatment with L-fucose or fucoidan. It would be interesting to determine if the reestablishment of lost fucosylation affects the other branches, or if the effect overpowers them; for example, will rescue of α(1,2) fucosylation in melanoma impact or mask the tumor promoting effect of α(1,6) fucosylation? There are several cancer types in which certain branching has been observed both up- and downregulated. A number of studies have shown that fucosylation can

change between cancer stages, and especially between primary and metastatic tumors. Very few, if any, studies have investigated the role that cell surface fucosylation might play in the differing stages of tumor progression and invasion through the local tissue and basement membrane on the way to the lymphatics and vasculature. By identifying fucosylation, and more generally glycosylation, changes between cancer stages, investigators might be able to determine new methods of detection and potential treatments.

4.1.2 Role of STIM1 in Melanoma Development and Progression

STIM1 and ORAI1 have been the topic of many studies in cancer investigating how modulation of SOCE can promote tumorigenic properties. The second project aimed to develop a novel transgenic mouse model to examine the role of STIM1 in tumor formation, growth, and metastasis. Melanocyte specific $BRAF^{CA/CA}$/$PTEN^{lox/lox}$/Cre^{+} mice were crossed with $STIM1^{lox/lox}$/$STIM2^{lox/lox}$ mice to generate mice with $BRAF^{V600E}$, $PTEN^{lox/lox}$, Cre^{+} genotypes coupled with various allelic expression of STIM1 and $STIM2^{WT/WT}$ or $STIM2^{lox/lox}$. After birth, 4-hydroxytamoxifen (4OHT) was used to induce the mutation of BRAF and deletions of PTEN, STIM1, and STIM2. Contrary to our hypothesis, we found that the loss of STIM1 promoted tumor growth after 4OHT treatment compared to $STIM1^{WT/WT}$ mice. Additionally, the time to tumor development was significantly shorter in $STIM1^{lox/lox}$ mice compared to $STIM1^{WT/WT}$ mice. Although we were excited to see what appeared to be metastatic activity in many lymph nodes examined, limitations of observational data alone make it difficult to derive a conclusion from our data. Examination of tumor tissues by immunohistochemistry determined that our knockouts might not be complete, thus adding confounding variables to our study.

Our *in vitro* work suggested that the loss of STIM1 inhibits melanoma cell migration and colony formation, whereas our *in vivo* work indicates loss of STIM1 exacerbates tumor formation and growth. This dichotomy might be explained by the inherent differences between *in vitro* and *in vivo* experiments. Experiments in 2D provide maximal concentration of nutrients and oxygen to all cells, and therefore do

not recapitulate the nutrient and oxygen gradients that are observed within tumors.[296] In order to remedy this *in vitro*, we moved to anchorage independent assays, which allow for the formation of suspended spheres in agarose and can recapitulate the nutrient and oxygen gradients mentioned. In this manner, we believed that the loss of STIM1 inhibited colony growth, which would be observed in murine tumors. However, colony formation assays do not take into account the interaction between melanoma cells and other cells in the tumor stroma, such as endothelial cells, fibroblasts, immune cells, and other types of skin cells.[297,298]

Being that our model appears to have incomplete knockout of STIM1, our first priority lies in confirming the extent of the knockout and ensuring a complete knockout of our model. Continuous treatment of the mice with 4OHT is not feasible as it leads to aggressive systemic tumors. There are several approaches that could be used to address this issue. The first is to conduct an orthotopic allograft in syngeneic wild type C57BL/6 mice using tumor tissue from our generated models. Our current models of mice would be treated with 4OHT to induce tumor formation. The tumors would then be excised, and implanted into a wild type C57BL/6 mouse. The allograft mice would be treated with high-dose tamoxifen to induce complete STIM1 and STIM2 knockout. In this manner, tumor growth could be accurately measured, as well as metastasis and possibly immune infiltration. Another model to be considered would be a skin graft. Skin from our generated mice could be grafted to control mice, which would then undergo 4OHT treatment. By starting 4OHT treatment after grafting, our experimental conditions can begin with the same amount of grafted tissue to observe differences in melanoma initiation, as well as progression and metastasis. Furthermore, the graft will prevent any spontaneous tumors from untreated sites, which has confounded the interpretation of data in our studies.

References Cited

1. Siegel, R. L., Miller, K. D. & Jemal, A. Cancer statistics, 2018. *CA. Cancer J. Clin.* **68,** 7–30 (2018).
2. Kosmidis, C. *et al.* Melanoma from Molecular Pathways to Clinical Treatment: An Up to Date Review. *J. Biomed.* **2,** 94–100 (2017).
3. Strickland, L. R., Pal, H. C., Elmets, C. A. & Afaq, F. Targeting drivers of melanoma with synthetic small molecules and phytochemicals. *Cancer Lett.* **359,** 20–35 (2015).
4. Glazer, A. M., Winkelmann, R. R., Farberg, A. S. & Rigel, D. S. Analysis of trends in US melanoma incidence and mortality. *JAMA Dermatology* **153,** 225–226 (2017).
5. Damsky, W., Theodosakis, N. & Bosenberg, M. Melanoma metastasis: new concepts and evolving paradigms. *Oncogene* **33,** 2413–2422 (2014).
6. Winnepenninckx, V. *et al.* Gene expression profiling of primary cutaneous melanoma and clinical outcome. *J. Natl. Cancer Inst.* **98,** 472–482 (2006).
7. Dickson, P. V & Gershenwald, J. E. Staging and prognosis of cutaneous melanoma. *Surg. Oncol. Clin. N. Am.* **20,** 1–17 (2011).
8. Gershenwald, J. E. *et al.* Melanoma Staging: Evidence-Based Changes in the American Joint Committee on Cancer Eighth Edition Cancer Staging Manual. *CA. Cancer J. Clin.* **67,** 472–492 (2017).
9. Shaikh, W. R. *et al.* Melanoma Thickness and Survival Trends in the United States, 1989-2009. *J. Natl. Cancer Inst.* **108,** (2016).
10. Shain, A. H. & Bastian, B. C. From melanocytes to melanomas. *Nat. Rev. Cancer* **16,** 345–358 (2016).
11. Heistein, J. B. & Acharya, U. *Cancer, Melanoma, Malignant*. *StatPearls* (StatPearls Publishing, 2018).
12. Tímár, J., Vizkeleti, L., Doma, V., Barbai, T. & Rásó, E. Genetic progression of malignant melanoma. *Cancer Metastasis Rev.* **35,** 93–107 (2016).
13. Arozarena, I. & Wellbrock, C. Targeting invasive properties of melanoma cells. *FEBS J.* **284,** 2148–2162 (2017).
14. Ma, Q., Dieterich, L. C. & Detmar, M. Biology of Melanoma Metastasis. in *Melanoma* 1–17 (Springer New York, 2017). doi:10.1007/978-1-4614-7322-0_27-1
15. Lund, A. W. *et al.* Lymphatic vessels regulate immune microenvironments in human and murine melanoma. *J. Clin. Invest.* **126,** 3389–3402 (2016).
16. Fidler, I. J. The Biology of Melanoma Metastasis. *J. Dermatology Surg.* **14,** 875–881 (1988).
17. Zbytek, B. *et al.* Current concepts of metastasis in melanoma. *Expert Review of Dermatology* **3,** 569–585 (2008).
18. Chambers, A. F., Groom, A. C. & MacDonald, I. C. Dissemination and growth of cancer cells in metastatic sites. *Nat. Rev. Cancer* **2,** 563–572 (2002).
19. Gupta, G. & Massague, J. Leading Edge Cancer Metastasis: Building a Framework. *Cell* **127,** 679–695 (2006).
20. Nicolson, G. L. Organ Specificity of Tumor Metastasis: Role of Preferential Adhesion, Invasion and Growth of Malignant Cells at Specific Secondary Sites. *Cancer Metastasis Rev.* **7,** 143–188 (1988).
21. Patel, J. K., Didolkar, M. S., Pickren, J. W. & Moore, R. H. Metastatic Pattern of Malignant

Melanoma. A study of 216 Autopsy Cases. *Am. J. Surg.* **135,** 807–810 (1978).
22. Lee, Y.-T. N. Malignant Melanoma: Pattern of Metastasis. *CA- A Cancer J. Clin.* **30,** 137–142 (1980).
23. Reintgen, D. *et al.* The orderly progression of melanoma nodal metastases. *Ann. Surg.* **220,** 759–767 (1994).
24. Nguyen, D. X., Bos, P. D. & Massague, J. Metastasis: from dissemination to organ-specific colonization. *Nat. Rev. Cancer* **9,** 274–284 (2009).
25. Karachaliou, N. *et al.* Melanoma: oncogenic drivers and the immune system. *Ann. Transl. Med.* **3,** 265 (2015).
26. Jakob, J. A. *et al.* NRAS mutation status is an independent prognostic factor in metastatic melanoma. *Cancer* **118,** 4014–4023 (2012).
27. Kunz, M. Oncogenes in melanoma: An update. *European Journal of Cell Biology* **93,** 1–10 (2014).
28. Reddy, B. Y., Miller, D. M. & Tsao, H. Somatic driver mutations in melanoma. *Cancer* **123,** 2104–2117 (2017).
29. Thomas, N. E. *et al.* Association between NRAS and BRAF mutational status and melanoma-specific survival among patients with higher-risk primary melanoma. *JAMA Oncol.* **1,** 359–368 (2015).
30. Bucheit, A. D. *et al.* Complete loss of PTEN protein expression correlates with shorter time to brain metastasis and survival in stage IIIB/C melanoma patients with BRAFV600mutations. *Clin. Cancer Res.* **20,** 5527–5536 (2014).
31. Gorden, A. *et al.* Analysis of BRAF and N-RAS mutations in metastatic melanoma tissues. *Cancer Res.* **63,** 3955–3957 (2003).
32. Perna, D. *et al.* BRAF inhibitor resistance mediated by the AKT pathway in an oncogenic BRAF mouse melanoma model. *Proc. Natl. Acad. Sci.* **112,** E536–E545 (2015).
33. Colombino, M. *et al.* BRAF/NRAS mutation frequencies among primary tumors and metastases in patients with melanoma. *J. Clin. Oncol.* **30,** 2522–2529 (2012).
34. Carlino, M. S. *et al.* Correlation of BRAF and NRAS mutation status with outcome, site of distant metastasis and response to chemotherapy in metastatic melanoma. *Br. J. Cancer* **111,** 292–299 (2014).
35. Bennett, D. C. Genetics of melanoma progression: The rise and fall of cell senescence. *Pigment Cell Melanoma Res.* **29,** 122–140 (2016).
36. Lade-Keller, J. *et al.* Immunohistochemical analysis of molecular drivers in melanoma identifies p16 as an independent prognostic biomarker. *J. Clin. Pathol.* **67,** 520–528 (2014).
37. Abildgaard, C. & Guldberg, P. Molecular drivers of cellular metabolic reprogramming in melanoma. *Trends Mol. Med.* **21,** 164–171 (2015).
38. Griffin, M. *et al.* BRAF inhibitors: resistance and the promise of combination treatments for melanoma. *Oncotarget* **8,** 78174–78192 (2017).
39. Rizos, H. *et al.* BRAF inhibitor resistance mechanisms in metastatic melanoma: Spectrum and clinical impact. *Clin. Cancer Res.* **20,** 1965–1977 (2014).
40. Long, G. V *et al.* Combined BRAF and MEK Inhibition versus BRAF Inhibition Alone in Melanoma. *N. Engl. J. Med.* **371,** 1877–1888 (2014).
41. Roesch, A. Tumor heterogeneity and plasticity as elusive drivers for resistance to MAPK pathway inhibition in melanoma. *Oncogene* **34,** (2014).
42. Li, Z. *et al.* Encorafenib (LGX818), a potent BRAF inhibitor, induces senescence accompanied by autophagy in BRAFV600E melanoma cells. *Cancer Lett.* **370,** 332–344 (2016).
43. Long, G. V. *et al.* Overall survival and durable responses in patients with BRAF V600-mutant metastatic melanoma receiving dabrafenib combined with trametinib. *J. Clin. Oncol.* **34,** 871–878 (2016).

44. Signorelli, J. & Shah Gandhi, A. Cobimetinib: A Novel MEK Inhibitor for Metastatic Melanoma. *Ann. Pharmacother.* **51,** 146–153 (2017).
45. Grimaldi, A. M. *et al.* MEK Inhibitors in the Treatment of Metastatic Melanoma and Solid Tumors. *Am. J. Clin. Dermatol.* **18,** 745–754 (2017).
46. Larkin, J. *et al.* Combined Vemurafenib and Cobimetinib in BRAF -Mutated Melanoma. *N. Engl. J. Med.* **371,** 1867–1876 (2014).
47. Long, G. V *et al.* Increased MAPK reactivation in early resistance to dabrafenib/trametinib combination therapy of BRAF-mutant metastatic melanoma. *Nat. Commun.* **5,** (2014).
48. Wellbrock, C. & Arozarena, I. The Complexity of the ERK/MAP-Kinase Pathway and the Treatment of Melanoma Skin Cancer. *Front. Cell Dev. Biol.* **4,** 1–9 (2016).
49. Wagle, N. *et al.* Dissecting Therapeutic Resistance to RAF Inhibition in Melanoma by Tumor Genomic Profiling. *J Clin Oncol* **29,** 3085–3096 (2011).
50. Wagle, N. *et al.* MAP kinase pathway alterations in BRAF -mutant melanoma patients with acquired resistance to combined RAF/MEK inhibition. *Cancer Discov.* **4,** 61–68 (2014).
51. Van Allen, E. M. *et al.* The Genetic Landscape of Clinical Resistance to RAF Inhibition in Metastatic Melanoma. *Cancer Discov* **4,** 94–109 (2013).
52. Johannessen, C. M. *et al.* COT drives resistance to RAF inhibition through MAP kinase pathway reactivation. *Nature* **468,** 968–974 (2010).
53. Konieczkowski, D. J. *et al.* A melanoma cell state distinction influences sensitivity to MAPK pathway inhibitors. *Cancer Discov.* **4,** 816–827 (2014).
54. Nazarian, R. *et al.* Melanomas acquire resistance to B-RAF(V600E) inhibition by RTK or N-RAS upregulation. *Nature* **468,** (2010).
55. Villanueva, J. *et al.* Acquired Resistance to BRAF Inhibitors Mediated by a RAF Kinase Switch in Melanoma Can Be Overcome by Cotargeting MEK and IGF-1R/PI3K. *Cancer Cell* **18,** 683–695 (2010).
56. Yadav, V. *et al.* Reactivation of Mitogen-activated Protein Kinase (MAPK) pathway by FGF Receptor 3 (FGFR3)/Ras mediates resistance to vemurafenib in human B-RAF V600E mutant melanoma. *J. Biol. Chem.* **287,** 28087–28098 (2012).
57. Meierjohann, S. Hypoxia-Independent Drivers of Melanoma Angiogenesis. *Front. Oncol.* **5,** 1–7 (2015).
58. Chang, F., Syrjänen, S., Tervahauta, A. & Syrjänen, K. Tumourigenesis associated with the p53 tumour suppressor gene. *Br. J. Cancer* **68,** 653–661 (1993).
59. Sinha, R. P. & Häder, D.-P. UV-induced DNA damage and repair: a review. *Photochem. Photobiol. Sci.* **1,** 225–236 (2002).
60. Zhan, Q., Carrier, F. & Fornace Jr., A. J. Induction of cellular p53 activity by DNA-damaging agents and growth arrest. *Mol. Cell. Biol.* **13,** 4242–4250 (1993).
61. Guan, J., Gupta, R. & Filipp, F. V. Cancer systems biology of TCGA SKCM: Efficient detection of genomic drivers in melanoma. *Sci. Rep.* **5,** (2015).
62. Bartek, J., Bartkova, J. & Lukas, J. DNA damage signalling guards against activated oncogenes and tumour progression. *Oncogene* **26,** 7773–7779 (2007).
63. Barker, C. A. & Postow, M. A. Combinations of radiation therapy and immunotherapy for melanoma: A review of clinical outcomes. *Int. J. Radiat. Oncol. Biol. Phys.* **88,** 986–997 (2014).
64. Maverakis, E. *et al.* Metastatic melanoma – A review of current and future treatment options. *Acta Derm. Venereol.* **95,** 516–524 (2015).
65. Senft, D. & Ronai, Z. A. Immunogenic, cellular, and angiogenic drivers of tumor dormancy-a melanoma view. *Pigment Cell Melanoma Res.* **29,** 27–42 (2016).
66. Atkins, B. M. B. *et al.* High-Dose Recombinant Interleukin 2 Therapy for Patients With Metastatic Melanoma: Analysis of 270 Patients Treated. *J. Clin. Oncol.* **17,** 2105–2116 (1999).

67. Rosenberg, S. A. *et al.* Use of Tumor-Infiltrating Lymphocytes and Interleukin-2 in the Immunotherapy of Patients with Metastatic Melanoma. A Preliminary Report. *N. Engl. J. Med.* **319,** 1676–80 (1988).
68. Sanlorenzo, M. *et al.* Melanoma immunotherapy. *Cancer Biology and Therapy* **15,** 665–674 (2014).
69. McCoy, K. D. & Le Gros, G. The role of CTLA-4 in the regulation of T cell immune responses. *Immunol. Cell Biol.* **77,** 1–10 (1999).
70. Ahmed, K. A. *et al.* Clinical outcomes of melanoma brain metastases treated with stereotactic radiation and anti-PD-1 therapy. *Ann. Oncol.* **27,** 434–441 (2016).
71. Weide, B. *et al.* Baseline biomarkers for outcome of melanoma patients treated with pembrolizumab. *Clin. Cancer Res.* **22,** 5487–5496 (2016).
72. Tumeh, P. C. *et al.* PD-1 blockade induces responses by inhibiting adaptive immune resistance. *Nature* **515,** 568–571 (2014).
73. Long, G. V *et al.* Dabrafenib plus trametinib versus dabrafenib monotherapy in patients with metastatic BRAF V600E/K-mutant melanoma: long-term survival and safety analysis of a phase 3 study. *Ann. Oncol.* **28,** 1631–1639 (2017).
74. Robert, C. *et al.* Improved Overall Survival in Melanoma with Combined Dabrafenib and Trametinib. *N. Engl. J. Med.* **372,** 30–39 (2015).
75. Eggermont, A. M. M. *et al.* Adjuvant ipilimumab versus placebo after complete resection of high-risk stage III melanoma (EORTC 18071): A randomised, double-blind, phase 3 trial. *Lancet Oncol.* **16,** 522–530 (2015).
76. Ackerman, A. *et al.* Outcomes of patients with metastatic melanoma treated with immunotherapy prior to or after BRAF inhibitors. *Cancer* **120,** 1695–1701 (2014).
77. Friedl, P. & Wolf, K. Molecular mechanisms of cell migration. *Cancer* **3,** 362–374 (2003).
78. Mattila, P. K. & Lappalainen, P. Filopodia: Molecular architecture and cellular functions. *Nat. Rev. Mol. Cell Biol.* **9,** 446–454 (2008).
79. Albiges-Rizo, C., Destaing, O., Fourcade, B., Planus, E. & Block, M. R. Actin machinery and mechanosensitivity in invadopodia, podosomes and focal adhesions. *J. Cell Sci.* **122,** 3037–3049 (2009).
80. Schoumacher, M., Goldman, R. D., Louvard, D. & Vignjevic, D. M. Actin, microtubules, and vimentin intermediate filaments cooperate for elongation of invadopodia. *J. Cell Biol.* **189,** 541–556 (2010).
81. Ridley, A. J. *et al.* Cell Migration: Integrating Signals from Front to Back. *Science (80-.).* **302,** 1704–1709 (2003).
82. Le Clainche, C. & Carlier, M.-F. Regulation of Actin Assembly Associated With Protrusion and Adhesion in Cell Migration. *Physiol. Rev.* **88,** 488–513 (2008).
83. Yamaguchi, H., Pixley, F. & Condeelis, J. Invadopodia and podosomes in tumor invasion. *Eur. J. Cell Biol.* **85,** 213–218 (2006).
84. Sibony-Benyamini, H. & Gil-Henn, H. Invadopodia: The leading force. *Eur. J. Cell Biol.* **91,** 896–901 (2012).
85. Oser, M. & Condeelis, J. The cofilin activity cycle in lamellipodia and invadopodia. *J. Cell. Biochem.* **108,** 1252–1262 (2009).
86. Bravo-Cordero, J. J. *et al.* A novel spatiotemporal RhoC activation pathway locally regulates cofilin activity at invadopodia. *Curr. Biol.* **21,** 635–644 (2011).
87. Sadok, A. *et al.* Rho kinase inhibitors block melanoma cell migration and inhibit metastasis. *Cancer Res.* **75,** 2272–2284 (2015).
88. Eddy, R. J., Weidmann, M. D., Sharma, V. P. & Condeelis, J. S. Tumor Cell Invadopodia: Invasive Protrusions that Orchestrate Metastasis. *Trends Cell Biol.* **27,** 595–607 (2017).

89. Murphy, D. A. & Courtneidge, S. A. The 'ins' and 'outs' of podosomes and invadopodia: characteristics, formation and function. *Nat. Rev.* **12,** 413–426 (2011).
90. Artym, V. V, Zhang, Y., Seillier-Moiseiwitsch, F., Yamada, K. M. & Mueller, S. C. Dynamic interactions of cortactin and membrane type 1 matrix metalloproteinase at invadopodia: Defining the stages of invadopodia formation and function. *Cancer Res.* **66,** 3034–3043 (2006).
91. Murphy, G. & Gavrilovic, J. Proteolysis and cell migration: Creating a path? *Current Opinion in Cell Biology* **11,** 614–621 (1999).
92. Hood, J. D. & Cheresh, D. A. Role of Integrins in Cell Invasion and Migration. *Nat. Rev. Cancer* **2,** 91–100 (2002).
93. Buccione, R., Orth, J. D. & McNiven, M. A. Foot and Mouth: Podosomes, Invadopodia and Circular Dorsal Ruffles. *Nat. Rev.* **5,** 647–657 (2004).
94. Bowden, E. T., Barth, M., Thomas, D., Glazer I, R. & Mueller, S. C. An invasion-related complex of cortactin, paxillin and PKCμ associates with invadopodia at sites of extracellular matrix degradation. *Oncogene* **18,** 4440–4449 (1999).
95. Pourfarhangi, K. E., Bergman, A. & Gligorijevic, B. ECM cross-linking regulates invadopodia dynamics. *bioRxiv* 198580 (2018). doi:10.1101/198580
96. Clark, E. S. & Weaver, A. M. A new role for cortactin in invadopodia: Regulation of protease secretion. *Eur. J. Cell Biol.* **87,** 581–590 (2008).
97. Mueller, S. C. *et al.* A novel protease-docking function of integrin at invadopodia. *J. Biol. Chem.* **274,** 24947–24952 (1999).
98. Ayala, I., Baldassarre, M., Caldieri, G. & Buccione, R. Invadopodia: A guided tour. *European Journal of Cell Biology* **85,** 159–164 (2006).
99. Hoshino, D. *et al.* Exosome secretion is enhanced by invadopodia and drives invasive behavior. *Cell Rep.* **5,** 1159–1168 (2013).
100. Hood, J. L., San Roman, S., San Roman, S. B. & Wickline, S. A. Exosomes released by melanoma cells prepare sentinel lymph nodes for tumor metastasis. *Cancer Res.* **71,** 1–10 (2011).
101. Paz, H., Pathak, N. & Yang, J. Invading one step at a time: the role of invadopodia in tumor metastasis. *Oncogene* **33,** 4193–4202 (2013).
102. Linder, S. The matrix corroded: podosomes and invadopodia in extracellular matrix degradation. *Trends in Cell Biology* **17,** 107–117 (2007).
103. Pichot, C. S. *et al.* Cdc42-interacting protein 4 promotes breast cancer cell invasion and formation of invadopodia through activation of N-WASp. *Cancer Res.* **70,** 8347–8356 (2010).
104. Parekh, A. & Weaver, A. M. Regulation of invadopodia by mechanical signaling. *Exp. Cell Res.* **343,** 89–95 (2016).
105. Stylli, S. S., Kaye, A. H. & Lock, P. Invadopodia: At the cutting edge of tumour invasion. *J. Clin. Neurosci.* **15,** 725–737 (2008).
106. Yamaguchi, H. *et al.* Lipid rafts and caveolin-1 are required for invadopodia formation and extracellular matrix degradation by human breast cancer cells. *Cancer Res.* **69,** 8594–8602 (2009).
107. Yamaguchi, H. & Oikawa, T. Membrane lipids in invadopodia and podosomes: key structures for cancer invasion and metastasis. *Oncotarget* **1,** 320–8 (2010).
108. Hoshino, D., Branch, K. M. & Weaver, A. M. Signaling inputs to invadopodia and podosomes. *J. Cell Sci.* **126,** 2979–2989 (2013).
109. Stylli, S. S. *et al.* Nck adaptor proteins link Tks5 to invadopodia actin regulation and ECM degradation. *J. Cell Sci.* **122,** 2727–2740 (2009).
110. Weaver, A. M. Invadopodia: Specialized cell structures for cancer invasion. *Clinical and Experimental Metastasis* **23,** 97–105 (2006).
111. Lorenz, M., Yamaguchi, H., Wang, Y., Singer, R. H. & Condeelis, J. Imaging sites of N-WASP activity in lamellipodia and invadopodia of carcinoma cells. *Curr. Biol.* **14,** 697–703 (2004).

112. Monsky, W. L. *et al.* A Potential Marker Protease of Invasiveness, Seprase, Is Localized on Invadopodia of Human Malignant Melanoma Cells. *Cancer Res.* **54,** 5702–5710 (1994).
113. Blanco, A. & Blanco, G. Carbohydrates. in *Medical Biochemistry* (eds. Versteeg-Buschman, L. & Coulthurst, F.) 73–97 (Sara Tenney, 2017). doi:10.1016/B978-0-12-803550-4.00004-5
114. NCBI. L-Fucose. Available at: https://pubchem.ncbi.nlm.nih.gov/compound/6-deoxy-L-galactose#section=Top.
115. Becker, D. J. & Lowe, J. B. Fucose: biosynthesis and biological function in mammals. *Glycobiology* **13,** 41R–53R (2003).
116. Chan, J. Y., Nwokoro, N. A. & Schachter, H. L-Fucose Metabolism in Mammals. *J. Biol. Chem.* **254,** 7060–7068 (1979).
117. Wang, X. & Taniguchi, N. Core Fucosylation of N-Linked Glycan for Fine-Tuning TGF b Receptor Function 122. *Glycosci. Biol. Med.* **2014,** 991–997 (2015).
118. Vanhooren, P. T. & Vandamme, E. J. L-Fucose: occurence, physiological role, chemical, enzymatic and microbial synthesis. *J. Chem. Technol. Biotechnol.* **74,** 479–497 (1999).
119. Ezawa, I. *et al.* A novel p53 target gene FUCA1 encodes a fucosidase and regulates growth and survival of cancer cells. *Cancer Sci.* **107,** n/a-n/a (2016).
120. Listinsky, J. J., Listinsky, C. M., Alapati, V. & Siegal, G. P. Cell surface fucose ablation as a therapeutic strategy for malignant neoplasms. *Adv. Anat. Pathol.* **8,** 330–337 (2001).
121. Agrawal, P. *et al.* A Systems Biology Approach Identifies FUT8 as a Driver of Melanoma Metastasis. *Cancer Cell* **31,** 804–819.e7 (2017).
122. Eccles, M. R., Chatterjee, A. & Rodger, E. J. Identifying drivers of metastasis; towards a systematic approach. *Transl. Cancer Res.* **6,** S1273–S1276 (2017).
123. Blanas, A., Sahasrabudhe, N. M., Rodríguez, E., van Kooyk, Y. & van Vliet, S. J. Fucosylated Antigens in Cancer: An Alliance toward Tumor Progression, Metastasis, and Resistance to Chemotherapy. *Front. Oncol.* **8,** 1–14 (2018).
124. Moriwaki, K. & Miyoshi, E. Fucosylation and gastrointestinal cancer. *World J. Hepatol.* **2,** 151–161 (2010).
125. Fernández-Rodríguez, J., De La Cadena, M. P., Martínez-Zorzano, V. S. & Rodríguez-Berrocal, F. J. Fucose levels in sera and in tumours of colorectal adenocarcinoma patients. *Cancer Lett.* **121,** 147–153 (1997).
126. Christiansen, M. N. *et al.* Cell surface protein glycosylation in cancer. *Proteomics* **14,** 525–546 (2014).
127. Ishihara, H., Massaro, D. J. & Heath, E. C. The Metabolism of L-Fucose. *J. Biol. Chem.* **243,** 1103–1109 (1968).
128. Lau, E. *et al.* The transcription factor ATF2 promotes melanoma metastasis by suppressing protein fucosylation. *Sci. Signal.* **8,** 1–12 (2015).
129. de Vries, T., Knegtel, R. M. A., Holmes, E. H. & Macher, B. A. Fucosyltransferases: structure/function studies. *Glycobiology* **11,** 119R–128R (2001).
130. Mollicone, R. *et al.* Activity, splice variants, conserved peptide motifs, and phylogeny of two New α1,3-fucosyltransferase families (FUT10 and FUT11). *J. Biol. Chem.* **284,** 4723–4738 (2009).
131. Prestegard, J. H., Liu, J. & Widmalm, G. Oligosaccharides and Polysaccharides. in *Essentials of Glycobiology* (Cold Spring Harbor Laboratory Press, 2015). doi:10.1101/GLYCOBIOLOGY.3E.003
132. Mcnaught, A. D., Royal, T., House, T. G. & Park, S. Nomenclature of Carbohydrates. *Pure Appl. Chem.* 1–91 (1996).
133. Tu, Z., Lin, Y.-N. & Lin, C.-H. Development of fucosyltransferase and fucosidase inhibitors. *Chem. Soc. Rev.* **42,** 4459 (2013).
134. Liang, W. *et al.* Core fucosylation of the T cell receptor is required for T cell activation. *Front. Immunol.* **9,** 1–14 (2018).

135. Miyoshi, E., Moriwaki, K. & Nakagawa, T. Biological Function of Fucosylation in Cancer Biology. *J. Biochem.* **143,** 725–729 (2008).
136. Isozaki, T. *et al.* Fucosyltransferase 1 mediates angiogenesis, cell adhesion and rheumatoid arthritis synovial tissue fibroblast proliferation. *Arthritis Res. Ther.* **16,** R28 (2014).
137. Gao, N. *et al.* C-Jun transcriptionally regulates alpha 1, 2-fucosyltransferase 1 (FUT1) in ovarian cancer. *Biochimie* **107,** 286–292 (2014).
138. Weiss, F. U. *et al.* Fucosyltransferase 2 (FUT2) non-secretor status and blood group B are associated with elevated serum lipase activity in asymptomatic subjects, and an increased risk for chronic pancreatitis: A genetic association study. *Gut* **64,** 646–656 (2015).
139. McGovern, D. P. B. *et al.* Fucosyltransferase 2 (FUT2) non-secretor status is associated with Crohn's disease. *Hum. Mol. Genet.* **19,** 3468–3476 (2010).
140. Lowe, J. B. & Marth, J. D. A Genetic Approach to Mammalian Glycan Function. *Annu. Rev. Biochem.* **72,** 643–691 (2003).
141. Holst, S., Wuhrer, M. & Rombouts, Y. Glycosylation characteristics of colorectal cancer. *Adv. Cancer Res.* **126,** 203–256 (2015).
142. Gorelik, E., Xu, F., Henion, T., Anaraki, F. & Galili, U. Reduction of metastatic properties of BL6 melanoma cells expressing terminal fucoseα1-2-galactose after α1,2-fucosyltransferase cDNA transfection. *Cancer Res.* **57,** 332–336 (1997).
143. Keeley, T., Lin, S., Lester, D. K., Lau, E. K. & Yang, S. The fucose salvage pathway inhibits invadopodia formation and extracellular matrix degradation in melanoma cells. *PLoS One* **13,** e0199128 (2018).
144. Furukawa, K. *et al.* Lewis y antigen is expressed in oral squamous cell carcinoma cell lines and tissues, but disappears in the invasive regions leading to the enhanced malignant properties irrespective of sialyl-Lewis x. *Glycoconj. J.* **30,** 585–597 (2013).
145. Chandrasekaran, E. V *et al.* Potential tumor markers for human gastric cancer: an elevation of glycan:sulfotransferases and a concomitant loss of alpha1,2-fucosyltransferase activities. *J. Cancer Res. Clin. Oncol.* **133,** 599–611 (2007).
146. Aubert, M. *et al.* Restoration of alpha(1,2) fucosyltransferase activity decreases adhesive and metastatic properties of human pancreatic cancer cells. *Cancer Res.* **60,** 1449–56 (2000).
147. Mathieu, S. *et al.* Transgene Expression of α(1,2)-Fucosyltransferase-I (FUT1) in Tumor Cells Selectively Inhibits Sialyl- Lewis x Expression and Binding to E-Selectin without Affecting Synthesis of Sialyl-Lewis a or Binding to P-Selectin. *Am. J. Pathol.* **164,** 371–383 (2004).
148. Hutchinson, W. L., Du, M. -Q, Johnson, P. J. & Williams, R. Fucosyltransferases: Differential plasma and tissue alterations in hepatocellular carcinoma and cirrhosis. *Hepatology* **13,** 683–688 (1991).
149. Laidler, P. *et al.* Characterization of glycosylation and adherent properties of melanoma cell lines. *Cancer Immunol. Immunother.* **55,** 112–118 (2006).
150. Yuan, K. *et al.* Alterations in human breast cancer adhesion-motility in response to changes in cell surface glycoproteins displaying alpha-L-fucose moieties. *Int. J. Oncol.* **32,** 797–807 (2008).
151. Carrascal, M. A. *et al.* Inhibition of fucosylation in human invasive ductal carcinoma reduces E-selectin ligand expression, cell proliferation, and ERK1/2 and p38 MAPK activation. *Mol. Oncol.* **12,** 579–593 (2018).
152. Guo, Q. *et al.* Functional analysis of alpha1,3/4-fucosyltransferase VI in human hepatocellular carcinoma cells. *Biochem. Biophys. Res. Commun.* **417,** 311–317 (2012).
153. Sanders, D. S. A., Milne, D. M. & Kerr, M. A. The expression of Lewisa and Lewisb antigens reflects changes in fucosylation between normal and neoplastic cervical squamous epithelium. *J. Pathol.* **162,** 23–28 (1990).
154. Escrevente, C. *et al.* Different expression levels of alpha3/4 fucosyltransferases and Lewis

determinants in ovarian carcinoma tissues and cell lines. *Int. J. Oncol.* **29,** 557–566 (2006).
155. Mas, E. *et al.* Fucosyltransferase activities in human pancreatic tissue: comparative study between cancer tissues and established tumoral cell lines. *Glycobiology* **8,** 605–613 (1998).
156. Aubert, M. *et al.* Peritoneal colonization by human pancreatic cancer cells is inhibited by antisense FUT3 sequence. *Int. J. Cancer* **88,** 558–565 (2000).
157. Watanabe, K. *et al.* Fucosylation is associated with the malignant transformation of intraductal papillary mucinous neoplasms: a lectin microarray-based study. *Surg. Today* **46,** 1217–1223 (2016).
158. Aziz, F., Gao, W. & Yan, Q. Fucosyltransferase-4 and Oligosaccharide Lewis Y Antigen as potentially Correlative Biomarkers of Helicobacter pylori CagA Associated Gastric Cancer. *Pathol. Oncol. Res.* **23,** 173–179 (2017).
159. Padró, M., Cobler, L., Garrido, M. & De Bolós, C. Down-regulation of FUT3 and FUT5 by shRNA alters Lewis antigens expression and reduces the adhesion capacities of gastric cancer cells. *Biochim. Biophys. Acta - Gen. Subj.* **1810,** 1141–1149 (2011).
160. Ogawa, J., Inoue, H. & Koide, S. a-2,3-Sialyltransferase Type 3N and a-1,3-Fucosyltransferase Type VII Are Related to Sialyl Lewisx Synthesis and Patient Survival from Lung Carcinoma. *Cancer* **79,** 1678–1685 (1997).
161. Barthel, S. R. *et al.* Alpha 1,3 fucosyltransferases are master regulators of prostate cancer cell trafficking. *Proc. Natl. Acad. Sci.* **106,** 19491–19496 (2009).
162. Inaba, Y. *et al.* Gene transfer of α1,3-fucosyltransferase increases tumor growth of the PC-3 human prostate cancer cell line through enhanced adhesion to prostatic stromal cells. *Int. J. Cancer* **107,** 949–957 (2003).
163. Yin, X., Rana, K., Ponmudi, V. & King, M. R. Knockdown of fucosyltransferase III disrupts the adhesion of circulating cancer cells to E-selectin without affecting hematopoietic cell adhesion. *Carbohydr. Res.* **345,** 2334–2342 (2010).
164. Ohyama, C., Tsuboi, S. & Fukuda, M. Dual roles of sialyl Lewis X oligosaccharides in tumor metastasis and rejection by natural killer cells. *EMBO J.* **18,** 1516–1525. (1999).
165. Fukuda, M. N. *et al.* A peptide mimic of E-selectin ligand inhibits sialyl Lewis X-dependent lung colonization of tumor cells. *Cancer Res.* **60,** 450–456 (2000).
166. Zhang, J. *et al.* Sialyl Lewis X-dependent lung colonization of B16 melanoma cells through a selectin-like endothelial receptor distinct from E- or P-selectin. *Cancer Res.* **62,** 4194–4198 (2002).
167. Liu, F., Zhang, Y., Zhang, X.-Y. & Chen, H.-L. Transfection of the nm23-H1 gene into human hepatocarcinoma cell line inhibits the expression of sialyl Lewis X, alpha1,3 fucosyltransferase VII, and metastatic potential. *J. Cancer Res. Clin. Oncol.* **128,** 189–96 (2002).
168. Hirakawa, M. *et al.* Fucosylated TGF-β receptors transduces a signal for epithelial-mesenchymal transition in colorectal cancer cells. *Br. J. Cancer* **110,** 156–163 (2014).
169. Shan, X. *et al.* Ginsenoside Rg3-induced EGFR/MAPK pathway deactivation inhibits melanoma cell proliferation by decreasing FUT4/LeY expression. *Int. J. Oncol.* **46,** 1667–1676 (2015).
170. Xu, J., Lamouille, S. & Derynck, R. TGF-β-induced epithelial to mesenchymal transition. *Cell Res.* **19,** 156–172 (2009).
171. Wang, H., Wang, Q.-Y., Zhang, Y., Shen, Z.-H. & Chen, H.-L. Alpha1,3 Fucosyltransferase-VII modifies the susceptibility of apoptosis induced by ultraviolet and retinoic acid in human hepatocarcinoma cells. *Glycoconj. J.* **24,** 207–20 (2007).
172. Wi, G. R. *et al.* A lectin-based approach to detecting carcinogenesis in breast tissue. *Oncol. Lett.* **11,** 3889–3895 (2016).
173. Ji, J. *et al.* Expression of alpha 1,6-fucosyltransferase 8 in hepatitis B virus-related hepatocellular carcinoma influences tumour progression. *Dig. liver Dis.* **45,** 414–421 (2013).

174. Takahasi, T. *et al.* α1,6 Fucosyltransferase is Highly and Specifically Expressed in Human Ovarian Serous Adenocarcimomas. *Int. J. Cancer* **88,** 914–919 (2000).
175. Kim, H. J. *et al.* Aberrant sialylation and fucosylation of intracellular proteins in cervical tissue are critical markers of cervical carcinogenesis. *Oncol. Rep.* **31,** 1417–1422 (2014).
176. Osumi, D. *et al.* Core fucosylation of E-cadherin enhances cell-cell adhesion in human colon carcinoma WiDr cells. *Cancer Sci.* **100,** 888–895 (2009).
177. Osuga, T. *et al.* Relationship between increased fucosylation and metastatic potential in colorectal cancer. *J. Natl. Cancer Inst.* **108,** (2016).
178. Liu, L. *et al.* The Identification and Characterization of Novel N-glycan-based Biomarkers in Gastric Cancer. *PLoS One* **8,** (2013).
179. Kim, Y. S. *et al.* Identification of target proteins of N-acetylglucosaminyltransferase V and fucosyltransferase 8 in human gastric tissues by glycomic approach. *Proteomics* **4,** 3353–3358 (2004).
180. Zhao, Y. P. *et al.* Decreased core-fucosylation contributes to malignancy in gastric cancer. *PLoS One* **9,** (2014).
181. Honma, R. *et al.* Expression of fucosyltransferase 8 is associated with an unfavorable clinical outcome in non-small cell lung cancers. *Oncology* **88,** 298–308 (2015).
182. Chen, C.-Y. *et al.* Fucosyltransferase 8 as a functional regulator of non-small cell lung cancer. *Proc. Natl. Acad. Sci.* **110,** 630–635 (2013).
183. Geng, F., Zhi SHI, B., Feng YUAN, Y. & Zhong, X. W. The expression of core fucosylated E-cadherin in cancer cells and lung cancer patients: prognostic implications. *Cell Res.* **14,** 423–433 (2004).
184. Wang, X. *et al.* Overexpression of α (1,6) fucosyltransferase associated with aggressive prostate cancer. *Glycobiology* **24,** 935–944 (2014).
185. Tu, C. F., Wu, M. Y., Lin, Y. C., Kannagi, R. & Yang, R. B. FUT8 promotes breast cancer cell invasiveness by remodeling TGF-β receptor core fucosylation. *Breast Cancer Res.* **19,** (2017).
186. Wang, Y. *et al.* Loss of α1,6-fucosyltransferase inhibits chemical-induced hepatocellular carcinoma and tumorigenesis by down-regulating several cell signaling pathways. *FASEB J.* **29,** 3217–3227 (2015).
187. Mehta, A. *et al.* Intrinsic hepatocyte dedifferentiation is accompanied by upregulation of mesenchymal markers, protein sialylation and core alpha 1,6 linked fucosylation. *Sci. Rep.* **6,** (2016).
188. Zhou, Y. *et al.* Inhibition of fucosylation by 2-fluorofucose suppresses human liver cancer HepG2 cell proliferation and migration as well as tumor formation. *Sci. Rep.* **7,** (2017).
189. Hu, P. *et al.* E-cadherin core fucosylation regulates nuclear beta-catenin accumulation in lung cancer cells. *Glycoconj. J.* **25,** 843–50 (2008).
190. Liu, Y.-C. *et al.* Sialylation and fucosylation of epidermal growth factor receptor suppress its dimerization and activation in lung cancer cells. *Proc. Natl. Acad. Sci.* **108,** 11332–11337 (2011).
191. Sun, J. *et al.* STIM1- and Orai1-mediated Ca2+oscillation orchestrates invadopodium formation and melanoma invasion. *J. Cell Biol.* **207,** 535–548 (2014).
192. Sun, J. *et al.* GATA3 transcription factor abrogates Smad4 transcription factor-mediated fascin overexpression, invadopodium formation, and breast cancer cell invasion. *J. Biol. Chem.* **288,** 36971–36982 (2013).
193. Yang, S., Zhang, J. J. & Huang, X.-Y. Methods in Molecular Biology. in *Methods in Molecular Biology* (ed. Yi Zheng) 221–228 (Springer, 2012).
194. Xu, L. *et al.* Gene Expression Changes in an Animal Melanoma Model Correlate with Aggressiveness of Human Melanoma Metastases. *Mol. Cancer Res.* **6,** 760–9 (2008).
195. Kabbarah, O. *et al.* Integrative Genome Comparison of Primary and Metastatic Melanomas. *PLoS One* **5,** (2010).

196. Riker, A. I. *et al.* The gene expression profiles of primary and metastatic melanoma yields a transition point of tumor progression and metastasis. *BMC Med. Genomics* **1,** 13 (2008).
197. Raskin, L. *et al.* Transcriptome Profiling Identifies HMGA2 as a Biomarker of Melanoma Progression and Prognosis. *J. Invest. Dermatol.* **133,** 2585–2592 (2013).
198. Sun, J. *et al.* Fascin protein is critical for transforming growth factor β protein-induced invasion and filopodia formation in spindle-shaped tumor cells. *J. Biol. Chem.* **286,** 38865–38875 (2011).
199. Lin, S. *et al.* Monoubiquitination inhibits the actin bundling activity of fascin. *J. Biol. Chem.* **291,** 27323–27333 (2016).
200. Mullen, J. *et al.* Fucose Therapy in Rat Mammary Cancer II. *J. Surg. Oncol.* **5,** 61–69 (1973).
201. Ghosh, K., Yadav, N. & Kanade, S. R. A novel L-fucose-binding lectin from Fenneropenaeus indicus induced cytotoxicity in breast cancer cells Biji Chatterjee. *J. Biochem.* **161,** 87–97 (2017).
202. Zhang, Z., Teruya, K., Eto, H. & Shirahata, S. Induction of Apoptosis by Low-Molecular-Weight Fucoidan through Calcium- and Caspase-Dependent Mitochondrial Pathways in MDA-MB-231 Breast Cancer Cells. *Biosci. Biotechnol. Biochem.* **77,** 235–242 (2013).
203. Chen, S., Zhao, Y., Zhang, Y. & Zhang, D. Fucoidan induces cancer cell apoptosis by modulating the endoplasmic reticulum stress cascades. *PLoS One* **9,** (2014).
204. Tsao, S. M. & Hsu, H. Y. Fucose-containing fraction of Ling-Zhi enhances lipid rafts-dependent ubiquitination of TGFβ receptor degradation and attenuates breast cancer tumorigenesis. *Sci. Rep.* **6,** (2016).
205. Zhang, Z., Teruya, K., Yoshida, T., Eto, H. & Shirahata, S. Fucoidan extract enhances the anti-cancer activity of chemotherapeutic agents in MDA-MB-231 and MCF-7 breast cancer cells. *Mar. Drugs* **11,** 81–98 (2013).
206. Wang, C. Y. *et al.* Antioxidant activity and growth inhibition of human colon cancer cells by crude and purified fucoidan preparations extracted from Sargassum cristaefolium. *J. Food Drug Anal.* **23,** 766–777 (2015).
207. Usoltseva, R. V. *et al.* Polysaccharides from brown algae Sargassum duplicatum: the structure and anticancer activity in vitro. *Carbohydr. Polym.* **175,** 547–556 (2017).
208. Usoltseva, R. V. *et al.* Structural characteristics and anticancer activity in vitro of fucoidan from brown alga Padina boryana. *Carbohydr. Polym.* **184,** 260–268 (2018).
209. Ale, M. T., Maruyama, H., Tamauchi, H., Mikkelsen, J. D. & Meyer, A. S. Fucose-containing sulfated polysaccharides from brown seaweeds inhibit proliferation of melanoma cells and induce apoptosis by activation of caspase-3 in vitro. *Mar. Drugs* **9,** 2605–2621 (2011).
210. Ciołczyk-Wierzbicka, D. *et al.* Expression of fucosyltransferases contributes to melanoma invasive phenotype. *Med. Chem. (Los. Angeles).* **3,** 418–424 (2007).
211. Sawanobori, A., Moriwaki, K., Takamatsu, S., Kamada, Y. & Miyoshi, E. A glycoproteomic approach to identify novel glycomarkers for cancer stem cells. *Proteomics* **16,** 3073–3080 (2016).
212. Smith, P. L. *et al.* Conditional control of selectin ligand expression and global fucosylation events in mice with a targeted mutation at the FX locus. *J. Cell Biol.* **158,** 801–815 (2002).
213. Senbanjo, L. T. & Chellaiah, M. A. CD44: A Multifunctional Cell Surface Adhesion Receptor Is a Regulator of Progression and Metastasis of Cancer Cells. *Front. Cell Dev. Biol.* **5,** (2017).
214. Dietrich, A., Tanczos, E., Vanscheidt, W., Schöpf, E. & Simon, J. C. High CD44 surface expression on primary tumours of malignant melanoma correlates with increased metastatic risk and reduced survival. *Eur. J. Cancer Part A* **33,** 926–930 (1997).
215. Seiter, S. *et al.* Expression of CD44 variant isoforms in malignant melanoma. *Clin. Cancer Res.* **2,** 447–456 (1996).
216. Taniguchi, N. *et al.* A glycomic approach to the identification and characterization of glycoprotein function in cells transfected with glycosyltransferase genes. *Proteomics* **1,** 239–247 (2001).
217. Mori, H. *et al.* CD44 directs membrane-type 1 matrix metalloproteinase to lamellipodia by

associating with its hemopexin-like domain. *EMBO J.* **21,** 3949–3959 (2002).
218. Vikesaa, J. *et al.* RNA-binding IMPs promote cell adhesion and invadopodia formation. *EMBO J.* **25,** 1456–1468 (2006).
219. Listinsky, J. J., Siegal, G. P. & Listinsky, C. M. The emerging importance of α-L-fucose in human breast cancer: a review. *Am. J. Transl. Res.* **3,** 292–322 (2011).
220. Labarriere, N. *et al.* H Blood Group Antigen Carried by CD44V Modulates Tumorigenicity of Rat Colon Carcinoma Cells. *Cancer Res.* **54,** 6275–6281 (1994).
221. Nakahara, H. *et al.* Activation of β1 integrin signaling stimulates tyrosine phosphorylation of p190(RhoGap) and membrane-protrusive activities at invadopodia. *J. Biol. Chem.* **273,** 9–12 (1998).
222. Link-Lenczowski, P. & Lityńska, A. Glycans in melanoma screening. Part 2. Towards the understanding of integrin N-glycosylation in melanoma. *Biochem. Soc. Trans.* **39,** 374–7 (2011).
223. Zhao, Y. *et al.* Deletion of core fucosylation on α3β1 integrin down-regulates its functions. *J. Biol. Chem.* **281,** 38343–38350 (2006).
224. Zipin, A. *et al.* Tumor-Microenvironment Interactions: The Fucose-Generating FX Enzyme Controls Adhesive Properties of Colorectal Cancer Cells. *Cancer Res.* **64,** 6571–6578 (2004).
225. Lu, Y. *et al.* Calreticulin activates β1 integrin via fucosylation by fucosyltransferase 1 in J82 human bladder cancer cells. *Biochem. J.* **460,** 69–78 (2014).
226. Pocheć, E., Lityńska, A., Amoresano, A. & Casbarra, A. Glycosylation profile of integrin α3β1changes with melanoma progression. *Biochim. Biophys. Acta - Mol. Cell Res.* **1643,** 113–123 (2003).
227. Liang, J., Gao, W. & Cai, L. Fucosyltransferase VII promotes proliferation via the EGFR/AKT/mTOR pathway in A549 cells. *Onco. Targets. Ther.* **10,** 3971–3978 (2017).
228. Zheng, Q. *et al.* miR-200b inhibits proliferation and metastasis of breast cancer by targeting fucosyltransferase IV and α1,3-fucosylated glycans. *Oncogenesis* **6,** e358 (2017).
229. Newton, A. C., Bootman, M. D. & Scott, J. D. Second Messengers. *Cold Spring Harb. Perspect. Biol.* **8,** a005926 (2016).
230. Déliot, N. & Constantin, B. Plasma membrane calcium channels in cancer: Alterations and consequences for cell proliferation and migration. *Biochim. Biophys. Acta - Biomembr.* **1848,** 2512–2522 (2015).
231. Humeau, J. *et al.* Calcium signaling and cell cycle: Progression or death. *Cell Calcium* **70,** 3–15 (2018).
232. Kohn, E. C., Alessandro, R., Spoonster, J., Wersto, R. P. & Liotta, L. A. Angiogenesis: role of calcium-mediated signal transduction. *Proc. Natl. Acad. Sci.* **92,** 1307–11 (1995).
233. Redondo, P. C. & Rosado, J. A. Store-Operated Calcium Entry: Unveiling the Calcium Handling Signalplex. *Int. Rev. Cell Mol. Biol.* **316,** 183–226 (2015).
234. Hogan, P. G. & Rao, A. Store-operated calcium entry: Mechanisms and modulation. *Biochem. Biophys. Res. Commun.* **460,** 40–49 (2015).
235. Krebs, J., Agellon, L. B. & Michalak, M. Ca2+ homeostasis and endoplasmic reticulum (ER) stress: An integrated view of calcium signaling. *Biochem. Biophys. Res. Commun.* **460,** 114–121 (2015).
236. Jardín, I. *et al.* Fine-tuning of store-operated calcium entry by fast and slow Ca2+-dependent inactivation: Involvement of SARAF. *Biochim. Biophys. Acta - Mol. Cell Res.* **1865,** 463–469 (2018).
237. Faouzi, M., Kilch, T., Horgen, F. D., Fleig, A. & Penner, R. The TRPM7 channel kinase regulates store-operated calcium entry. *J. Physiol.* **595,** 3165–3180 (2017).
238. Ambudkar, I. S., Brito De Souza, L. & Ong, H. L. TRPC1, Orai1, and STIM1 in SOCE: Friends in tight spaces. *Cell Calcium* **63,** 33–39 (2017).
239. Prakriya, M. & Lewis, R. S. Store-Operated Calcium Channels. *Physiol. Rev.* **95,** 1383–1436 (2015).
240. Giorgi, C., Danese, A., Missiroli, S., Patergnani, S. & Pinton, P. Calcium Dynamics as a Machine for

Decoding Signals. *Trends in Cell Biology* (2018). doi:10.1016/j.tcb.2018.01.002
241. Pinto, M. C. X. *et al.* Calcium signaling and cell proliferation. *Cell. Signal.* **27,** 2139–2149 (2015).
242. Wu, M. M., Buchanan, J., Luik, R. M. & Lewis, R. S. Ca 2+ store depletion causes STIM1 to accumulate in ER regions closely associated with the plasma membrane. *J. Cell Biol.* **174,** 803–813 (2006).
243. Stewart, T. A., Yapa, K. T. D. S. & Monteith, G. R. Altered calcium signaling in cancer cells. *Biochimica et biophysica acta* **1848,** 2502–2511 (2015).
244. Yang, S., Zhang, J. J. & Huang, X. Y. Orai1 and STIM1 Are Critical for Breast Tumor Cell Migration and Metastasis. *Cancer Cell* **15,** 124–134 (2009).
245. Chen, Y.-F. *et al.* Calcium store sensor stromal-interaction molecule 1-dependent signaling plays an important role in cervical cancer growth, migration, and angiogenesis. *Proc. Natl. Acad. Sci.* **108,** 15225–15230 (2011).
246. Chen, Y. T. *et al.* Microtubule-associated histone deacetylase 6 supports the calcium store sensor STIM1 in mediating malignant cell behaviors. *Cancer Res.* **73,** 4500–4509 (2013).
247. Xu, J.-M. *et al.* Stromal interaction molecule 1 plays an important role in gastric cancer progression. *Oncol. Rep.* **35,** 3496–504 (2016).
248. Xia, J. *et al.* Elevated Orai1 and STIM1 expressions upregulate MACC1 expression to promote tumor cell proliferation, metabolism, migration, and invasion in human gastric cancer. *Cancer Lett.* **381,** 31–40 (2016).
249. Hooper, R., Zaidi, M. R. & Soboloff, J. The heterogeneity of store-operated calcium entry in melanoma. *Sci. China Life Sci.* **59,** 764–769 (2016).
250. Wang, J. Y. *et al.* STIM1 overexpression promotes colorectal cancer progression, cell motility and COX-2 expression. *Oncogene* **34,** 4358–4367 (2015).
251. Zhang, Z. *et al.* STIM1, a direct target of microRNA-185, promotes tumor metastasis and is associated with poor prognosis in colorectal cancer. *Oncogene* **34,** 4808–4820 (2015).
252. Wong, H. S.-C. & Chang, W.-C. Correlation of clinical features and genetic profiles of stromal interaction molecule 1 (STIM1) in colorectal cancers. *Oncotarget* **6,** 42169–42182 (2015).
253. Wang, Y. *et al.* Elevated expression of STIM1 is involved in lung tumorigenesis. *Oncotarget* **5,** 86584–86593 (2016).
254. Wang, Y. *et al.* STIM1 silencing inhibits the migration and invasion of A549 cells. *Mol. Med. Rep.* **16,** 3283–3289 (2017).
255. Yang, N. *et al.* Blockade of store-operated Ca2+entry inhibits hepatocarcinoma cell migration and invasion by regulating focal adhesion turnover. *Cancer Lett.* **330,** 163–169 (2013).
256. Zhou, Y. *et al.* Suppression of STIM1 inhibits the migration and invasion of human prostate cancer cells and is associated with PI3K/Akt signaling inactivation. *Oncol. Rep.* **38,** 2629–2636 (2017).
257. Umemura, M. *et al.* Store-operated Ca2+ entry (SOCE) regulates melanoma proliferation and cell migration. *PLoS One* **9,** (2014).
258. Cheon, D.-J. & Orsulic, S. Mouse Models of Cancer. *Annu. Rev. Pathol. Mech. Dis.* **6,** 95–119 (2011).
259. Sharma, A., Kuzu, O. F., Nguyen, F. D., Sharma, A. & Noory, M. Current State of Animal (Mouse) Modeling in Melanoma Research. *Cancer Growth Metastasis* **8,** 81 (2015).
260. Rozenberg, G. I., Monahan, K. B., Torrice, C., Bear, J. E. & Sharpless, N. E. Metastasis in an orthotopic murine model of melanoma is independent of RAS/RAF mutation. *Melanoma Res.* **20,** 361–71 (2010).
261. Bobek, V. *et al.* A Clinically Relevant, Syngeneic Model of Spontaneous, Highly Metastatic B16 Mouse Melanoma. *Anticancer Res.* **30,** 4799–4808 (2010).
262. Rgen, J. *et al.* Mouse models for melanoma: a personal perspective. *Exp. Dermatol.* **19,** 157–164 (2010).

263. Zhang, Y. *et al.* Fate of allogeneic or syngeneic cells in intravenous or portal vein injection: Possible explanation for the mechanism of tolerance induction by portal vein injection. *Eur. J. Immunol.* **24,** 1558–1565 (1994).
264. Fidler, I. J. & Nicolson, G. L. Organ Selectivity for Implantation Survival and Growth of B16 Melanoma Variant Tumor Lines 2. *J. Natl. Cancer Inst.* **57,** 1199–1202 (1976).
265. Arguello, F., Baggs, R. B. & Frantz3, C. N. *A Murine Model of Experimental Metastasis to Bone and Bone Marrow*. *Cancer Research* **48,** (1988).
266. Pérez-Guijarro, E., Day, C.-P., Merlino, G. & Zaidi, M. R. Genetically engineered mouse models of melanoma. *Cancer* **123,** 2089–2103 (2017).
267. Lesche, R. *et al.* Cre/loxP-mediated inactivation of the murine Pten tumor suppressor gene. *Genesis* **32,** 148–149 (2002).
268. Dankort, D. *et al.* A new mouse model to explore the initiation , progression , and therapy tumors. *Genes Dev.* **21,** 379–384 (2007).
269. Dankort, D. *et al.* BrafV600Ecooperates with Pten loss to induce metastatic melanoma. *Nat. Genet.* **41,** 544–552 (2009).
270. Oh-hora, M. *et al.* Dual functions for the endoplasmic reticulum calcium sensors STIM1 and STIM2 in T cell activation and tolerance. *Nat. Immunol.* **9,** 432–443 (2008).
271. Weidinger, C., Shaw, P. J. & Feske, S. STIM1 and STIM2-mediated Ca2+ influx regulates antitumour immunity by CD8+ T cells. *EMBO Mol. Med.* **5,** 1311–1321 (2013).
272. Matsumoto, M. *et al.* The Calcium Sensors STIM1 and STIM2 Control B Cell Regulatory Function through Interleukin-10 Production. *Immunity* **34,** 703–714 (2011).
273. Zamponi, G. W. Targeting voltage-gated calcium channels in neurological and phychiatric diseases. *Nat. Rev.* **15,** 19–34 (2016).
274. Aytes, A. *et al.* Stromal interaction molecule 2 (STIM2) is frequently overexpressed in colorectal tumors and confers a tumor cell growth suppressor phenotype. *Mol. Carcinog.* **51,** 746–753 (2012).
275. Bergthorsson, J. T. *et al.* A genome-wide study of allelic imbalance in human testicular germ cell tumors using microsatellite markers. *Cancer Genet. Cytogenet.* **164,** 1–9 (2006).
276. Perri, P. *et al.* Weak linkage at 4p16 to predisposition for human neuroblastoma. *Oncogene* **21,** 8356–8360 (2002).
277. Pershouse, M. A. *et al.* Deletion mapping of chromosome 4 in head and neck squamous cell carcinoma. *Oncogene* **14,** 369–373 (1997).
278. Polascik, T. J., Cairns, P., Chang, W. Y., Schoenberg, M. P. & Sidransky, D. Distinct regions of allelic loss on chromosome 4 in human primary bladder carcinoma. *Cancer Res.* **55,** 5396–9 (1995).
279. Shivapurkar, N. *et al.* Multiple Regions of Chromosome 4 Demonstrating Allelic Losses in Breast Carcinomas. *Cancer Res.* **59,** 3576–3580 (1999).
280. Xu, X. L. *et al.* Inactivation of Human SRBC , Located within the 11p15 . 5-p15 . 4 Tumor Suppressor Region , in Breast and Lung Cancers 1. *Cancer Res.* **61,** 7943–7949 (2001).
281. Hu, R.-J. *et al.* A 2.5-Mb Transcript Map of a Tumor-Suppressing Subchromosomal Transferable Fragment from 11p15.5, and Isolation and Sequence Analysis of Three Novel Genes. *Genomics* **46,** 9–17 (1997).
282. Reid, L. H. *et al. Localization of a tumor suppressor gene in 11p15.5 using the G401 Wilms' tumor assay*. *Human Molecular Genetics* **5,** (1996).
283. Sabbioni, S. *et al.* Exon structure and promoter identification of STIM1 (alias GOK), a human gene causing growth arrest of the human tumor cell lines G401 and RD. *Cytogenet. Cell Genet.* **86,** 214–8 (1999).
284. Darbellay, B., Arnaudeau, S., Bader, C. R., Konig, S. & Bernheim, L. STIM1L is a new actin-binding splice variant involved in fast repetitive Ca2+ release. *J. Cell Biol.* **194,** 335–46 (2011).

285. Bogeski, I., Kilch, T. & Niemeyer, B. A. ROS and SOCE: recent advances and controversies in the regulation of STIM and Orai. *J. Physiol.* **590,** 4193–4200 (2012).
286. Xu, Y. *et al.* STIM1 accelerates cell senescence in a remodeled microenvironment but enhances the epithelial-to-mesenchymal transition in prostate cancer. *Sci. Rep.* **5,** 1–17 (2015).
287. Chiu, W.-T., Tang, M.-J., Jao, H.-C. & Shen, M.-R. Soft substrate up-regulates the interaction of STIM1 with store-operated Ca2+ channels that lead to normal epithelial cell apoptosis. *Mol. Biol. Cell* **19,** 2220–30 (2008).
288. Flourakis, M. *et al.* Orai1 contributes to the establishment of an apoptosis-resistant phenotype in prostate cancer cells. *Cell Death Dis.* **1,** (2010).
289. Abeele, F. Vanden *et al.* Bcl-2-dependent modulation of Ca2+ homeostasis and store-operated channels in prostate cancer cells. *Cancer Cell* **1,** 169–179 (2002).
290. Li, G. *et al.* Suppression of {STIM1} inhibits human glioblastoma cell proliferation and induces {G0/G1} phase arrest. *J. Exp. Clin. Cancer Res.* **32,** 1–9 (2013).
291. Aulestia, F. J. *et al.* Quiescence status of glioblastoma stem-like cells involves remodelling of Ca2+signalling and mitochondrial shape. *Sci. Rep.* **8,** 1–12 (2018).
292. Massagué, J. TGFβ in Cancer. *Cell* **134,** 215–230 (2008).
293. Sridurongrit, S. Tumor-suppressive and tumor-promoting role of Tgf-Beta in Hepatocellular Carcinoma. *Int. J. Biol.* **9,** 41 (2016).
294. Stanková, J. Fucose-activated killer cells. I. Enhanced TNF-alpha mRNA accumulation and protein production. *J. Leukoc. Biol.* **52,** 188–96 (1992).
295. Teas, J. & Irhimeh, M. R. Melanoma and brown seaweed: an integrative hypothesis. *J. Appl. Phycol.* **29,** 941–948 (2017).
296. Beaumont, K. A., Mohana-Kumaran, N. & Haass, N. K. Modeling Melanoma In Vitro and In Vivo. *Healthcare* **2,** 27–46 (2014).
297. Smalley, K. S., Lioni, M., Noma, K., Haass, N. K. & Herlyn, M. In vitro three-dimensional tumor microenvironment models for anticancer drug discovery. *Expert Opin. Drug Discov.* **3,** 1–10 (2008).
298. Egeblad, M., Nakasone, E. S. & Werb, Z. Tumors as organs: Complex tissues that interface with the entire organism. *Developmental Cell* **18,** 884–901 (2010).
299. Maio, M. *et al.* Five-year survival rates for treatment-naive patients with advanced melanoma who received ipilimumab plus dacarbazine in a phase III trial. *J. Clin. Oncol.* **33,** 1191–1196 (2015).
300. Chapman, P. B. *et al.* Improved Survival with Vemurafenib in Melanoma with BRAF V600E Mutation. *N. Engl. J. Med.* **364,** 2507–2516 (2011).
301. Hodi, F. S. *et al.* Combined nivolumab and ipilimumab versus ipilimumab alone in patients with advanced melanoma: 2-year overall survival outcomes in a multicentre, randomised, controlled, phase 2 trial. *Lancet Oncol.* **17,** 1558–1568 (2016).
302. Hodi, F. S. *et al.* Improved Survival with Ipilimumab in Patients with Metastatic Melanoma. *N. Engl. J. Med.* **363,** 711–723 (2010).
303. Postow, M. A. *et al.* Nivolumab and Ipilimumab versus Ipilimumab in Untreated Melanoma. *N. Engl. J. Med.* **372,** 2006–2017 (2015).
304. Weber, J. *et al.* Phase I/II Study of Metastatic Melanoma Patients Treated with Nivolumab Who Had Progressed after Ipilimumab. *Cancer Immunol. Res.* **4,** 345–353 (2016).
305. Larkin, J. *et al.* Combined Nivolumab and Ipilimumab or Monotherapy in Untreated Melanoma. *N. Engl. J. Med.* **373,** 23–34 (2015).
306. Robert, C. *et al.* Ipilimumab plus Dacarbazine for Previously Untreated Metastatic Melanoma. *N. Engl. J. Med.* **364,** 2517–2526 (2011).
307. Hao, Y. *et al.* C-Fos mediates α1, 2-fucosyltransferase 1 and Lewis y expression in response to

TGF-β1 in ovarian cancer. *Oncol. Rep.* **38,** 3355–3366 (2017).
308. Fukushima, K., Satoh, T., Baba, S. & Yamashita, K. α1,2-Fucosylated and β-N-acetylgalactosaminylated prostate-specific antigen as an efficient marker of prostatic cancer. *Glycobiology* **20,** 452–460 (2009).
309. Kosanović, M. M. & Janković, M. M. Sialylation and fucosylation of cancer-associated prostate specific antigen. *J. B.U.ON.* **10,** 247–250 (2005).
310. Misonou, Y. *et al.* Comprehensive clinico-glycomic study of 16 colorectal cancer specimens: Elucidation of aberrant glycosylation and its mechanistic causes in colorectal cancer cells. *J. Proteome Res.* **8,** 2990–3005 (2009).
311. Domino, S. E., Karnak, D. M. & Hurd, E. A. Cell surface fucosylation does not affect development of colon tumors in mice with germline Smad3 mutation. *Tumor Biol.* **28,** 77–83 (2007).
312. Desiderio, V. *et al.* Increased fucosylation has a pivotal role in invasive and metastatic properties of head and neck cancer stem cells. *Oncotarget* **1,** 71–84 (2010).
313. Yang, H. F. *et al.* Fentanyl promotes breast cancer cell stemness and epithelial-mesenchymal transition by upregulating α1, 6-fucosylation via Wnt/β-catenin signaling pathway. *Front. Physiol.* **8,** 1–12 (2017).
314. Höti, N. *et al.* Overexpression of α (1,6) fucosyltransferase in the development of castration-resistant prostate cancer cells. *Prostate Cancer Prostatic Dis.* **21,** 137–146 (2018).
315. Tuccillo, F. M. *et al.* Aberrant glycosylation as biomarker for cancer: Focus on CD43. *Biomed Res. Int.* **2014,** (2014).
316. Ito, Y. *et al.* Expression of α1,6-fucosyltransferase (FUT8) in papillary carcinoma of the thyroid: Its linkage to biological aggressiveness and anaplastic transformation. *Cancer Lett.* **200,** 167–172 (2003).
317. Kaptan, E., Sancar-Bas, S., Sancakli, A., Bektas, S. & Bolkent, S. The effect of plant lectins on the survival and malignant behaviors of thyroid cancer cells. *J. Cell. Biochem.* 1–14 (2018). doi:10.1002/jcb.26875

Appendix

Permissions

Citation: Keeley T, Lin S, Lester DK, Lau EK, Yang S (2018) The fucose salvage pathway inhibits invadopodia formation and extracellular matrix degradation in melanoma cells. PLoS ONE 13(6): e0199128. https://doi.org/10.1371/journal.pone.0199128

Editor: Marco Magalhaes, University of Toronto, CANADA

Received: February 26, 2018

Accepted: June 3, 2018

Published: June 20, 2018

Data Availability Statement: The expression data of FUT1 and FUT2 in human melanoma patients are available from the NCBI (https://www.ncbi.nlm.nih.gov/geo/), GSE8401, GSE46517, GSE 7553, GSE15605 and GSE3189. All other relevant data are contained within the paper.

Funding: This study is supported by a grant from the National Cancer Institute (R01 CA175741) (SY). There was no additional external funding received for this study.